PHASE AND AMPLITUDE STABILIZATION OF SUPERCONDUCTING RESONATORS

Thesis by

Jean Roger Delayen

In Partial Fulfillment of the Requirements

for the Degree of

Doctor of Philosophy

California Institute of Technology

Pasadena, California

1978

(Submitted August 8, 1977)

TO JEROME, HIS MOTHER, AND HIS GRANDPARENTS

ACKNOWLEGMENTS

I would like to express my sincere appreciation to the following persons for their direct or indirect contributions:

Professor J. E. Mercereau for his leadership and advice.

Drs. G. J. Dick and K. W. Shepard who, besides teaching me the tricks of the trade, showed me the subtle difference between having fun and messing around.

Dr. H. A. Notarys for always being there at the right time with the right answer.

All the L. T. P. graduate students, past and present, who made the laboratory a fine place to be; particularly, H. C. Yen and T. Yogi whose close cooperation was appreciated.

Mr. S. Santantonio and Mr. E. P. Boud for their invaluable technical assistance.

Ms G. Kusudo who, although her coffee was getting weaker and weaker, kept the lab going; Ms S. Reagan who is pursuing, with the same cheerfulness, the task of administrative assistance.

The California Institute of Technology for financial assistance.

The Institute of Electrical and Electronics Engineers for their permission to use Figures (4.1) and (5.1) which appeared in IEEE trans. NS - 24.

My wife, Linda, for her expert typing, and for providing extra stimulus by showing me that, sometimes, being able to afford a dishwasher could be as important as having fun in a lab; and to Jérôme

who soon realized it was in everybody's interest if he slept through the night.

ABSTRACT

This thesis, which stemmed from the superconducting heavy-ion accelerator project at Caltech, deals with the problem of phase and amplitude stabilization of the fields in superconducting resonators. The problem arises from the fast (∿50 Hz) resonator eigenfrequency modulation of magnitude (∿100 Hz) which is much larger than the resonator bandwidth (∿10 Hz). The problem is compounded by the fact that the coupling between the electrical and mechanical modes of the resonator can lead to instabilities (ponderomotive instabilities). The solution suggested involves operating the resonators in self-excited loops, and electronically modifying the loop parameters in order to lock the loop oscillations to an external phase and amplitude reference without attempt to modify the instantaneous resonator eigenfrequency. It is found that this method of phase stabilization is well suited to resonators with small energy contents and small eigenfrequency deviations since the power required is equal to their product; this occurs when the loaded bandwidth of the resonator is twice the maximum eigenfrequency deviation to be compensated for. It is also found that when the loop is free-running, the field amplitude is stable and no ponderomotive instabilities are present as long as the non-ideal effects are limited. When the loop is locked to an external phase and amplitude reference, ponderomotive instabilities can occur; however, the loop can be made stable by adjustment of the loop phase shift, and the stable range can be increased by using high amplitude and phase feedback gains. It is also found that under

certain feedback conditions, the error on the particle energy gain can be made to vanish, although residual phase and amplitude errors are still present. A microprocessor-controlled feedback system based on this analysis is then described and results of experiments performed in conjunction with a 150 MHz lead (Pb) plated superconducting split-ring resonator are presented. The experiments show excellent agreement with the analysis.

TABLE OF CONTENTS

Chapter I

INTRODUCTION

Superconductivity in metals, usually associated with zero D.C. resistance and expulsion of magnetic field, was discovered in 1911. However, since it is a macroscopic quantum state, it was not understood and explained until 1957 when the tools to describe such a state became available (B1). With the help of the BCS theory of superconductivity, the behavior of superconductors under various conditions could be predicted. It soon became apparent that superconductivity had great application potential, and it slowly shifted from the realm of physics to the one of applied physics. As of this date, there are three major areas of application of superconductivity (N1):

1. Low power superconductivity which uses the properties of Josephson junctions
2. High power D.C. superconductivity (magnets, motors, etc.)
3. High power RF superconductivity (resonators)

Item 2 has already entered the engineering stage and industrial applications abound. Item 1 and 3 are still in the developmental stage, and should enter the industrial world in a few years.

This thesis deals with one aspect of item 3; namely RF superconducting resonators. In the early 1960's, it was noticed that although superconducting surfaces operating at radio-frequencies* had a non-zero surface resistance, this surface resistance was still very small; and, in any case, much smaller than that of normal

---

*By radio-frequency, we mean the 10 MHz - 10 GHz range.

materials like copper operating at room temperature. It then became apparent that superconductivity could be used to great advantage in applications where metals had to carry large RF currents. One such application was in particle accelerators where particles gain energy by interacting with large electromagnetic fields present in a series of resonators.* Using superconducting materials to build these resonators has two main advantages. Firstly, from the economics point of view, the power required to achieve a given energy gain is greatly reduced. The surface resistance of superconductors in the 100 - 200 MHz range is about 10^5 - 10^6 times smaller than the one of copper. However, because the Joule losses are so small in superconductors, other loss mechanisms which were negligible in normal resonators can become important; namely dielectric and field emission losses. Furthermore, each Watt dissipated in liquid helium requires about 1,000 W to be extracted to room temperature. The total power consumption is thus reduced by a factor of about 10 instead of 10^5; since even small accelerators require amounts of power measured in tens of MW, this factor of 10 is still very significant. The second advantage in using superconductivity is more important to nuclear physicists. Since the Joule dissipation in normal resonators is so large, normal accelerators usually have to be operated with a

---

*In this particular application of superconducting resonators, superconductivity improves what can be done with normal resonators. There are other applications, however, where superconductivity is absolutely required as in a new electromechanical conversion scheme recently proposed (D4, Y1).

low duty cycle (∿5%) in order to keep their temperature at a reasonable level. Superconducting accelerators, on the other hand, can be operated with a duty cycle of 1, thus reducing the length of an experiment by a significant factor.

The first proposals of superconducting accelerators were about high energy electron linear accelerators (F1, S1). Despite the very large amount of effort invested in superconducting electron accelerators, some problems have still proven to be insurmountable at this date, and their future is uncertain. A few years later, superconducting linear heavy-ion and proton accelerators were proposed, and are now entering the final stage of development; they should be operating in the very near future (B3,K2).

It should be pointed out now that most of the problems which have to be solved in high power RF superconductivity are not consequences of superconductivity in itself, but are consequences of the fact that the resonators are superconducting. By this we mean that all the phenomena which had to be dealt with were already present in normal resonators; however, they were overshadowed by the large surface resistance of the normal metal, and their influence was negligible. Because of the small surface resistance of superconductors (or small bandwidth, or large Q of superconducting resonators), these phenomena become very important, and new solutions have to be found.

In order to successfully build a superconducting heavy-ion linear accelerator, three main problems have to be solved. Firstly, an electromagnetic structure has to be found in which the field

distribution is such that the particle interacts efficiently with the field and gains as much energy as possible. The first requirement on the structure, then, is that the wave velocity in the resonator closely matches the velocity of the particle. Since this kind of accelerator is intended to accelerate particles from a velocity of about 0.04c to about 0.15c, this implies that the electromagnetic structure has to be very strongly loaded in order to decrease the phase velocity. Another requirement placed on the structure, whether it is normal or superconducting, is that the power dissipated at a given energy gain is minimal. This can be expressed by:

$$\frac{\langle B_{//}^2 \rangle}{\langle E_z \rangle^2} \quad \text{minimum} \qquad (1.1)$$

where $\langle B_{//}^2 \rangle$ represents the average of the square of the magnetic field at the surface, and $\langle E_z \rangle$ is the average electric field experienced by the particle. There are also other requirements which are specific to superconducting resonators. A superconducting resonator will operate up to the field level at which at any point of the surface the parallel magnetic field reaches the critical field of the superconductor -- however small the area of high magnetic field is and however small the magnetic field is everywhere else on the surface. This can be expressed by:

$$\frac{B_{// \max}}{\langle E_z \rangle} \quad \text{minimum} \qquad (1.2)$$

Since resistive losses are small in superconducting resonators, other loss mechanisms can become important and even dominant. One of them is field emission from points of the surface where the normal electric field is high. A new requirement is then:

$$\frac{E_{\perp max}}{\langle E_z \rangle} \quad \text{minimum} \qquad (1.3)$$

Finally, for reasons which will become apparent in Chapter II, it is very desirable that the energy content U of the resonator be as small as possible at a given energy gain:

$$\frac{U}{\langle E_z \rangle^2} \quad \text{minimum} \qquad (1.4)$$

There are also other requirements placed on superconducting resonators which cannot be stated as simply. One of them is that the currents flowing through joints between different parts of the resonator be as small as possible since these joints, which are necessary for fabrication, usually have lowered superconducting properties. Another requirement is that the resonator be made as mechanically rigid as possible so as to minimize the eigenfrequency variations caused by vibrations and radiation pressure.

As the above requirements became better understood, several electromagnetic structures were developed; among them we may cite the helical resonator (S2), the reentrant resonator (B2), the spiral

resonator (D1), and the split-ring resonator (S3). With the advent of the split-ring resonator, this area of the development program has probably reached its final stage, and it is unlikely that a new structure will be introduced which will provide improvements for this kind of application. It is interesting to note that the most favored structures for normal and superconducting heavy-ion LINAC are different. In the normal case, spiral resonators are usually preferred; whereas, in the superconducting case, split-ring resonators are preferred. This is due to the different requirements placed upon the structure in the two cases. The spiral resonator has the advantage of easier fabrication while the split-ring resonator has the advantage of lower surface fields and small RF currents flowing through the joints.

The second main area of research dealt with the material aspect. Once a structure had been found which had an optimal field distribution, it was necessary to find a superconducting surface which would allow the highest field magnitude. Actually, the development of the structure and of the material occurred simultaneously and were interrelated. Since some of the requirements placed on the structure are incompatible with each other (for example: modifying the structure to decrease the maximum surface magnetic field usually increases the maximum surface electric field), the structure had to be optimized in such a way that the maximum electric field and the maximum magnetic field allowable by the superconductor would be reached simultaneously. When work began on superconducting heavy-ion accelerators, there were two candidates for the superconductor; namely niobium (Nb) and

lead* (Pb). Although considerable improvements have been made on these two materials, these improvements have been parallel, and the question as to which one is preferable is still open. The main advantage of Nb over Pb is in its superconducting properties; its critical temperature is higher (9.5°K compared to 7.2°K), and so is its critical field (1950 G compared to 800 G). On the other hand, the Cu-Pb composite offers the advantage of better mechanical and thermal properties and easier fabrication. Recently, work has begun on a Cu-Nb composite which would improve the thermal stability of Nb structures (S5). Other materials are also being investigated such as Nb_3Sn (H1); this work, however, is still in the experimental stage, and such a surface is not yet suitable for a full-scale application.

The third area of research is in the control and stabilization of the accelerator. Once the fields of the desired profile and magnitude have been achieved, it is necessary to assure that the interaction between the particle and the electromagnetic field takes place in a controllable and predictable way. The problem arises because of the very narrow bandwidth ($\sim$10Hz) of the resonators, and the aim of this thesis is to provide a solution to this problem.

A heavy-ion linear accelerator is composed of a series of resonators; each of them sustaining a longitudinal electric field along the particle trajectory of the form:

$$E_z = E(z) \cos(\omega t + \phi) \qquad (1.5)$$

---

*By lead, we mean a structure made of copper, electroplated with 5 - 10 μ of lead (D6).

To find the energy gain of a particle of charge q traversing such a resonator, we will assume that the resonator is centered at $z = 0$, extends from $z = -\frac{\ell}{2}$ to $z = +\frac{\ell}{2}$, that the field profile is symetrical ($E(z)$ is even), that the particle of velocity $v = \beta c$ reaches the center of the resonator at $t = 0$, and that the energy gain is small (v = constant). With these assumptions, the energy gain W is:

$$W = q \cos \phi \int_{-\frac{\ell}{2}}^{+\frac{\ell}{2}} E(z) \cos \left(\frac{\omega}{\beta c} z\right) dz \qquad (1.6)$$

This can also be represented as:

$$W = q \cos \phi \, E(\beta_0) \, \ell \, T(\beta) \qquad (1.7)$$

where $E(\beta_0)$ is the average electric field seen by a particle whose velocity is matched to the resonator, and $T(\beta)$, called the transit time factor, characterizes the velocity acceptance of such a resonator. Figure 1.1 shows the transit time factor of two split-ring resonators.

Equation (1.7) clearly shows that the energy gain is maximum when the particle is in phase with the field ($\phi = 0$). Under this condition, however, the beam of particles is unstable under deviations of the time of arrival of the particles, and it is preferable to operate with $\phi < 0$ so that particles arriving early will experience less acceleration than particles arriving late assuring longitudinal

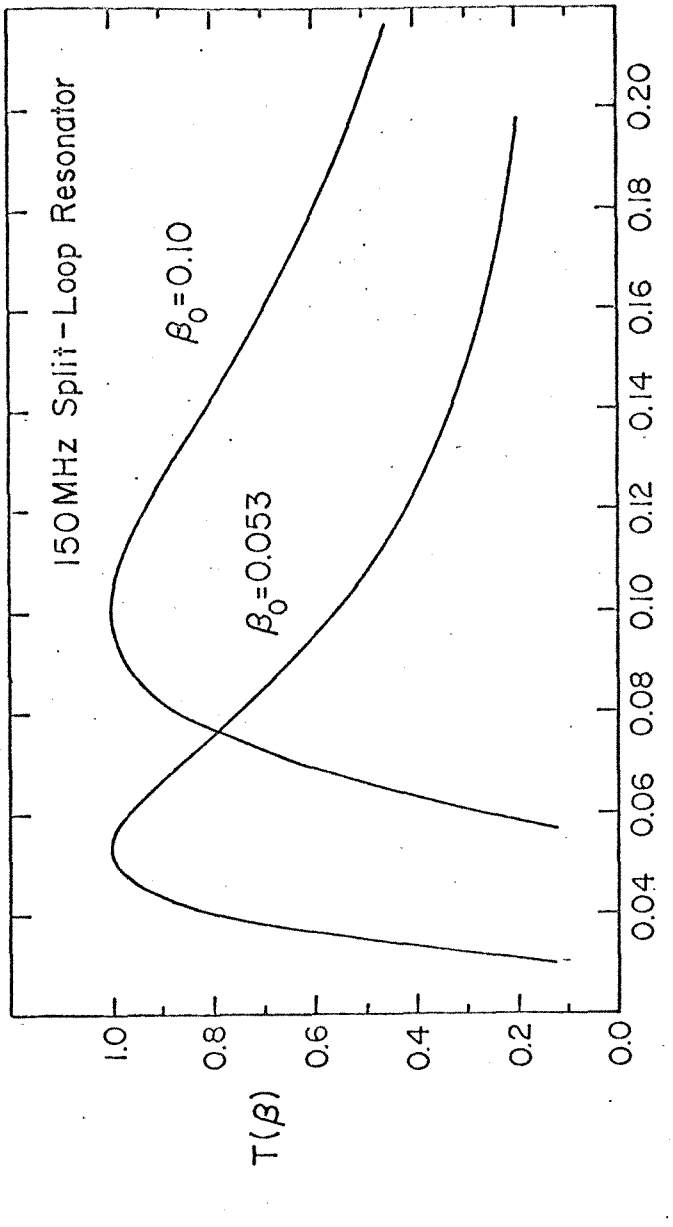

Fig. 1.1. Transit time factor of two 150 MHz split-ring resonators

stability of the beam. An acceptable operating phase, also called synchronous phase is:

$$\phi_s = -20^o \qquad (1.8)$$

which is a compromise between $\phi_s = 0$ where acceleration is maximum, but the beam is unstable, and $\phi_s = -90^o$ where the beam is most stable, but no acceleration is provided.

From equation (1.7), it is also apparent that in order to conserve the monochromaticity of the beam, the RF field amplitude and the phase between the particle and the RF field have to be as stable as possible. Since the particles will traverse successively all the resonators, this implies that all the amplitudes have to be stable, and that the fields in all the resonators have to be locked to a common phase (or frequency) reference.

When normal resonators are used, these requirements are automatically satisfied since the eigenfrequency variations of the resonators are much smaller than their bandwidths so their eigenfrequencies can be considered for all practical purposes as being identical and constant, and all the resonators are driven by a common oscillator. When superconducting resonators are used, however, because of their very narrow bandwidths, their instantaneous eigenfrequencies differ from the reference frequency by many bandwidths, so that if the resonators were driven by a common oscillator, the field amplitude and phase would be random.

The eigenfrequency deviations occur on three different time

scales:

1. static: several resonators cannot be fabricated with a frequency matching better than 50 kHz which corresponds to mechanical tolerances of less than 1 mil
2. quasi-static: variations of eigenfrequency due to temperature drifts and radiation pressure
3. dynamic: excitation of the mechanical modes of the resonator by external noise and the radiation pressure (ponderomotive effects)

Effects 1 and 2 can be dealt with easily by mechanical tuning (deformation of the resonator walls), so we will concentrate on the dynamical effects which occur on a time scale of the order of the period of the mechanical modes of the resonator ($\sim$20msec).

In order to show how sensitive superconducting resonators are to mechanical deformations, let's consider a 150 MHz split-ring resonator with a Q of 10^7 (bandwidth = 15 Hz). In such a resonator, the characteristic length (the length which determines the eigenfrequency; in this case, the distance between the drift tubes) is of the order of 1 cm. This means that a variation of the characteristic length of 10 $\mathring{A}$ will produce a change of the eigenfrequency of the order of the bandwidth. Clearly, such variations will be easily produced by excitation of the resonator by acoustical noise and vibrations. Such vibrations can be kept to a minimum, but cannot be eliminated, and random eigenfrequency variations of the order of 100 Hz or more are to be expected. Another source of mechanical deformation of the

resonator is the pressure exerted by the field on the walls of the resonators, i.e. the radiation pressure. If the field amplitude were absolutely stable, the radiation pressure-induced frequency shift would be constant, and could be compensated for easily; however, since it is quite large at operating field amplitude (from 400 Hz for a split-ring resonator up to 400 kHz for a helical resonator), even a small modulation of the field amplitude can produce large modulations of the eigenfrequency. The problem is compounded by the fact that such a coupling between the electrical and mechanical modes of the resonator through the radiation pressure can lead to instabilities of the electromechanical system (ponderomotive effects) (K1, S4). Such a coupling implies a power flow between the electrical and mechanical modes; if the power transfered from the electrical mode to the mechanical mode is larger than the power dissipated by the mechanical mode, instability will occur. This instability takes the form of a building up of the mechanical mode (oscillatory instability). Another instability, called monotonic instability, can be present. It is analogous to the jump phenomenon in many non-linear oscillators where there is an unstable region of amplitude between two stable levels.

The task before us is then to find a way to stabilize the amplitude and phase of the field in a resonator, although its eigenfrequency can change rapidly by many bandwidths, and at the same time prevent or eliminate the instabilities produced by the electromechanical coupling.

Until now, the solutions to this problem involved direct

modification of the eigenfrequency of the resonator. One method was to connect an external reactance to the resonator through a PIN diode switch (D2, H2, D3, P1). The diode was turned on and off with a duty cycle such that the average frequency of the resonator would be equal to the frequency reference it had to be locked to, and with a switching rate such that the residual phase jitter would be acceptable. Another method was to produce rapid mechanical deformation of the resonator via a piezoelectric feedback system (B2).

In this thesis, we present a solution which is novel in several ways. Firstly, we do not use a generator to drive the resonator, but we operate it in a self-excited loop. Secondly, we make no attempt to modify the instantaneous resonator eigenfrequency; instead, we modify the self-excited loop so it will oscillate at a constant frequency. It will be shown that such a system has the advantage that even when no feedbacks are present, the loop is still oscillating at its nominal field amplitude (amplitude of the fields in the resonator) and that the amplitude is stable, and that the ponderomotive instabilities are easily removed. Furthermore, the feedback parameters can be chosen so that the error on the energy gain vanishes, although residual errors on the phase and amplitude are still present.

This thesis is divided as follows: Chapter II presents the principle of phase stabilization of a self-excited loop. In Chapter III we first determine the equations describing the behavior of a resonator in a self-excited loop, we then determine the stability of a free-running self-excited loop (unlocked state) in presence of electromechanical coupling, the stability analysis is then pursued

to the case where amplitude and phase feedback are present (loop locked to an external amplitude and phase reference), and finally we determine the performance of such a system (residual phase, amplitude and energy gain errors). In Chapter IV, we describe a system which was built based on the analysis of Chapter III, and in Chapter V we present experimental results obtained with this system and a 150 MHz superconducting split-ring resonator shown in Figure (1.2).

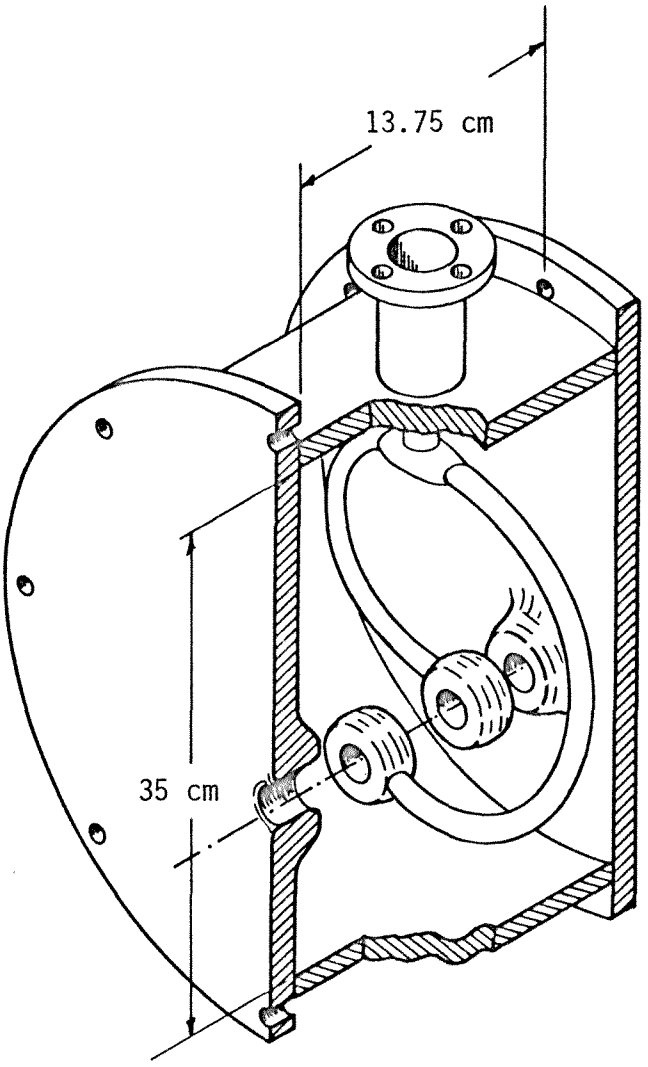

Fig. 1.2. Drawing of a 150 MHz split-ring resonator.

Chapter II

PRINCIPLE OF STABILIZATION OF A SELF-EXCITED LOOP

The principle of a self-excited loop is shown in Fig. 2.1. A self-excited loop is composed of a filter,which will be assumed to be linear, a phase shifter, and a limiter. Two other elements which are usually present in a self-excited loop but are not essential in the understanding are an attenuator and an amplifier. The output of the filter is used as its input after going through the phase shifter and the limiter. A self-excited loop is in essence an unstable positive feedback loop where the limit cycle or amplitude of the oscillations is set by the nonlinear element in the loop,i.e. the limiter. The frequency of oscillation is the one at which the total loop phase shift is a multiple of 2π.

The filter is characterized by its transfer function:

$$\Phi(i\omega) = A(\omega)\ e^{i\theta(\omega)} \tag{2.1}$$

where $A(\omega)$ is the amplitude characteristic and $\theta(\omega)$ is the phase chatacteristic .

The loop will then oscillate at the frequency ω, such that:

$$\theta(\omega) + \theta_{\ell} = 0 \quad \text{modulo } 2\pi \tag{2.2}$$

where θ_{ℓ} is the phase shift introduced by the loop phase shifter.

Depending upon the complexity of $\Phi(i\omega)$, there may be several frequencies which satisfy (2.2). We will, however, assume, for the

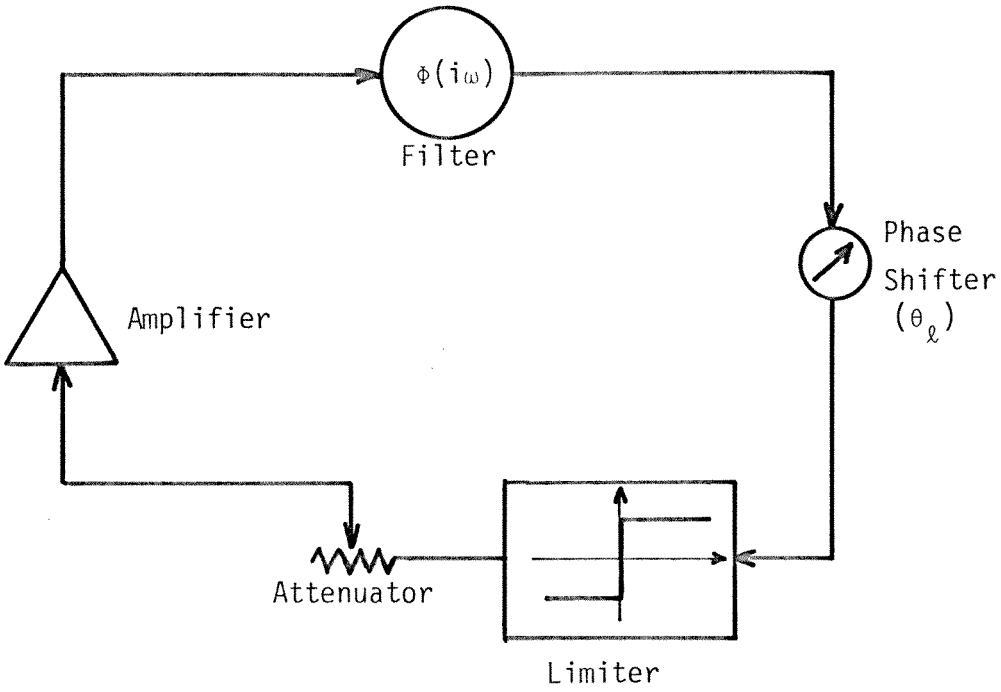

Fig. 2.1 Block diagram of a self-excited loop containing a filter of transfer function $\Phi(i\omega)$

sake of simplicity, that the loop oscillates at a single frequency.

We will now assume that the filter transfer function also depends on a parameter p, which is not controllable. As the parameter p varies, the loop oscillation frequency will vary in such a way as to keep the phase shift across the filter constant:

$$\theta(p,\omega) + \theta_\ell = 0 \qquad (2.3)$$

On the other hand, if the loop phase shift θ_ℓ is varied, the loop oscillation frequency will also vary in order to satisfy (2.3). Thus phase stabilization* of a self-excited loop can be accomplished by introducing a controllable amount of additional loop phase shift in order to compensate for the variation of the loop oscillation frequency caused by the uncontrollable parameter p. We will now go into more details in the specific case of a second order filter which accurately represents an isolated mode of an electromagnetic resonator.

To eliminate the constant phase shifts in the loop (along cables, across the limiter and amplifier), we will define the phase shifts across the resonator and the phase shifter as the difference between the actual phase shift and the one when the loop oscillation frequency is equal to the resonator eigenfrequency ω_c. With this convention, if $\theta_c(\omega)$ is the phase shift across the resonator at frequency ω, and θ_ℓ is the phase shift across the loop phase shifter, the loop oscilla-

* By phase stabilization we mean locking the phase of the loop oscillation to an external phase reference.

tion frequency is defined by:

$$\theta_c(\omega) + \theta_\ell = 0 \qquad (2.4)$$

and:

$$\theta_c(\omega_c) = 0 \qquad (2.5)$$

The relationships between the amplitude characteristic $A(\omega)$ of the resonator, the loop oscillation frequency ω, and the loop phase shift θ_ℓ, are shown in Fig. (2.2).

From Fig. (2.2), we see that the loop phase shift θ_ℓ does not actually set the loop oscillation frequency but the difference between the resonator eigenfrequency and the loop oscillation frequency. That means that even if the resonator eigenfrequency varies because of vibrations or other causes, the operating point will be fixed on the amplitude characteristic curve. Thus, a self-excited loop, although not stable in frequency, is stable in amplitude.

We will now assume that the loop phase shifter is adjusted so that the loop oscillates at the resonator eigenfrequency ($\theta_c = \theta_\ell = 0$), and we will add a signal in quadrature as shown in Fig. (2.3). The two different signals will be referred to as "in phase" of amplitude A_p, and "in quadrature" of amplitude A_q.

By adding a signal in quadrature, we introduce an additional phase shift ϕ_i defined by:

$$\tan \phi_i = \frac{A_q}{A_p} \qquad (2.6)$$

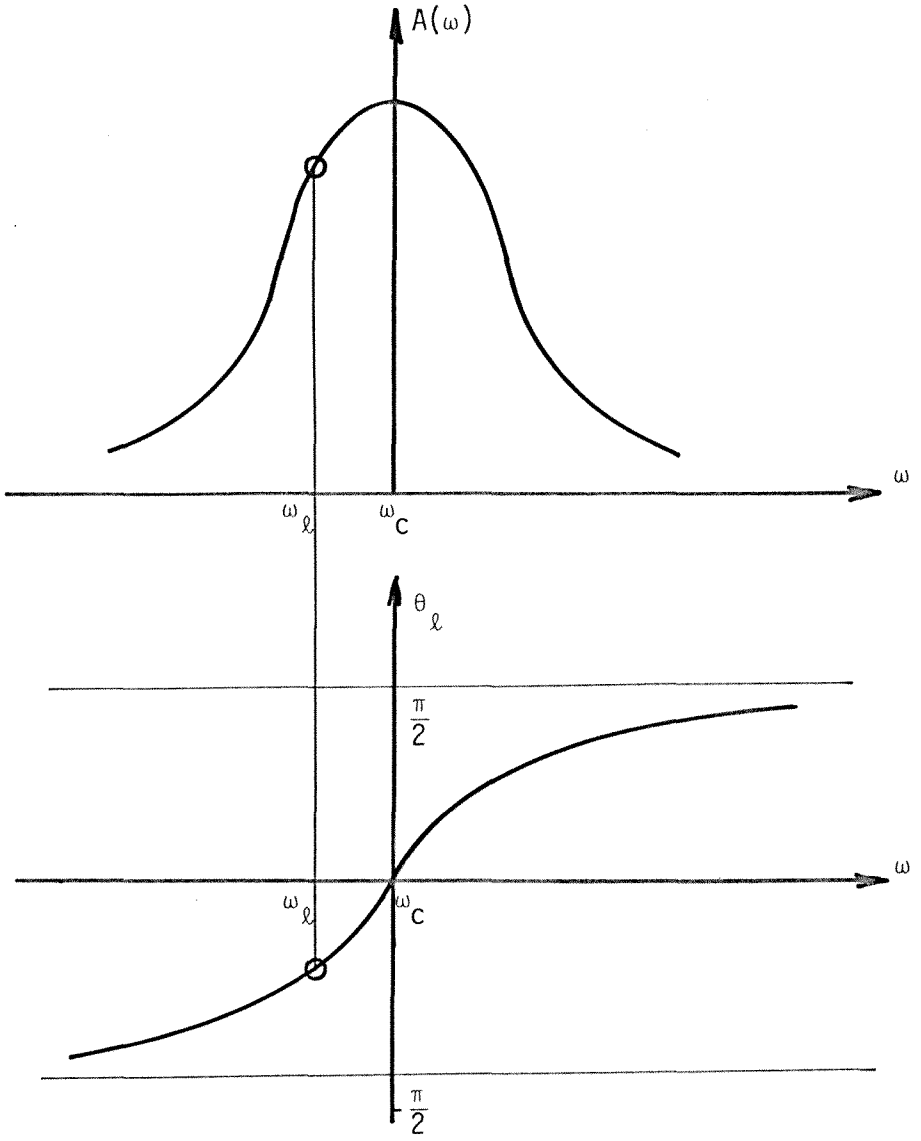

Fig. 2.2 Relationships between the amplitude characteristic $A(\omega)$, the loop oscillation frequency ω, and the loop phase shift θ_ℓ of a self-excited loop containing a resonator

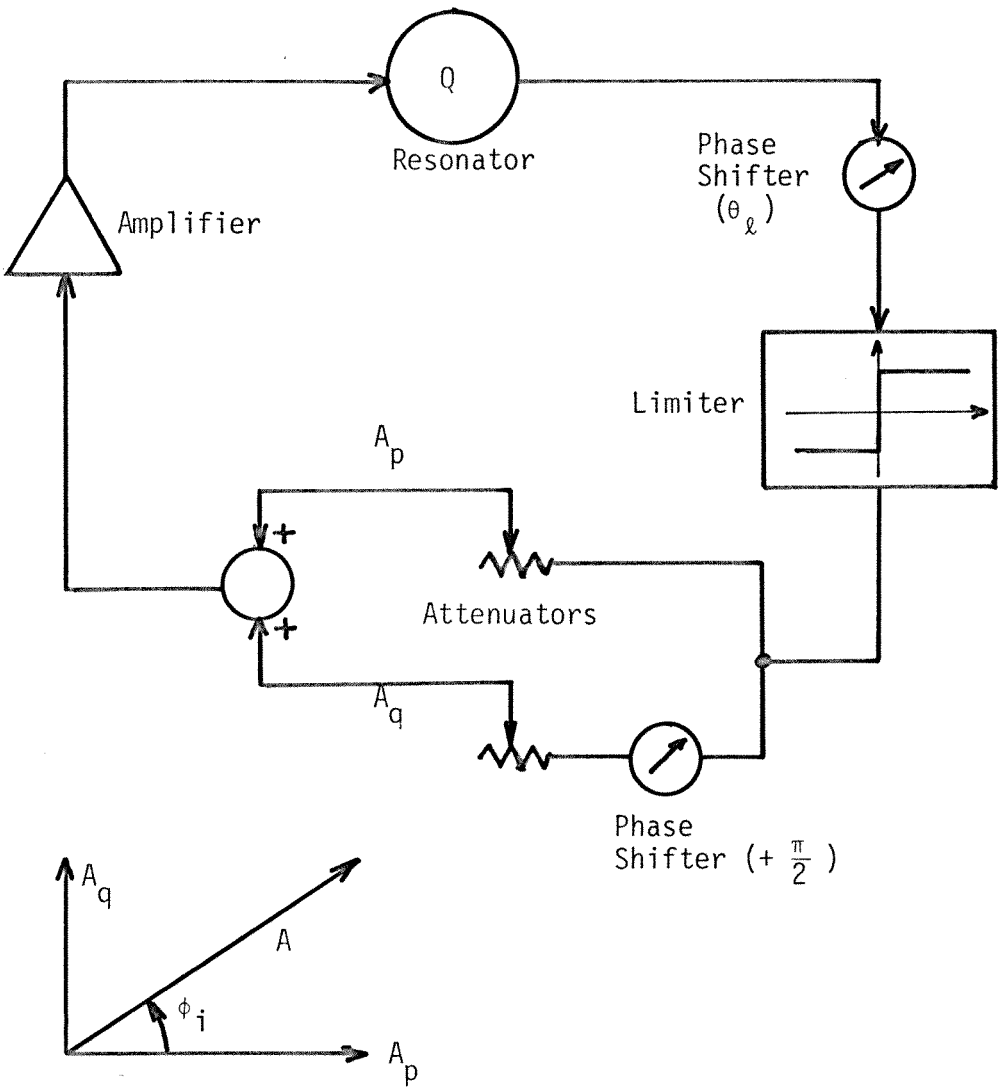

Fig. 2.3 Principle of stabilization of a self-excited loop by addition of a signal in quadrature

and the amplitude of the driving signal is now:

$$A = \sqrt{A_p^2 + A_q^2} \tag{2.7}$$

The loop oscillates now at the frequency $\omega_\ell = \omega_c + \delta\omega$ such that:

$$\theta_c(\omega_\ell) = -\phi_i \tag{2.8}$$

Therefore, adding a signal in quadrature introduces a frequency shift. The principle of phase stabilization is then to add an amount of signal in quadrature A_q such that the frequency shift $\delta\omega$ which is produced compensates for the frequency excursion of the resonator:

$$\omega_c + \delta\omega = \omega_r = \text{constant} \tag{2.9}$$

We will now make a quantitative study to see if this scheme can be used to stabilize superconducting resonators.

We will start by defining the parameters of the resonator.

τ_o : Intrinsic amplitude decay time

$\Delta\omega_o = \frac{2}{\tau_o}$: Intrinsic bandwidth

$Q_o = \frac{\omega_c \tau_o}{2}$: Intrinsic quality factor

β : Coupling constant

$\tau = \frac{\tau_o}{1 + \beta}$: Loaded amplitude decay time

$\Delta\omega = \Delta\omega_o(1 + \beta)$: Loaded bandwidth

$Q = \frac{Q_o}{1 + \beta}$: Loaded quality factor

The energy content $U(\omega)$ is related to the incident power P_{inc} by (T1):

$$U(\omega) = \frac{4\,Q}{(1 + \beta)\omega_c} \quad \frac{P_{inc}}{1 + \left(\frac{2Q(\omega - \omega_c)}{\omega_c}\right)^2} \qquad (2.10)$$

The resonator phase shift is related to the loop frequency by:

$$\tan \theta_c(\omega) = Q\left(1 - \frac{\omega^2}{\omega_c^2}\right) \simeq -2\,\frac{\delta\omega}{\omega_c}\,Q \qquad (2.11)$$

where $\delta\omega = \omega - \omega_c$

The incident power P_{inc} can be divided into two different powers: P_p which energizes the resonator to an energy content U, and P_q which produces the frequency shift at this energy content. They are related to the incident power P_{inc} by:

$$\frac{P_{inc}}{A^2} = \frac{P_p}{A_p^2} = \frac{P_q}{A_q^2} \qquad (2.12)$$

Using (2.6), (2.8), (2.11) and (2.12), (2.10) transforms to:

$$U(\omega) = \frac{4\beta Q_o}{(1+\beta)^2 \omega_c} \frac{P_p\left(1 + \frac{A_q^2}{A_p^2}\right)}{1 + \left(\frac{2\delta\omega Q}{\omega_c}\right)^2} = \frac{Q_o}{\omega_c} \frac{4\beta}{(1+\beta)^2} P_p \qquad (2.13)$$

Therefore, the energy content of the resonator and the field level are independent of the amount of frequency shift introduced by the signal in quadrature A_q and depend only on the amplitude of the signal in phase A_p. In other words, when the loop phase shift is adjusted so that the unlocked (free running) self-excited loop oscillates at the resonator eigenfrequency, the introduction of phase feedback will not alter the amplitude of the fields in the resonator, and the phase and amplitude feedback loops will be decoupled. It will be seen in Chapter III that it might be preferable to relinquish this condition, and to introduce a certain amount of coupling in order to decrease the phase jitter by increasing the amplitude jitter.

The criterion of practicality for this phase feedback system can be stated as follows: What amount of incident power P_{max} is required to produce a frequency shift $\delta\omega_{max}$ when the resonator operates at an energy content U?

The only parameter of the resonator system which can be varied is the coupling constant β. While P_p increases with increasing β (beyond critical coupling), P_q decreases, and an optimal coupling can be found which minimizes the required total power.

The incident power $P_{inc}(\delta\omega)$ which produces a frequency shift $\delta\omega$ at an energy content U is from (2.13):

$$P_{inc}(\delta\omega) = \left[1 + \left(\frac{2\,\delta\omega}{(1+\beta)\Delta\omega_o}\right)^2\right]\frac{(1+\beta)^2}{4\,\beta}\,P_{abs} \qquad (2.14)$$

where $P_{abs} = \omega_c \frac{U}{Q_o}$ is the power dissipated in the resonator.

The coupling constant β_{opt} which minimizes the incident power for $\delta\omega = \delta\omega_{max}$ is obtained by differentiation of (2.14):

$$\beta_{opt} = \sqrt{\Delta_o^2 + 1} \qquad (2.15)$$

where

$$\Delta_o = 2\,\frac{\delta\omega_{max}}{\Delta\omega_o} \qquad (2.16)$$

At this optimal coupling we have:

$$P_{inc}(\delta\omega) = U\,\delta\omega_{max}\,\frac{\left(1+\sqrt{\Delta_o^2+1}\right)^2}{2\Delta_o\sqrt{\Delta_o^2+1}}\left[1 + \left(\frac{\delta\omega}{\delta\omega_{max}}\right)\left(\frac{\Delta_o}{\sqrt{\Delta_o^2+1}+1}\right)^2\right] \qquad (2.17)$$

The maximum power required is then:

$$P_{max} = P_{inc}(\delta\omega_{max}) = U\,\delta\omega_{max}\,f(\Delta_o) \qquad (2.18)$$

where $f(\Delta_o)$ is shown in Fig. (2.4)

The proportionality between the power required and the energy

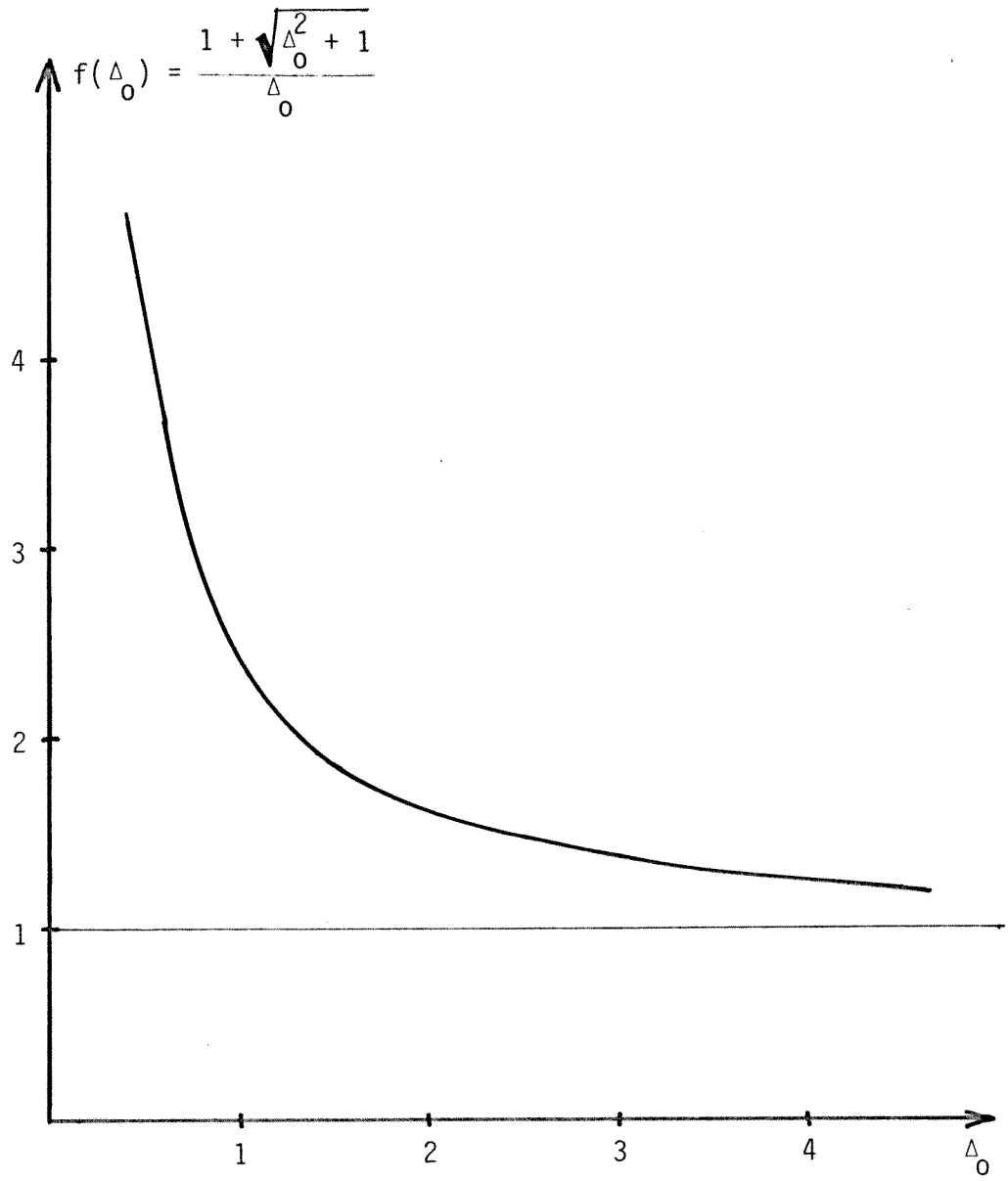

Fig. 2.4 Graph of the function relating the energy content, the frequency shift and the incident power (see Eq. 2.18)

content explains the importance of requirement (1.4); that is,to find a structure which has a small energy content at a given accelerating field.

The coupling constant is not a directly measurable quantity, but is inferred from the loaded bandwidth $\Delta\omega$. The optimal loaded bandwidth is related to the maximum frequency shift by:

$$\Delta\omega_{opt} = 2\, f(\Delta_o)\, \delta\omega_{max} \tag{2.19}$$

For typical superconducting resonators used for heavy ion acceleration, the frequency shift $\delta\omega_{max}$ which has to be compensated is much larger than the intrinsic bandwidth $\Delta\omega_o$ and in the limit $\Delta_o >> 1$, Equations (2.18) and (2.19) simplify to:

$$P_{max} = U\, \delta\omega_{max}$$

$$\Delta\omega_{opt} = 2\, \delta\omega_{max} \tag{2.20}$$

Equations (2.20) indicate that optimal coupling occurs when the loaded bandwidth is twice the frequency shift which has to be compensated, and that the incident power required is the product of the energy content at operating accelerating field and the frequency shift to be compensated.

The split-ring resonator has the feature that both $\delta\omega_{max}$ and U at the operating field are small. Typically $\delta\omega_{max}/2\pi$ = 100 Hz and

$U = 0.25$ J. Less than 200 W of RF power would then be sufficient to provide phase stability to such a split-ring resonator.

Chapter III

PHASE AND AMPLITUDE STABILIZATION OF A RESONATOR OPERATING IN A SELF-EXCITED LOOP

In this chapter we will make a detailed study of phase and amplitude stabilization of a resonator operating in a self-excited loop. First we will determine the equations governing the behavior of such a loop. Then we will summarize the results obtained by Schulze on the ponderomotive instabilities of generator-driven resonators. Lastly, we will study the behavior of a self-excited loop in the locked and unlocked state.

3.1 Differential equation of a self-excited loop

The difference between a generator-driven resonator and a resonator in a self-excited loop is in the nature of the input and output variables. In a generator-driven resonator, the input variables are the generator amplitude and frequency, the output variables being the amplitude of the field in the resonator and the phase shift across the resonator. In a self-excited loop, the input variables are the limiter output amplitude (which we will also call generator amplitude) and the loop phase shift, and the output variables are the amplitude of the field in the resonator and the frequency of the loop oscillations. This is shown in Fig. (3.1).

If we assume that the fields in the resonator can be expressed in terms of a single mode, which is valid when both the bandwidth and the frequency variation are small with respect to the mode separation, the resonator can be represented as a lumped-parameter circuit:

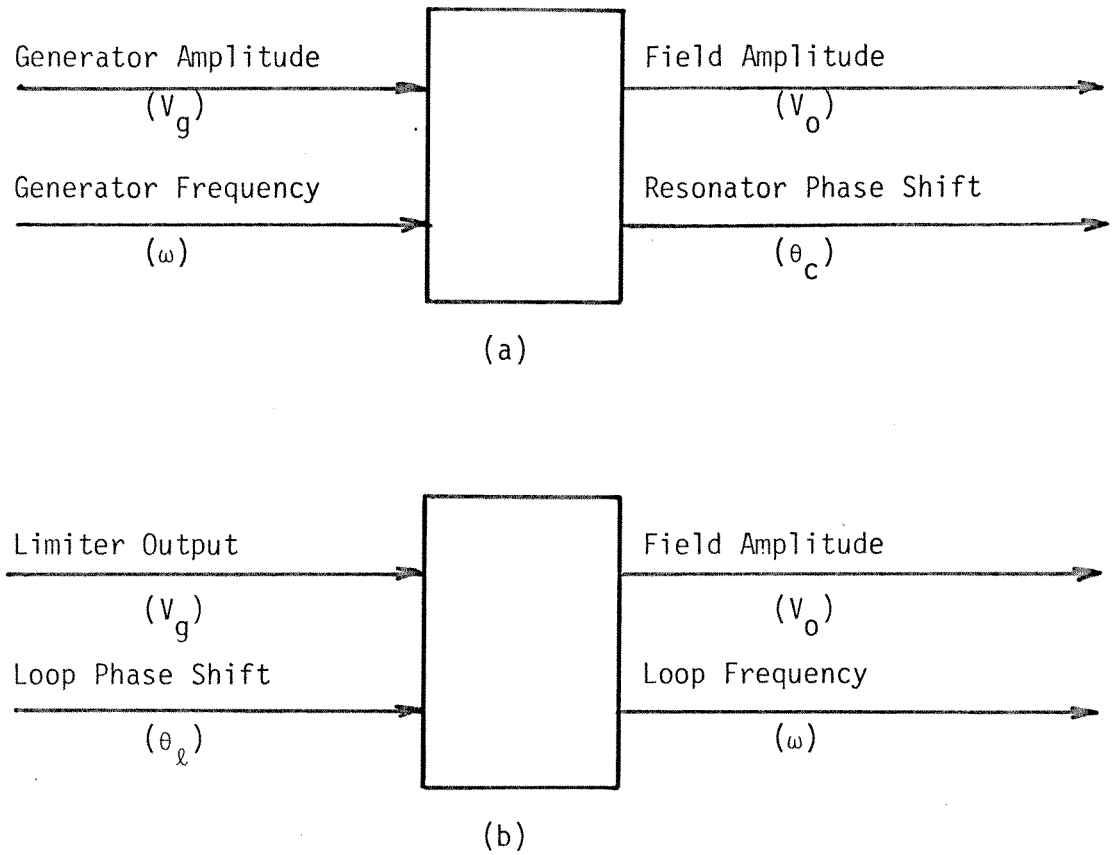

Fig. 3.1 Input and output variables of a resonator

(a) : Driven by a generator

(b) : Operated in a self-excited loop

$$\ddot{v} + \frac{2}{\tau}\dot{v} + \omega_c^2 v = \frac{2}{\tau}\dot{v}_g \qquad (3.1.1)$$

ω_c : instantaneous eigenfrequency of the resonator

τ : amplitude decay time of the resonator fields

In the case of a self-excited loop we have the following expressions for v and v_g (see Fig. 3.2):

$$\begin{aligned} v &= V e^{i\phi} \\ v_g &= V_g e^{i\phi} e^{i\theta_\ell} \end{aligned} \qquad (3.1.2)$$

V : real amplitude of the field in the resonator

ϕ : RF phase of the electromagnetic field

θ_ℓ: phase shift introduced by the loop phase shifter

Using equations (3.1.2) in (3.1.1) and identifying the derivative of the phase, $\dot{\phi}$, with the instantaneous frequency ω of the loop oscillations, we obtain the following differential equation:

$$\ddot{V} + \dot{V}\left(\frac{2}{\tau} + 2i\omega\right) + V\left(\omega_c^2 - \omega^2 + \frac{2}{\tau} i\omega + i\dot{\omega}\right) = \frac{2}{\tau}\left(i\omega V_g + \dot{V}_g\right) e^{i\theta_\ell} \qquad (3.1.3)$$

This equation looks quite similar to the case where the resonator is driven by an external generator of frequency ω, with the important difference that in Eq. (3.1.3) V represents the real amplitude of the field. For comparison with the generator-driven case, see Eq. (3.2.2) and Appendix A.

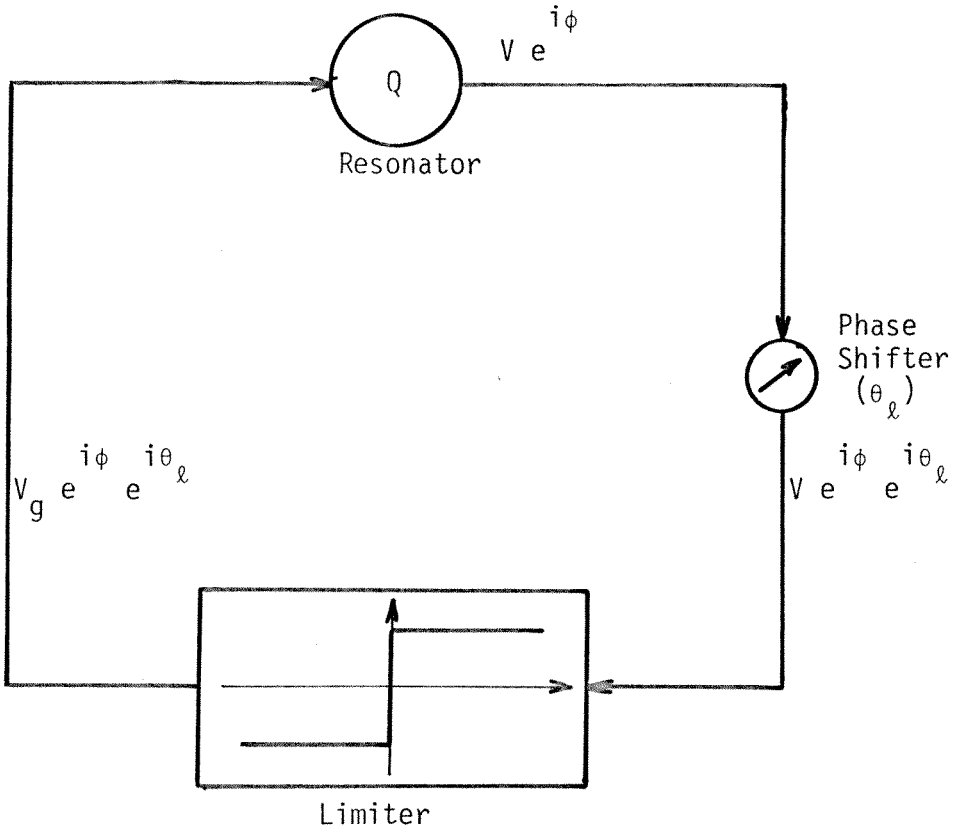

Fig. 3.2. Block diagram of a resonator operating in a self-excited loop

The following approximation will be used throughout this dissertation:

$$\omega_c^2 - \omega^2 \simeq -2\omega(\omega - \omega_c) \tag{3.1.4}$$

Also, we will assume that the generator amplitude changes negligibly during one RF period ($\dot{V}_g << \omega V_g$).

Separating real and imaginary parts of (3.1.3) and using (3.1.4), we obtain the following set of differential equations which describes the behavior of the fields in a resonator operating in a self-excited loop:

$$\begin{aligned} \tau\dot{V} + V\left(1 + \frac{\tau\omega}{2\omega}\right) &= V_g \cos\theta_\ell \\ -\frac{\tau\ddot{V}}{2\omega} - \frac{\dot{V}}{\omega} + \tau V(\omega - \omega_c) &= V_g \sin\theta_\ell \end{aligned} \tag{3.1.5}$$

The steady state solutions are:

$$\begin{aligned} V_o = V_g \cos\theta_\ell &= \frac{V_g}{1 + y_\ell^2} \\ (\omega - \omega_c)_o &= y_\ell \end{aligned} \tag{3.1.6}$$

where $y_\ell = \tan\theta_\ell$

3.2 Ponderomotive effects in RF resonators

Until now, we have considered a resonator as being equivalent to a single electromagnetic mode. However, since the walls of the

resonator are not infinitely rigid, a resonator has to be described also in terms of mechanical modes. For simplicity, we will consider a single mechanical mode of frequency Ω_μ and decay time τ_μ.

Ponderomotive effects in RF resonators result from a coupling between electromagnetic and mechanical modes of the resonator caused by radiation pressure. Electromagnetic fields confined in a resonator exert a pressure on the walls of the resonator given by (B4):

$$P = \frac{\mu_o}{4} H^2 - \frac{\varepsilon_o}{4} E^2 \qquad (3.2.1)$$

This pressure is proportional to the energy content of the resonator or to the square of the fields. It will produce a deformation of the walls of the resonator, resulting in a change in the eigenfrequency of the resonator and in the detuning between the generator and the resonator. This produces a variation of the energy content and, in turn, a variation of the driving force of the mechanical mode.

Thus, an RF resonator has to be represented by two coupled modes, one electromagnetic and one (or several) mechanical. Under certain conditions, this two-mode system can become unstable.

Ponderomotive instabilities were first observed in normal resonators (K1), and an analysis was provided in the limit where the electrical decay was much smaller than the mechanical period. The analysis was extended by Shapiro (S6) to the case where the electrical decay time is comparable or larger than the period of the mechanical mode by comparing the power flow between the electrical and mechanical

modes and the power dissipated in the mechanical mode. Ponderomotive instabilities in generator-driven resonators, both monotonic and oscillatory, were then studied in a systematic and unified way by Schulze (S4) who made use of the transfer function formalism. His results will be summarized here for comparison with instabilities in resonators operated in self-excited loops.

The resonator is represented by an electromagnetic mode:

$$\ddot{\tilde{V}} + \dot{\tilde{V}}\left(2i\omega + \frac{2}{\tau}\right) + \tilde{V}\left(\omega_c^2 - \omega^2 + \frac{2}{\tau} i\omega\right) = \frac{2}{\tau} i\omega V_g \qquad (3.2.2)$$

and a mechanical mode:

$$\ddot{\Delta\omega}_\mu + \frac{2}{\tau_\mu}\dot{\Delta\omega}_\mu + \Omega_\mu^2 \Delta\omega_\mu = -k_\mu \Omega_\mu^2 \tilde{V}\tilde{V}^* \qquad (3.2.3)$$

where

$\tilde{V} = Ve^{i\theta_c}$	:	complex amplitude of the fields in the resonator
ω	:	frequency of the generator
$\omega_c = \omega_o + \Delta\omega_\mu$	:	instantaneous resonator eigenfrequency
ω_o	:	resonator eigenfrequency at zero field
$\Delta\omega_\mu = -k_\mu V^2$	:	radiation pressure-induced frequency shift
k_μ	:	electromechanical coupling constant
$\Delta\omega_{\mu o} = -k_\mu V_o^2$	:	steady state radiation pressure-induced frequency shift at field level V_o

This electromechanical system can present two types of instabilities: a monotonic instability similar to the jump phenomenon

encountered in many non-linear oscillators, and an oscillatory instability.

The monotonic stability condition was found by Schulze as follows:

$$- y\, k_\mu V_o^2 < \frac{1 + y^2}{2\,\tau} \tag{3.2.4}$$

And the oscillatory stability condition as:

$$y\, k_\mu V_o^2 < \frac{(1 - \Omega_\mu^2\tau^2 + y^2)^2 + 4(1 + \frac{\tau}{\tau_\mu})(\Omega_\mu^2\tau^2 + \frac{\tau}{\tau_\mu}(1 + y^2))}{2\tau_\mu\tau^2\Omega_\mu^2(1 + \frac{\tau}{\tau_\mu})^2} \tag{3.2.5}$$

where $y = \tau(\omega - \omega_{co})$: normalized detuning between generator and resonator

$\omega_{co} = \omega_o + \Delta\omega_{\mu o}$: steady state resonator eigenfrequency at field level V_o.

Several remarks can be made about these results. The oscillatory stability condition was obtained from the linearized system which means it is a necessary condition for the nonlinear system, and the following approximation was used:

$$\frac{1}{2}\,\frac{\Omega_\mu}{\omega_o}\,(\Omega_\mu\tau + \frac{1}{\Omega_\mu\tau}) \ll 1 \tag{3.2.6}$$

which is valid since the mechanical frequency is always much smaller than the electrical frequency.

It can also be noted that the monotonic instability can occur

only on the low frequency side ($y < 0$), and the oscillatory instability on the higher frequency side ($y > 0$). When working at the resonance point ($y = 0$), no instability can occur at any field value. However, in practice, this is not feasible since y is not a controlled variable. y is related to the difference between the generator frequency which is fixed and the resonator eigenfrequency which is variable due to vibrations, and typically can vary by several electrical bandwidths.

Typically, for superconducting resonators, the monotonic instability can occur when the static radiation pressure frequency shift is of the order of the electrical bandwidth, and the oscillatory instability when it is of the order of the mechanical bandwidth.

Typical values for the split-loop resonator at operating field values are:

$$\frac{\Delta\omega_{\mu o}}{2\pi} \sim 500 \text{ Hz}$$

$$\frac{1}{\tau} \sim 10 \text{ Hz}$$

$$\frac{1}{\tau_{\mu}} \sim 0.1 \text{ Hz}$$

So these instabilities can occur at field values much smaller than the operating field.

The last remark is that these results apply to an unlocked generator-driven resonator. Phase and amplitude stabilization schemes which are required to use a resonator as an accelerating

structure will modify the stability conditions.

We will now study the stability of a resonator operating in a self-excited loop in the presence of ponderomotive coupling. We will study the stability firstly in the absence of phase and amplitude feedback (unlocked loop), and secondly in the presence of phase and amplitude feedback (loop locked to an external reference).

3.3 Ponderomotive stability of a resonator in a self-excited loop

To study the stability of a resonator operating in a self-excited loop, we will use the set of differential equations describing the electrical system which was obtained earlier:

$$\begin{aligned} \tau\dot{V} + V\left(1 + \frac{\tau\dot{\omega}}{2\omega}\right) &= V_g \cos\theta_\ell \\ -\frac{\tau\ddot{V}}{2\omega} - \frac{\dot{V}}{\omega} + \tau V(\omega - \omega_c) &= V_g \sin\theta_\ell \end{aligned} \qquad (3.3.1)$$

And we will also use the differential equation representing the mechanical oscillator which is coupled to the electrical oscillator through the radiation pressure:

$$\ddot{\Delta\omega}_\mu + \frac{2}{\tau_\mu}\dot{\Delta\omega}_\mu + \Omega_\mu^2 \Delta\omega_\mu = -k_\mu \Omega_\mu^2 V^2 \qquad (3.3.2)$$

The task is to find the range of values of the different parameters of the system where the system will be stable. The first problem lies in the fact that we are in the presence of a non-linear system, and an exact answer to the stability of this non-linear system is

impossible to find. As a consequence, we will study the stability of the associated linearized system. Throughout this thesis, a subscript $_o$ will represent a steady state value, and a δ in front of a variable will represent the deviation of this variable around its steady state value. We then obtain the linearized system:

$$\frac{\tau}{2\omega}\delta\ddot{V} - \frac{\delta\dot{V}}{\omega} + \delta V y_\ell + \tau V_o \delta\omega - \tau V_o \delta\omega_\mu = 0$$

$$\tau\delta\dot{V} + \delta V + \frac{\tau\delta\omega}{2\omega} = 0 \qquad (3.3.3)$$

$$\delta\ddot{\omega}_\mu + \frac{2}{\tau_\mu}\delta\dot{\omega}_\mu + \Omega_\mu^2\delta\omega_\mu = -2k_\mu\Omega_\mu^2 V_o \delta V$$

The steady state values are:

$$V_o = V_g \cos\theta_\ell$$

$$\tau(\omega - \omega_c)_o = \tan\theta_\ell = y_\ell \qquad (3.3.4)$$

$$\Delta\omega_{\mu o} = -k_\mu V_o^2$$

The next step is to apply the Laplace transform to this system. A function and its Laplace transform will be represented by the same symbol:

$$\delta V(s)(-\frac{\tau s^2}{2\omega} - \frac{s}{\omega} + y_\ell) = \tau V_o \delta\omega_\mu(s) - \tau V_o \delta\omega(s)$$

$$\delta V(s)(\tau s + 1) = -\frac{\tau s}{2\omega} V_o \delta\omega(s) \qquad (3.3.5)$$

$$\delta\omega_\mu(s)(s^2 + \frac{2}{\tau_\mu} s + \Omega_\mu^2) = -2k_\mu \Omega_\mu^2 V_o \delta V(s)$$

By eliminating $\delta\omega_\mu$ and $\delta\omega$ in the first equation, we obtain the characteristic equation of the system which is as follows:

$$(-\frac{\tau s^2}{2\omega} - \frac{s}{\omega} + y_\ell) + \frac{2\tau k_\mu \Omega_\mu^2 V_o^2}{s^2 + \frac{2}{\tau_\mu} s + \Omega_\mu^2} - \frac{2\omega}{s}(\tau s + 1) = 0 \qquad (3.3.6)$$

The stability of a linear system can, in principle, be determined from its characteristic equation. When this system is represented in block diagram form, the Laplace transform of its output is just the product of the Laplace transform of its input and the transfer function of this system. The denominator of the transfer function is the characteristic equation of the system (D5).

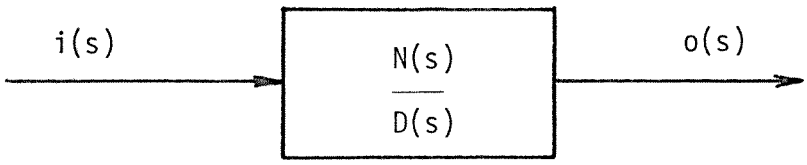

Fig. 3.3

In particular, if the input is a delta function, the Laplace

transform of the output is the transfer function. The system is considered as stable if any bounded input produces a bounded output, which is equivalent to the condition that an impulse input produces an output W(t) which satisfies (J1):

$$\int_{0-}^{\infty} |W(t)|\, dt < \infty \qquad (3.3.7)$$

Therefore, for the system to be stable, the function whose Laplace transform is the transfer function of the system has to satisfy Eq. (3.3.7).

If the transfer function is a rational fraction with poles s_i (the zeros of the characteristic equation), it can be expanded in partial fractions:

$$\frac{N(s)}{D(s)} = \sum_i \frac{K_i}{(s-s_i)} \qquad (3.3.8)$$

from which we obtain directly the time evolution of the output resulting from an impulse input:

$$W(t) = \sum_i K_i\, e^{s_i t} \qquad (3.3.9)$$

Therefore, for a linear system to be stable, all the roots of its characteristic equation have to have negative real parts.

Several methods have been devised to find the sign of the roots of an equation without actually calculating them (D5, O1); some

algebraic (Routh, Hurwitz), some graphical (Nyquist). However, the algebraic criteria become very lengthy when the degree of the characteristic equation is larger than 4, and the graphical methods are not suited to an analysis of a system whose stability has to be determined in function of parameters whose numerical values are not known.

If the roots of the characteristic equation are plotted in the complex plane, for the system to be stable, they all have to be situated in the left-hand side either on the real axis or in conjugate pairs as shown in Fig.(3.4).

When the parameters of the system are varied, the roots will move in the complex plane. When one of the roots moves in the right-hand side, the output of the system will increase exponentially (at least as long as the linear approximation is valid). Two kinds of instability can occur. When the characteristic equation has a positive real root, the output will increase exponentially yielding monotonic instability. When a complex root has a positive real part, the output will be an exponentially increasing sinusoid yielding oscillatory instability. Therefore, when the system starts from a set of parameters where it is stable and a parameter is varied, the boundary of monotonic stability region can be found from:

$$D(s)\Big|_{s=0} = 0 \qquad (3.3.10)$$

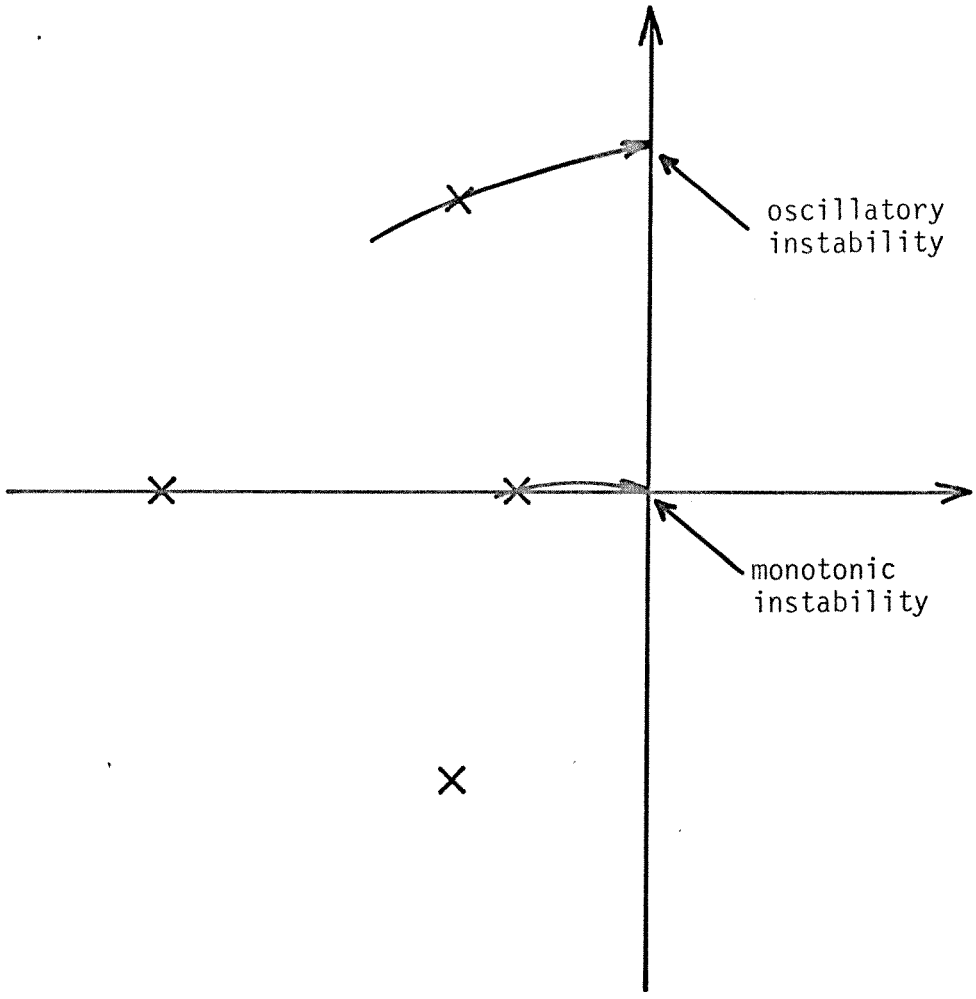

Fig. 3.4. Locus of the roots of the characteristics equation showing the locations of the two kinds of instabilities encountered

If a_o is the constant coefficient in D(s), this is equivalent to:

$$a_o = 0$$

In the case of monotonic stability, not only the boundary of the stability region, but also the region can be defined. A necessary (but not sufficient) condition for the stability of a linear system is that all the coefficients of the characteristic polynomial have to be positive. Thus, the monotonic stability condition can be expressed as:

$$a_o > 0 \qquad (3.3.11)$$

It should be noted that this condition is valid only when the system parameters are continuously varied from a set of stable parameters. For example, there might be isolated regions in the parameter space where this condition is satisfied, but where the system is not stable, i.e. regions where an even number of roots have a positive real part.

The other type of instability that can occur is the oscillatory instability. This will take place when a pair of complex conjugate roots crosses the imaginary axis. The boundary of oscillatory stability can thus be expressed by:

$$D(j\Omega) = 0 \qquad (3.3.12)$$

That is when a root of the characteristic equation is purely imaginary. It should be noted that Ω is an unknown, and that both Ω and the values of the parameters have to be found by equating the real and imaginary parts of $D(j\Omega)$ to 0.

In this case, the stability region cannot be simply extracted from the stability boundary, but can be found by taking the limit of the value of certain parameters (to 0 or ∞) where the stability region can be found by some other method.

In some cases, however, exact solutions cannot be found because of the complicated nature of the characteristic equation, and we will have to settle for approximate stability conditions.

In this particular problem, where we have to find the sign of the roots of equation (3.3.6), we will use Routh's stability criterion (D5). If the characteristic equation is of the form:

$$D(s) = \sum_{i=0}^{n} a_i s^i \qquad (3.3.13)$$

To use Routh's stability criterion, we build the following array:

$$\begin{array}{lllll}
s^n & a_n & a_{n-2} & a_{n-4} & \cdots\cdots\cdots \\
s^{n-1} & a_{n-1} & a_{n-3} & a_{n-5} & \cdots\cdots\cdots \\
s^{n-2} & b_1 & b_2 & b_3 & \cdots\cdots\cdots \\
s^{n-3} & c_1 & c_2 & \cdots\cdots\cdots\cdots & \\
\vdots & & & & \\
s^1 & j_1 & & & \\
s^0 & k_1 & & &
\end{array} \qquad (3.3.14)$$

where

$$b_1 = \frac{a_{n-1}a_{n-2} - a_n a_{n-3}}{a_{n-1}} \qquad b_2 = \frac{a_{n-1}a_{n-4} - a_n a_{n-5}}{a_{n-1}}$$

$$c_1 = \frac{b_1 a_{n-3} - a_{n-1}b_2}{b_1} \qquad c_2 = \frac{b_1 a_{n-5} - a_{n-1}b_3}{b_1}$$

The array is continued until the s^o row.

The number of positive roots of the characteristic equation is equal to the number of change of sign of the elements of the first column (with the assumption that $a_n > 0$).

In our case:

$$\begin{aligned}
a_5 &= \frac{\tau}{2\omega} \\
a_4 &= \frac{1}{\omega}\left(1 + \frac{\tau}{\tau_\mu}\right) \\
a_3 &= \frac{1}{\omega}\left(\frac{\tau\Omega_\mu^2}{2} + \frac{2}{\tau_\mu}\right) + 2\omega\tau - y_\ell \\
a_2 &= \frac{\Omega_\mu^2}{\omega} - \frac{2y_\ell}{\tau_\mu} + 2\omega\left(\frac{2\tau}{\tau_\mu} + 1\right) \\
a_1 &= -y_\ell\Omega_\mu^2 - 2\tau\Omega_\mu^2 k_\mu V_o^2 + 2\omega\left(\frac{2}{\tau_\mu} + \tau\Omega_\mu^2\right) \\
a_0 &= 2\omega\Omega_\mu^2
\end{aligned} \tag{3.3.15}$$

Finding an exact solution would be extremely lengthy, and it

would be so complicated that it would not provide much insight into the stability of the system. However, the different terms in the coefficients a_i have different order of magnitude, and we will keep only the terms which have the highest degree in ω and the ponderomotive term which will be responsible for any instability. We will also use the same approximation in all the elements of the Routh's array.

By looking at a_o, we see immediately that there can be no monotonic instability since (3.3.11) is always satisfied; only oscillatory instability can occur. To obtain the oscillatory stability condition, we build the following array:

$$
\begin{array}{lll}
s^5 & \frac{\tau}{2\omega} & 2\omega\tau \qquad\qquad 2(-\tau\Omega_\mu^2 k_\mu V_o^2+\omega(\frac{2}{\tau_\mu}+\tau\Omega_\mu^2)) \\
s^4 & \frac{1}{\omega}(1+\frac{\tau}{\tau_\mu}) & 2\omega(\frac{2\tau}{\tau_\mu}+1) \qquad\qquad 2\omega\Omega_\mu^2 \\
s^3 & \tau & 2(1+\frac{\tau}{\tau_\mu})(\frac{2}{\tau_\mu}+\tau\Omega_\mu^2-\tau\frac{\Omega_\mu^2}{\omega}k_\mu V_o^2)-\tau\Omega_\mu^2 \\
s^2 & 2\omega\tau(\frac{2\tau}{\tau_\mu}+1) & 2\omega\tau\Omega_\mu^2 \\
s^1 & -(\frac{2\tau}{\tau_\mu}+1)\tau\frac{\Omega_\mu^2}{\omega}k_\mu V_o^2+\frac{2}{\tau_\mu}(\tau^2\Omega_\mu^2+\frac{2\tau}{\tau_\mu}+1) & \qquad (3.3.16) \\
s^0 & 2\omega\tau\Omega_\mu^2 &
\end{array}
$$

All the elements of certain rows have been multiplied by positive constants to simplify these expressions without any consequence on the stability condition.

We see that the system will be stable if the element in the s^1 row is positive. This yields the oscillatory stability condition:

$$k_\mu V_o^2 < \frac{2}{\tau_\mu}\omega\tau\left[\frac{1}{1+\frac{2\tau}{\tau_\mu}}+\frac{1}{\tau^2\Omega_\mu^2}\right] \tag{3.3.17}$$

When the equality is satisfied (boundary of the stability region), we can obtain the frequency of the oscillations from the row s^2 by solving the following equation (D5):

$$2\omega\tau\left(\frac{2\tau}{\tau_\mu}+1\right)s^2 + 2\omega\tau\Omega_\mu^2 = 0 \tag{3.3.18}$$

Therefore, the instability oscillation has the frequency:

$$\Omega_c = \frac{\Omega_\mu}{\sqrt{1+\frac{2\tau}{\tau_\mu}}} \tag{3.3.19}$$

We see that the oscillation frequency is very close to the mechanical frequency.

We will now examine the stability condition. For all the resonators proposed for heavy-ion acceleration, the mechanical bandwidth is always much smaller than the electrical bandwidth ($\frac{\tau}{\tau_\mu} \ll 1$), and the term in the bracket is always larger than 1.

A self-excited loop will then present ponderomotive instability when the static radiation pressure frequency shift (in absolute value) is larger than the product of the mechanical bandwidth and the electrical Q of the resonator.

This stability condition can also be expressed as:

$$k_\mu V_o^2 < 2\Omega_\mu \frac{Q}{Q_\mu}\left[\frac{1}{1+\frac{2\tau}{\tau_\mu}} + \frac{1}{\tau^2\Omega_\mu^2}\right] \qquad (3.3.20)$$

where $Q = \frac{\omega\tau}{2}$: electrical quality factor

$Q_\mu = \frac{\Omega_\mu \tau_\mu}{2}$: mechanical quality factor

In this form, we see that instability will occur when the radiation pressure frequency shift is larger than twice the product of the mechanical frequency and the ratio of the electrical and mechanical Q's.

For all practical accelerating structures, this would occur at fields much larger than operating fields.

As an example, for a 150 MHz split-loop resonator:

$$Q \sim 5.10^7$$

$$Q_\mu \sim 3.10^3$$

$$\Omega_\mu \sim 3.10^2 \text{ rad/sec}$$

This would give:

$$k_\mu V_o^2 < 10^7 \text{ rad/sec}$$

At typical operating fields:

$$k_\mu V_o^2 \sim 3.10^3 \text{ rad/sec}$$

Therefore, this kind of structure can be considered as being unconditionally stable under ponderomotive coupling when operated in a self-excited loop.

Another perspective which might give more insight into the stability of such a system is to represent it in the block diagram form shown in Fig. 3.5 which was obtained from equation (3.3.5). In this form, it can easily be seen that since the numerator of the forward transfer function does not have a constant term, no monotonic instability (s = 0) can occur. Also, because of the very narrow bandwidth of the feedback transfer function, if oscillatory instability is to occur, the frequency of this instability will be close to Ω_μ.

Presented in this form, stability of the system can be determined using Nyquist analysis (D5). The Nyquist criterion can be simply stated as follows: At the frequency at which the imaginary part of the open loop transfer function is equal to 0, its real part has to be larger than -1. The open loop transfer function is the product

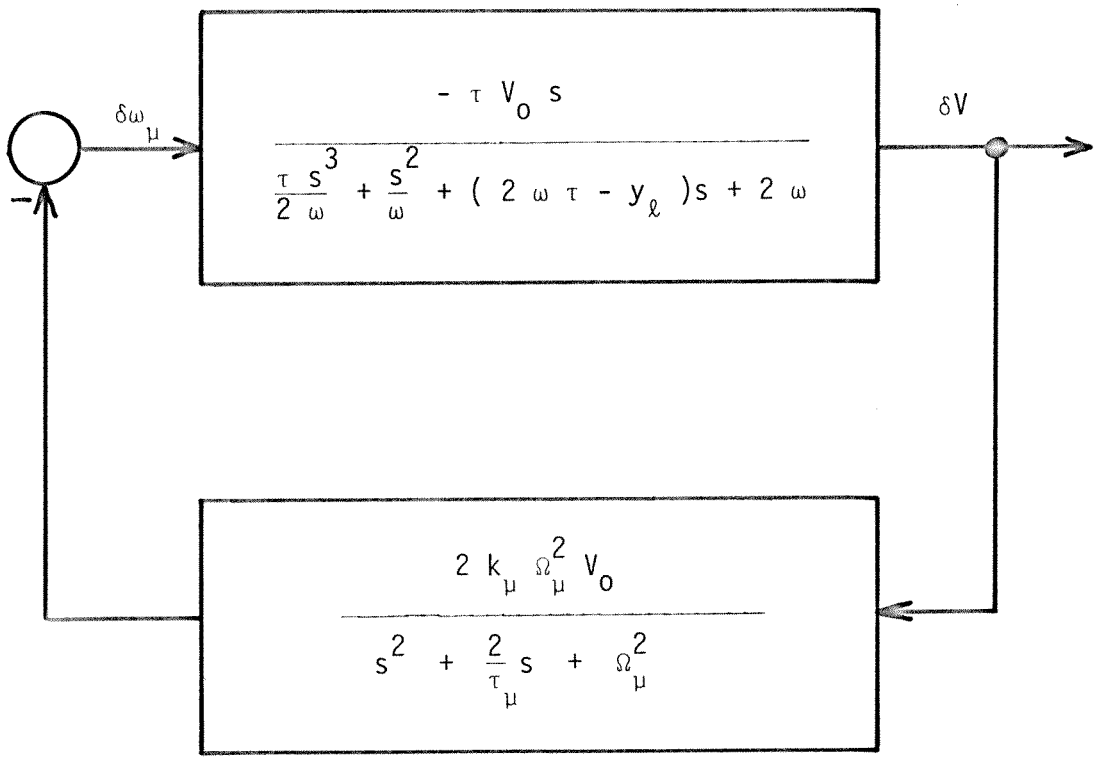

Fig. 3.5. Transfer functions block diagram of a resonator operating in a self-excited loop in presence of electromechanical coupling

of the forward and feedback transfer function.

By using this criterion, we obtain the following stability condition:

$$k_\mu V_o^2 < \frac{2}{\tau_\mu} \omega\tau \left(1 + \frac{1}{\tau^2 \Omega_\mu^2} \right) \qquad (3.3.21)$$

which, except for the term $\frac{\tau}{\tau_\mu}$ which is always much smaller than 1, is identical to the stability condition obtained previously. To obtain this condition, the following terms were neglected: $\frac{\tau s^3}{2\omega}$, $\frac{s^2}{\omega}$, $-y_\ell s$, and we assumed that the oscillation frequency was the mechanical frequency Ω_μ.

It can be noted that the term in the differential equations (3.3.1) responsible for the coupling which can lead to ponderomotive instabilities is $\frac{\tau\omega\dot{V}}{2\omega}$. The smallness of this term explains the stability of a self-excited loop.

The best way to get some physical insight into the absence of monotonic instability when the resonator is operated in a self-excited loop is to compare the steady state solutions of the generator-driven and self-excited cases.

When the resonator is driven by a fixed frequency generator, the steady-state solutions are (S4):

$$V_o = V_g \cos \theta_c$$

$$\tau (\omega - \omega_o) = -\tan \theta_c - \tau k_\mu V_o^2 \qquad (3.3.22)$$

When the resonator is operated in a self-excited loop, the steady-state solutions are obtained from (3.3.4):

$$V_o = V_g \cos \theta_\ell$$

$$\tau (\omega - \omega_o) = \tan \theta_\ell - \tau k_\mu V_o^2 \qquad (3.3.23)$$

If one recalls that θ_c and θ_ℓ are related by:

$$\theta_c + \theta_\ell = 0 \qquad (3.3.24)$$

we see that the two sets of relationships (3.3.22) and (3.3.23) are absolutely identical.

However, as was mentioned earlier, the main difference between a resonator driven by a generator and a resonator operating in a self-excited loop is in the nature of the input and output variables.

If one represents the output variables (V_o and θ_c) as a function of the input variables (V_g and ω) when the resonator is driven by a generator, one obtains Fig. (3.6).

And if the output variables (V_o and ω) are represented as functions of the input variables (V_g and θ_ℓ) when the resonator

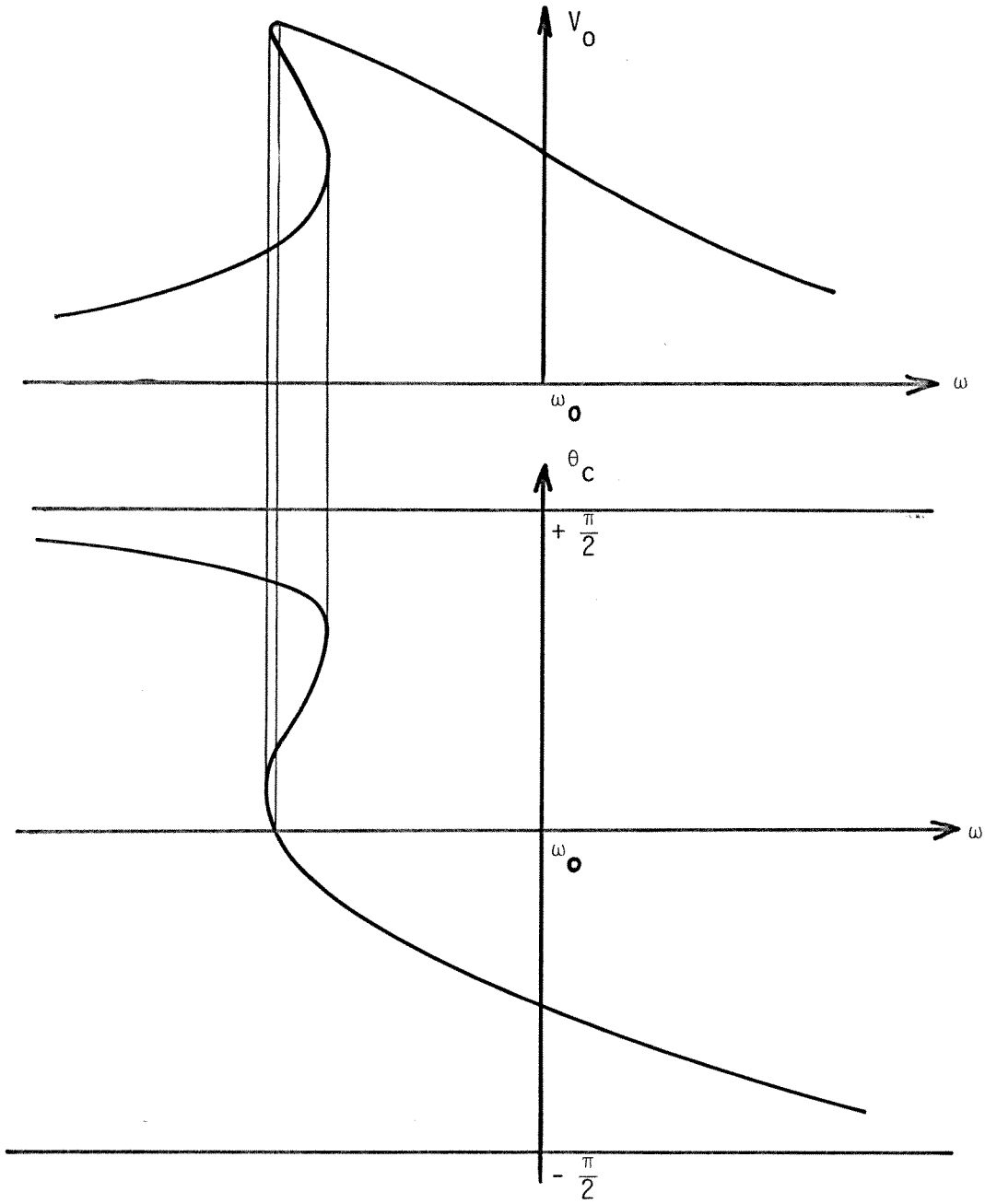

Fig. 3.6. Relationships between input and output variables of a generator-driven resonator in presence of electromechanical coupling

operates in a self-excited loop, one obtains Fig. 3.7.

Thus, we see that when the resonator is driven by a generator, under certain conditions ($\omega < \omega_o$, V_g sufficiently high), the output variables can become multivalued functions of the input variables, yielding monotonic instability. Whereas, when the resonator is operated in a self-excited loop, the output variables always are single-valued functions of the input variables which is equivalent to monotonic stability.

For instabilities to occur, there must be some coupling from amplitude modulation to eigenfrequency variation and back from eigenfrequency to amplitude. The coupling from amplitude to eigenfrequency is provided by the radiation pressure; and, in the case of generator-driven resonators, the coupling from eigenfrequency to amplitude is provided by the detuning between generator and resonator. When the resonator is operated in a self-excited loop, however, as was shown in Chapter II, the loop oscillation frequency tracks the resonator eigenfrequency so the amplitude is undisturbed, and the coupling from eigenfrequency to amplitude is very small. The only coupling existing comes from the inertia of the loop frequency in tracking the resonator eigenfrequency; however, this coupling is of the order of $\frac{\tau\Omega}{\omega}\mu$ and very small so it can lead to oscillatory instability only when the resonator is operated at a field level where the radiation pressure frequency shift is very high. Such a field is, in general, much higher than the operating field.

3.4 Ponderomotive stability of a non-ideal self-excited loop

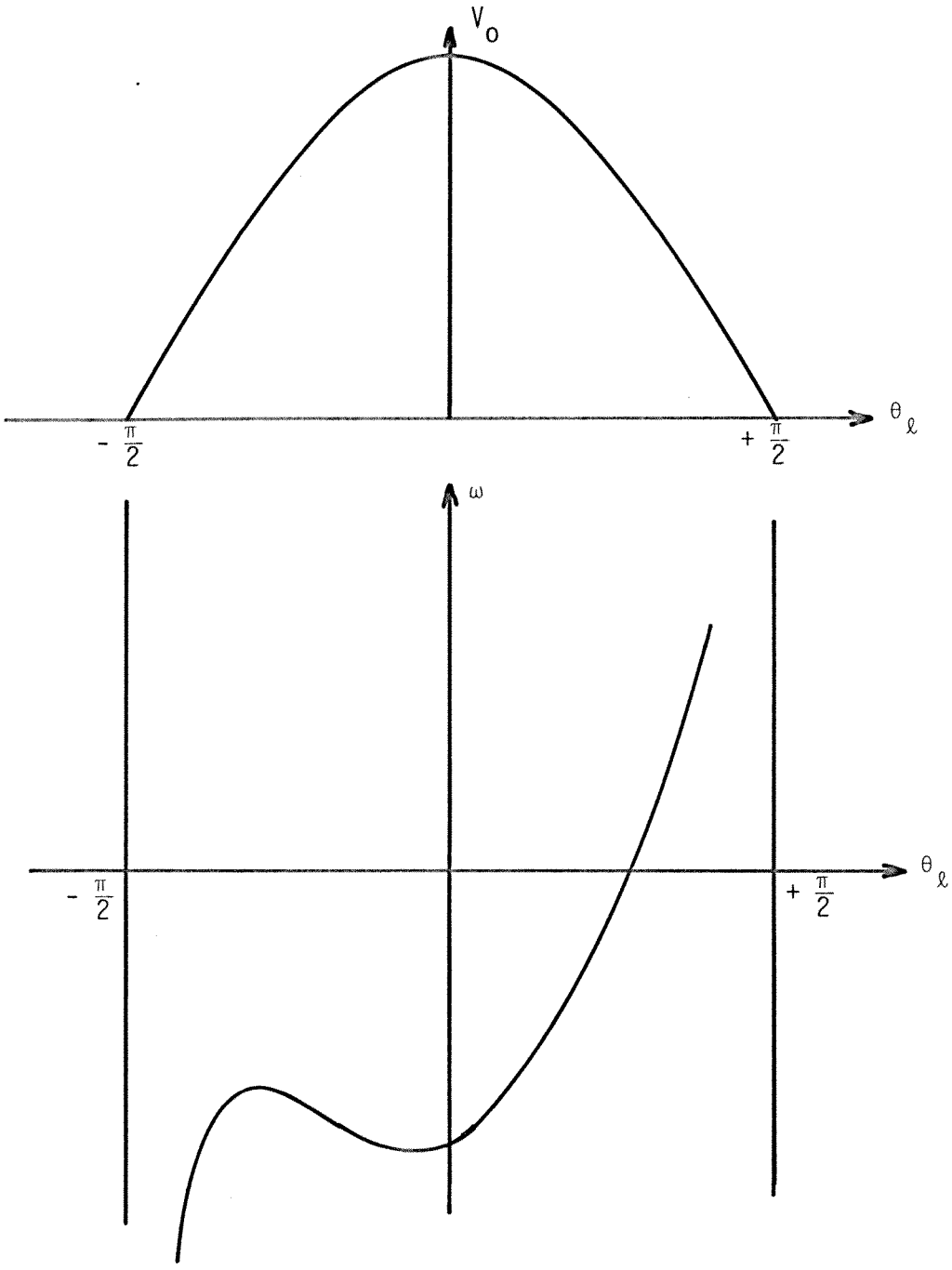

Fig. 3.7. Relationships between input and output variables of a resonator operating in a self-excited loop in presence of electromechanical coupling

In the previous section, we saw that when a resonator was operated in an ideal self-excited loop, it did not present ponderomotive instabilities. By ideal, we mean that the loop phase shift and the limiter output were constant. In practice, however, some non-ideal effects might be present and can originate in many places: detectors, phase shifter, limiter, power amplifier, etc. However, whatever their origin, the most important non-ideal effects, as far as stability is concerned, can be classified under:

- frequency dependent generator amplitude
- frequency dependent phase shift

In this section, we will study the stability of a self-excited loop in presence of ponderomotive coupling and of these non-ideal effects. This will allow us to put bounds on the allowable amount of non-ideal effects in order to preserve ponderomotive stability of the self-excited loop.

The ponderomotive instabilities which might be created by these non-ideal effects could, of course, be removed by the feedbacks which are required to lock the phase and amplitude of the fields in the resonator to external references, and will be discussed later. However, one great advantage of a self-excited loop is that even when no phase and amplitude feedbacks are present, the loop is still oscillating, and the amplitude is stable. It is important to keep this property.

3.4.1 Frequency dependent generator amplitude

We will use the same set of differential equations as before, with the exception that the terms in $\frac{1}{\omega}$ will be neglected since it was seen earlier that they do not create any instability in the field range of interest:

$$\tau V (\omega - \omega_c) = V_g \sin \theta_\ell$$

$$\tau \dot{V} + V = V_g \cos \theta_\ell \qquad (3.4.1.1)$$

$$\ddot{\Delta\omega}_\mu + \frac{2}{\tau_\mu} \dot{\Delta\omega}_\mu + \Omega_\mu^2 \Delta\omega_\mu = -k_\mu \Omega_\mu^2 V^2$$

However, in this case the generator amplitude V_g is a function of the loop oscillation frequency ω . It will be assumed to be of the form:

$$V_g = V_{go} \left[1 + \gamma_a \tau (\omega - \omega_{co}) \right] \qquad (3.4.1.2)$$

The frequency-amplitude coupling constant γ_a , thus defined, is the fractional change of the generator amplitude when the loop oscillation frequency varies by one-half an electrical bandwidth.

As before, the system is first linearized, then the Laplace transform is applied to it, and by elimination of $\delta\omega$ and $\delta\omega_\mu$, we obtain the following characteristic equation:

$$\sum_{i=0}^{3} a_i s^i = 0 \qquad (3.4.1.3)$$

where:

$$\begin{aligned} a_3 &= \tau (1 - \gamma_a y_\ell) \\ a_2 &= 1 + \frac{2\tau}{\tau_\mu} (1 - \gamma_a y_\ell) \\ a_1 &= \frac{2}{\tau_\mu} + \Omega_\mu^2 (1 - \gamma_a y_\ell) \\ a_0 &= \Omega_\mu^2 (1 + 2 \tau \gamma_a k_\mu V_o^2) \end{aligned} \qquad (3.4.1.4)$$

To determine the stability of this system, we will use Routh's criterion. When using this criterion, we always make the implicit assumption that:

$$a_n > 0 \qquad (3.4.1.5)$$

In our case, this would require:

$$\gamma_a y_\ell < 1 \qquad (3.4.1.6)$$

This condition is always satisfied since, in practice, γ_a is always a very small number; much smaller than 1. Also, it is very

inefficient to operate a resonator far away from resonance, and in practical operation y_ℓ is always confined in the range $[-1, +1]$, so that the above condition is satisfied.

From a_o and inequality (3.3.11), we obtain directly the monotonic stability condition as follows:

$$-\gamma_a k_\mu V_o^2 < \frac{1}{2\tau} \qquad (3.4.1.7)$$

After building the Routh's array, we obtain the following oscillatory stability condition:

$$\frac{1}{\tau_\mu} + \frac{\tau^2\Omega_\mu^2}{\tau_\mu}(1-\gamma_a y_\ell)^2 + \frac{2\tau}{\tau_\mu}(1-\gamma_a y_\ell) - (1-\gamma_a y_\ell)\gamma_a \tau^2 \Omega_\mu^2 k_\mu V_o^2 > 0 \qquad (3.4.1.8)$$

As was mentioned earlier, the following condition is often satisfied in practice:

$$| \gamma_a y_\ell | << 1 \qquad (3.4.1.9)$$

Under this condition, we obtain the simplified oscillatory stability condition:

$$\gamma_a k_\mu V_o^2 < \frac{1}{\tau_\mu}\left[\frac{1 + \frac{2\tau}{\tau_\mu}}{\tau^2\Omega_\mu^2} + 1\right] \qquad (3.4.1.10)$$

Thus, as expected, we find that there is a range for γ_a around

0 where ponderomotive stability is preserved. If γ_a is positive and sufficiently large, oscillatory instability will occur; and if γ_a is negative and sufficiently large in absolute value, monotonic instability will occur. This is shown in Fig. (3.8).

3.4.2 Frequency dependent phase shifter

The other main non-ideal effect which might lead to ponderomotive instability is a frequency dependent phase shifter. By this, we do not mean that this effect actually takes place in the phase shifter, but instead that the loop phase shift is frequency dependent. For example, a narrow band power amplifier can introduce a frequency dependent phase shift. It will probably also have a frequency dependent gain which is equivalent to a frequency dependent generator amplitude studied in the previous section.

We will again use the same set of differential equations with the exception that now:

$$\theta_\ell = \theta_{\ell o} + \gamma_\theta \tau(\omega - \omega_{co}) \qquad (3.4.2.1)$$

The frequency-phase shift coupling constant γ_θ is defined as the additional phase shift introduced when the loop oscillation frequency varies by half an electrical bandwidth.

After linearizing and applying the Laplace transform, we obtain the following characteristic equation:

$$\sum_{i=0}^{3} a_i s^i = 0 \qquad (3.4.2.2)$$

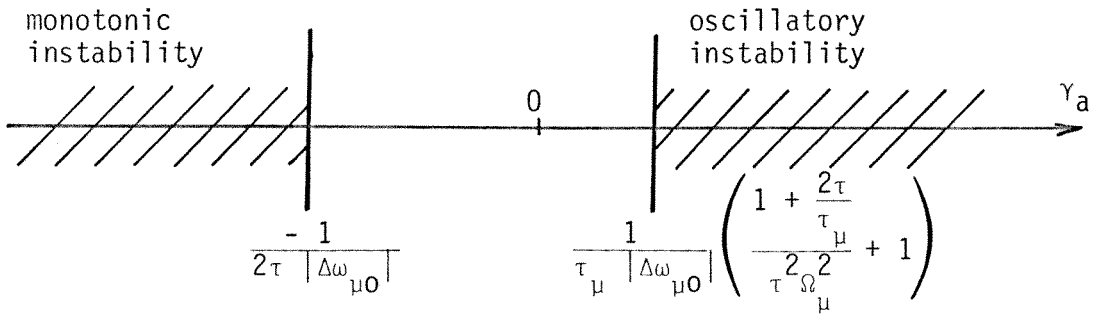

Fig. 3.8. Stability region of a resonator operating in a self-excited loop in presence of electromechanical coupling and a frequency dependent limiter output

where:

$$a_3 = \tau \left(1 - \gamma_\theta \right)$$

$$a_2 = 1 + \frac{2\tau}{\tau_\mu} \left(1 - \gamma_\theta \right) - \gamma_\theta \left(1 + y_\ell^2 \right) \qquad (3.4.2.3)$$

$$a_1 = \frac{2}{\tau_\mu} \left[1 - \gamma_\theta \left(1 + y_\ell^2 \right) \right] + \Omega_\mu^2 \left(1 - \gamma_\theta \right)$$

$$a_0 = \Omega_\mu^2 \left[1 - \gamma_\theta \left(1 + y_\ell^2 \right) - 2\gamma_\theta \tau \, y_\ell \, k_\mu \, V_o^2 \right]$$

Since in all practical applications:

$$| \gamma_\theta | << 1 \qquad (3.4.2.4)$$

we have:

$$a_3 > 0 \qquad (3.4.2.5)$$

and we can use Routh's criterion.

From a_0 and inequality (3.3.11), we directly obtain the monotonic stability condition:

$$\gamma_\theta(1 + y_\ell^2 + 2y_\ell\tau|\Delta\omega_{\mu o}|) \quad < \quad 1 \qquad (3.4.2.6)$$

This monotonic stability condition is more easily visualized in the figures (3.9 a, b, c, d). In those figures, the hatched regions are the regions of monotonic instability. It should be remembered, however, that to obtain them we made the assumption:

$$\left| \gamma_\theta \right| << 1 \qquad (3.4.2.7)$$

Following the same procedure, we build the Routh's array to obtain the following oscillatory stability condition:

$$\frac{2\tau}{\tau_\mu^2}(1 - \gamma_\theta)(1 - \gamma_\theta(1 + y_\ell^2)) + \frac{\tau^2\Omega_\mu^2}{\tau_\mu}(1 - \gamma_\theta)^2$$
$$+ \frac{1}{\tau_\mu}(1 - \gamma_\theta(1 + y_\ell^2)) + \tau^2\Omega_\mu^2(1 - \gamma_\theta)y_\ell\gamma_\theta k_\mu V_o^2 \quad > \quad 0 \qquad (3.4.2.8)$$

In this form it is not very useful; however, in the practical limit:

$$|\gamma_\theta|(1 + y_\ell) \quad << \quad 1 \qquad (3.4.2.9)$$

We obtain the simplified oscillatory stability condition:

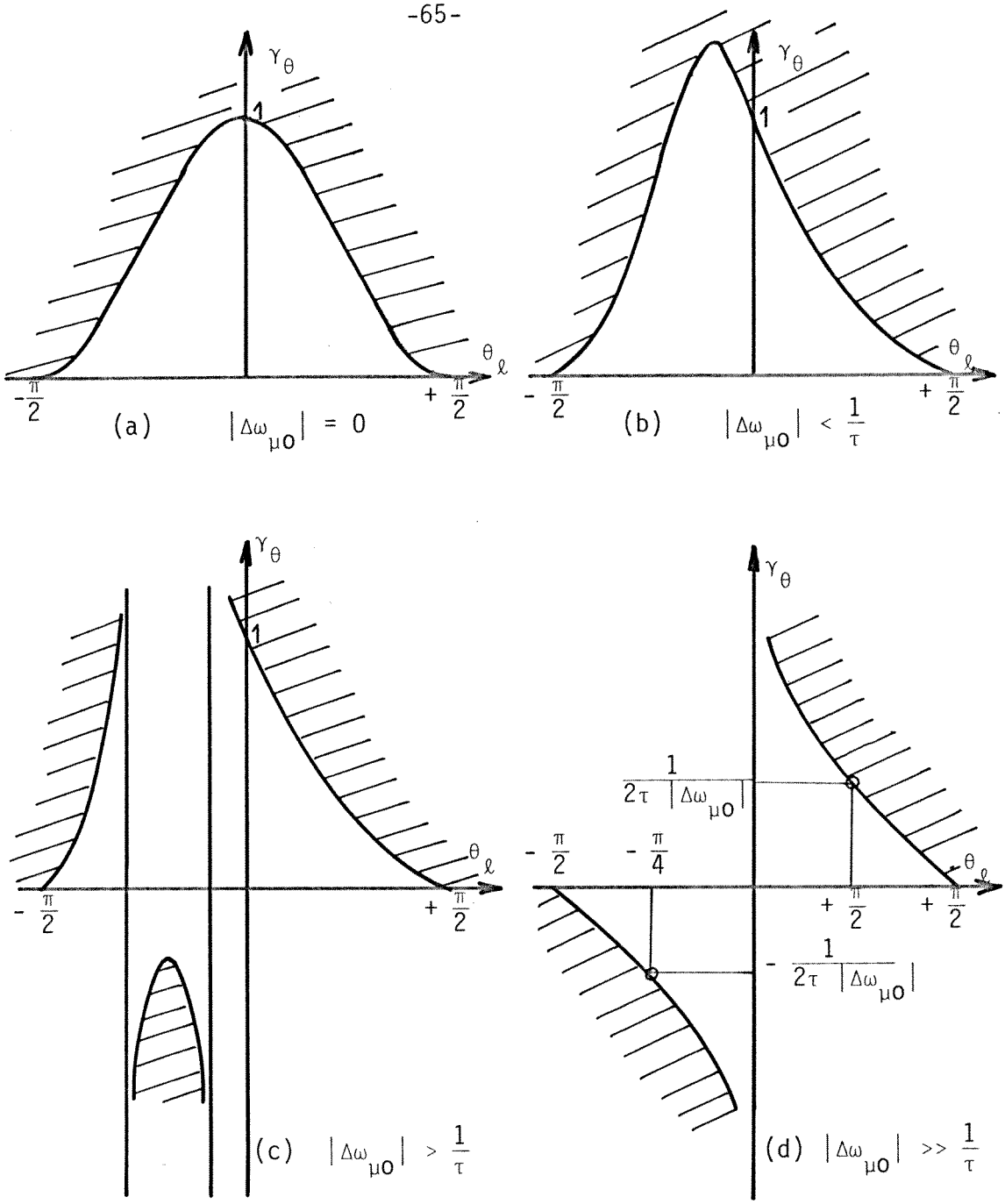

Fig. 3.9. Regions of monotonic stability of a resonator operating in a self-excited loop in presence of electromechanical coupling and a frequency-dependent phase shifter for different values of the static radiation pressure frequency shift

$$y_\ell \gamma_\theta > - \frac{1}{\tau_\mu |\Delta\omega_{\mu o}|} \left[\frac{1 + \frac{2\tau}{\tau_\mu}}{\tau^2 \Omega_\mu^2} + 1 \right] \qquad (3.4.2.10)$$

This condition is graphically represented in Fig. (3.10).

3.5 Ponderomotive stability of a resonator operating in a self-excited loop in presence of phase and amplitude feedback

In the previous sections, we saw that a resonator operating in a self-excited loop did not present ponderomotive instabilities if the non-ideal effects were limited, and that the field amplitude was stable. However, for this resonator to be useful as an accelerating structure, the phase and amplitude of the electromagnetic field have to be locked to an external phase and amplitude reference. In this section, we will study feedbacks which are required to provide phase and amplitude locking. As a consequence of phase feedback, the resonator will appear, in some respects, as being driven by a fixed frequency generator, and ponderomtoive instabilities are likely to appear. We will then have to study the influence of the feedback parameters on the stability of the system, and find what range of value they must have in order to provide enough phase and amplitude locking while preserving stability.

3.5.1 Equations and block diagram

When the self-excited loop is locked to an external phase (or frequency) reference, there are three frequencies of interest:

ω_c : eigenfrequency of the resonator

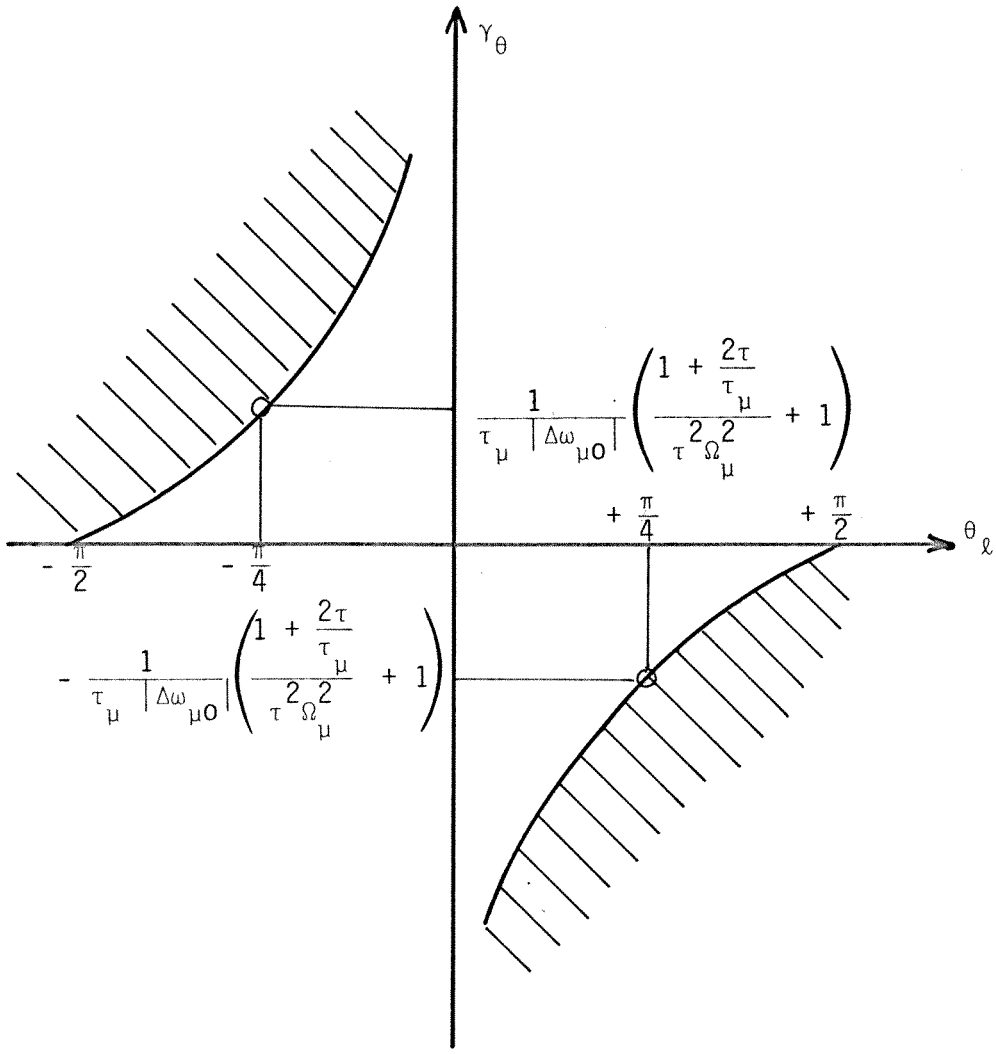

Fig. 3.10. Region of oscillatory stability of a resonator operating in a self-excited loop in presence of electromechanical coupling and a frequency-dependent phase shifter

ω_ℓ : oscillation frequency of the unlocked self-excited loop (no feedback)

ω_r : reference frequency (frequency at which the loop is to be locked

We define the following dimensionless parameters:

$$y_\ell = (\omega_{\ell o} - \omega_{co}) = \tan \theta_\ell \quad \text{where } \theta_\ell \text{ is the loop phase shift} \qquad (3.5.1.1)$$

$$y_r = (\omega_r - \omega_{co})$$

We recall that subscript $_o$ denotes a steady-state value, while δ represents a deviation around this steady-state.

The set of differential equations (3.3.1) and (3.3.2) will be used to describe the electromechanical system. Once again, the following terms $\frac{\tau \ddot{V}}{2\omega}$, $\frac{\dot{V}}{\omega}$ and $\frac{\tau \dot{\omega}}{2\omega} V$ will be neglected since they are much smaller than the others; and, as was seen earlier, do not contribute to the stability of the system.

In order to provide amplitude and phase locking, we have access to two input variables:

- generator amplitude (limiter output)
- loop phase shift

We can control these two input variables either individually, or control some combination of them. Amplitude feedback is more simply provided by modulating the generator amplitude (limiter output). In order to provide phase feedback, however, instead of controlling simply the loop phase shift, it is more advantageous to control a signal added in quadrature to the driving signal. This is equivalent to a simultaneous control of loop phase shift and generator amplitude which reduces the coupling between phase and amplitude feedback, as was shown in Chapter II.

The signal driving the resonator is then:

$$V_g = V_{go}(1 + \delta v_g)\, e^{i\theta_\ell}\, (1 + i(t_o + \delta t)) \qquad (3.5.1.2)$$

In the above expression, δv_g is responsible for the amplitude feedback, t_o provides the steady-state phase feedback, and δt provides additional phase feedback required by the presence of disturbances. The steady-state amplitude feedback was included in V_{go} so that δv_g also provides only the additional feedback required by the presence of disturbances.

The behavior of the electrical part of the system is then represented by the following set of differential equations:

$$\begin{aligned} \tau\dot{V} + V &= V_{go}(1 + \delta v_g)(\cos\theta_\ell - \sin\theta_\ell(t_o + \delta t)) \\ \tau V(\omega - \omega_c) &= V_{go}(1 + \delta v_g)(\sin\theta_\ell + \cos\theta_\ell(t_o + \delta t)) \end{aligned} \qquad (3.5.1.3)$$

To which we add the following equation describing the mechanical part of the system:

$$\ddot{\Delta\omega}_\mu + \frac{2}{\tau_\mu}\dot{\Delta\omega}_\mu + \Omega_\mu^2 \Delta\omega_\mu = -k_\mu \Omega_\mu^2 V^2 \qquad (3.5.1.4)$$

The steady-state solutions are:

$$V_o = \frac{V_{go}}{\cos\theta_\ell (1 + y_\ell y_r)}$$

$$t_o = \frac{y_r - y_\ell}{1 + y_\ell y_r} \qquad (3.5.1.5)$$

$$\Delta\omega_{\mu o} = -k_\mu V_o^2$$

We see that for the loop to be operating, the following condition must be satisfied:

$$1 + y_\ell y_r > 0 \qquad (3.5.1.6)$$

Inequality (3.5.1.6) means that the loop will be operating if the phase shift which has to be introduced in order to lock the loop oscillations to the frequency ω_r is in the range $\left] -\frac{\pi}{2} , +\frac{\pi}{2} \right[$. This is a direct consequence of the fact that we introduce the phase shift

by adding a signal in quadrature. The steady-state solutions are more easily presented in Fig. (3.11).

If the set of differential equations (3.5.1.3) is linearized around the steady-state values, we obtain:

$$\tau\delta\dot{v} + \delta v = \delta v_g - \sin\theta_\ell \cos\theta_\ell(1 + y_\ell y_r)\delta t$$

$$y_r\delta v + \tau\delta(\omega - \omega_c) = y_r\delta v_g + \cos^2\theta_\ell(1 + y_\ell y_r)\delta t \qquad (3.5.1.7)$$

$$\ddot{\delta\omega}_\mu + \frac{2}{\tau_\mu}\dot{\delta\omega}_\mu + \Omega_\mu^2\delta\omega_\mu = -2\Omega_\mu^2 k_\mu V_o^2\delta v$$

where we used:

$$V = V_o\ (\ 1 + \delta v\ ) \qquad (3.5.1.8)$$

It should be pointed out that when the loop was unlocked, we had:

$$\tau\ (\ \omega - \omega_c\ )_o = y_\ell \qquad (3.5.1.9)$$

Whereas in this case, when the loop is locked, we have:

$$\tau\ (\ \omega - \omega_c\ )_o = y_r \qquad (3.5.1.10)$$

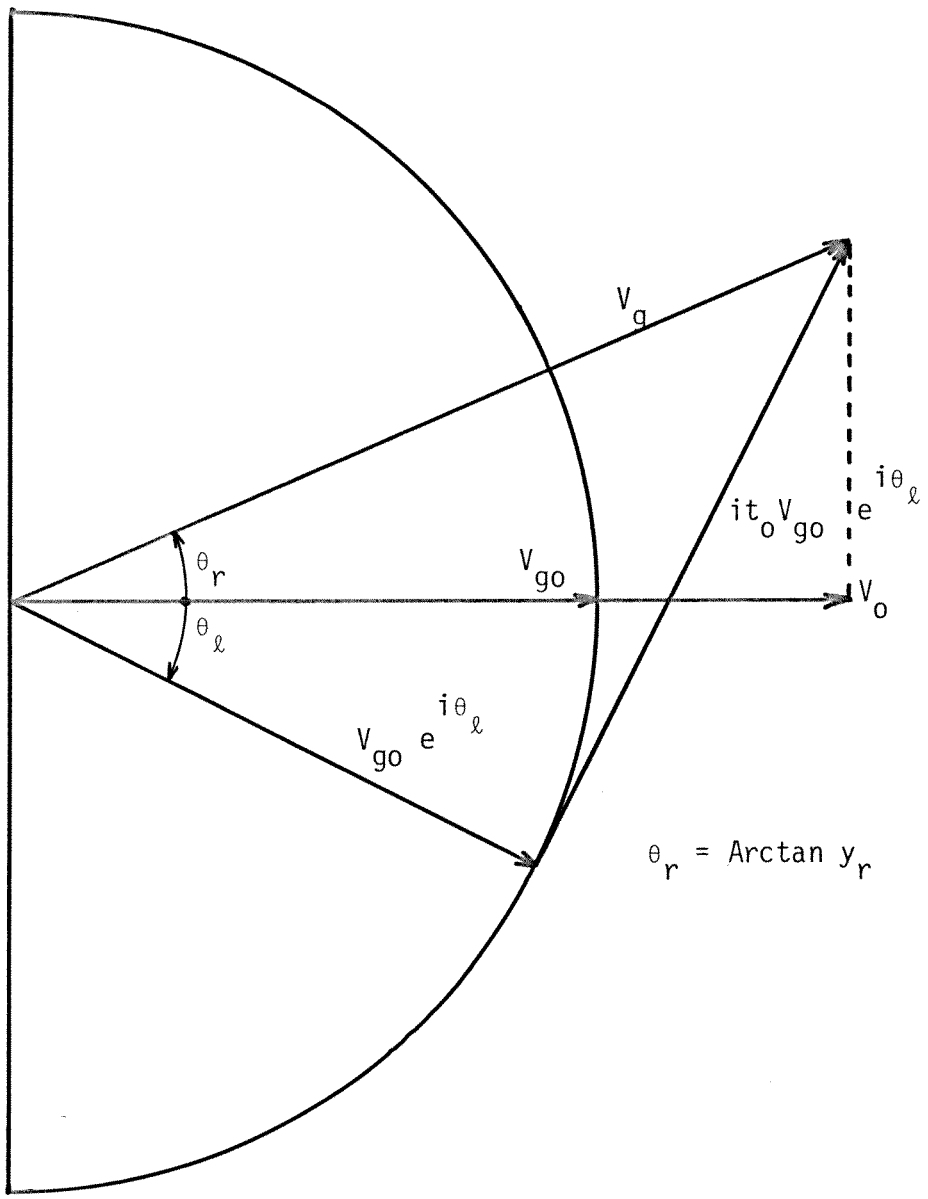

Fig. 3.11. Graphical representation of the steady-state solutions of the system (3.5.1.3)

We next apply the Laplace transform to the above system to get:

$$\delta v(s) = G_{aa}\delta v_g(s) + G_{ta}\delta t(s)$$

$$\delta(\omega - \omega_c)(s) = G_{a\omega}\delta v_g(s) + G_{t\omega}\delta t(s) \qquad (3.5.1.11)$$

$$\delta\omega_\mu(s) = G_\mu \delta v(s)$$

where we have defined the transfer functions:

$$G_{aa} = \frac{1}{\tau s + 1}$$

$$G_{ta} = \frac{-y_\ell(1 + y_\ell y_r)}{(1 + y_\ell^2)(\tau s + 1)}$$

$$G_{a\omega} = \frac{y_r s}{\tau s + 1} \qquad (3.5.1.12)$$

$$G_{t\omega} = \frac{1 + y_\ell y_r}{\tau(1 + y_\ell^2)} \quad \frac{\tau s + 1 + y_\ell y_r}{\tau s + 1}$$

$$G_\mu = \frac{-2\Omega_\mu^2 k_\mu V_o^2}{s^2 + \frac{2}{\tau_\mu} s + \Omega_\mu^2}$$

Until now, we assumed that the variation of the resonator eigenfrequency was due only to ponderomotive effects. However, there is another source of frequency variation which is responsible for the necessity of the feedback. It is the excitation of the mechanical modes of the resonator by noise and ambiant vibrations. Thus we have:

$$\delta\omega_c = \delta\omega_\mu + \delta\omega_{ex} \qquad (3.5.1.13)$$

$\delta\omega_\mu$: ponderomotive effects

$\delta\omega_{ex}$: external vibrations

The system of equations (3.5.1.11) can be best presented in the block diagram form shown in Fig. (3.12). In this block diagram, F_a and F_ϕ are respectively the amplitude and phase feedback transfer function. This block diagram can be simplified to the form shown in Fig. (3.13), where we used:

$$G_a = \frac{-F_\phi G_{ta}}{(s + F_\phi G_{t\omega})(1 + F_a G_{aa}) - F_\phi G_{ta}(G_{a\omega} F_a - G_\mu)}$$

$$G_\phi = \frac{1 + F_a G_{aa}}{(s + F_\phi G_{t\omega})(1 + F_a G_{aa}) - F_\phi G_{ta}(G_{a\omega} F_a - G_\mu)} \qquad (3.5.1.14)$$

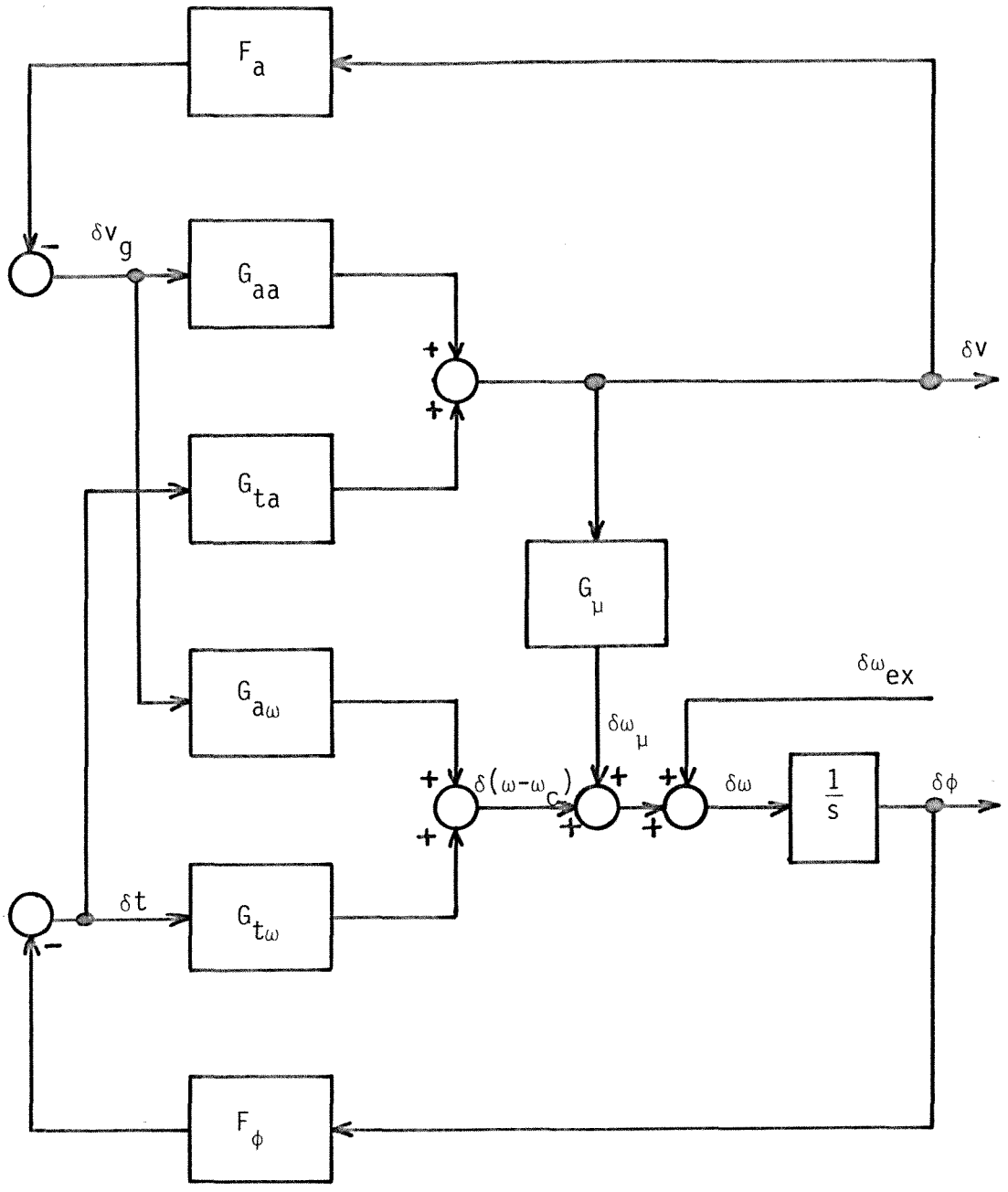

Fig. 3.12. General transfer functions block diagram of a resonator operating in a self-excited loop in presence of electromechanical coupling and phase and amplitude feedback

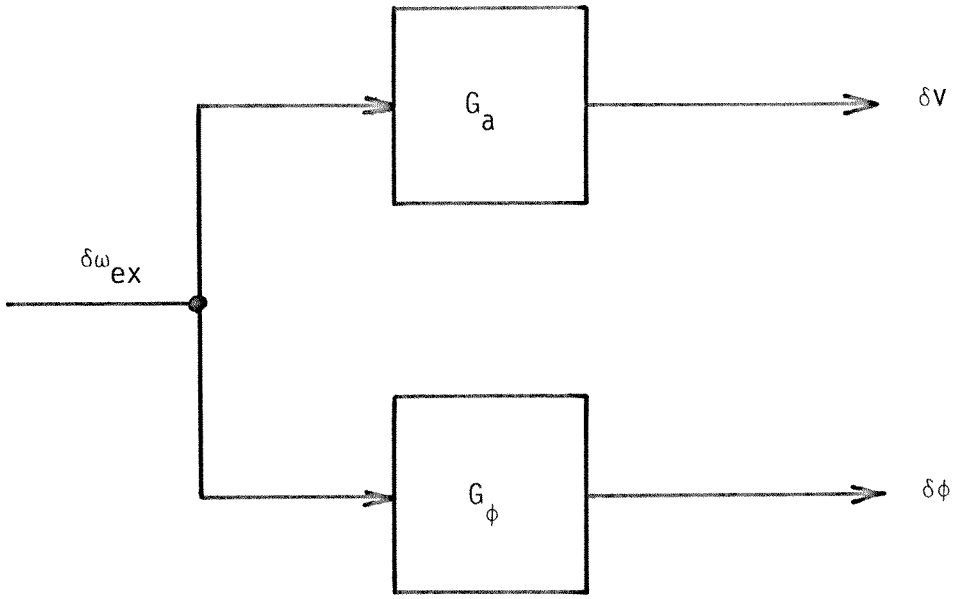

$$G_a = \frac{-F_\phi G_{ta}}{(s + F_\phi G_{t\omega})(1 + F_a G_{aa}) - F_\phi G_{ta}(G_{a\omega} F_a - G_\mu)}$$

$$G_\phi = \frac{1 + F_a G_{aa}}{(s + F_\phi G_{t\omega})(1 + F_a G_{aa}) - F_\phi G_{ta}(G_{a\omega} F_a - G_\mu)}$$

Fig. 3.13. Simplified representation of the block diagram of Fig. 3.12

Performance and stability of the feedback system can be found from the above transfer functions. In particular, stability can be determined from the common denominator of G_a and G_ϕ which is the characteristic equation of the system. As before, stability will be assured if all the roots of this common denominator have negative real parts.

Before proceeding further, however, we have to make some assumption about the form of the feedback transfer functions F_a and F_ϕ. Because of the already complicated nature of the system, it would be to our advantage to use transfer functions which, although realistic, are simple enough so the analysis can be pushed exactly as far as possible. The insight and experience gained this way can be used to analyze the system when more complicated transfer functions are used, and an exact analysis is impossible. Thus, we will assume that the amplitude feedback is proportional to the amplitude error, and that the phase feedback is proportional to the phase error. That is:

$$F_a = k_a \qquad k_a > 0$$

$$F_\phi = k_\phi \qquad k_\phi > 0 \tag{3.5.1.15}$$

We will define $H (k_a, k_\phi, k_\mu)$ as the common denominator of G_a and G_ϕ.

$$H(k_a,k_\phi,k_\mu) = (s + F_\phi G_{t\omega})(1 + F_a G_{aa}) - F_\phi G_{ta}(G_{a\omega} F_a - G_\mu)$$

(3.5.1.16)

Before studying the influence of ponderomotive effects on the stability of the system, we have to make sure that the presence of the phase and amplitude feedback does not introduce instabilities independently of the ponderomotive effects. This can be simply done by finding the sign of the roots of $H (k_a, k_\phi, 0) = 0$. After replacing the various transfer functions with their expressions found earlier, and after some manipulation, we obtain:

$$H(k_a,k_\phi,0) = \frac{\tau s^2 + \tau s\left[1 + k_a + \frac{k_\phi(1 + y_\ell y_r)}{1 + y_\ell^2}\right] + \frac{k_\phi(1 + k_a)(1 + y_\ell y_r)^2}{1 + y_\ell^2}}{\tau s(\tau s + 1)}$$

(3.5.1.17)

A simple necessary and sufficient condition can be obtained from Routh or Hurwitz' criterion in the case of a second order equation: the roots of a second order equation will have negative real parts if, and only if, the three coefficients are positive. (Actually they must be of the same sign, but we always assume that the coefficient of the highest power of s is positive.)

Therefore, from equation (3.5.1.17) we see that if the following condition is satisfied:

$$1 + y_\ell\, y_r > 0 \qquad (3.5.1.18)$$

the system will be stable for all values of k_a and k_ϕ when no ponderomotive effects are present. This is identical to inequality (3.5.1.6), which is a necessary condition for the loop to be operating.

3.5.2 Stability with zero amplitude feedback and infinite phase feedback

Before going to the general analysis of the feedback system, we will spend some time on the system which presents the most analogy to the generator-driven resonator so we can make some comparisons between the two. The system which presents such an analogy is the one where there is no amplitude feedback, and where there is infinite phase feedback.

That system has a characteristic equation which is proportional to:

$$G_{t\omega} + G_{ta}G_{\mu} = 0 \qquad (3.5.2.1)$$

or:

$$(\tau s + 1 + y_\ell y_r)(s^2 + \frac{2}{\tau_\mu} s + \Omega_\mu^2) + 2y_\ell \tau \Omega_\mu^2 k_\mu V_o^2 = 0 \qquad (3.5.2.2)$$

From the constant term of the above equation and condition (3.3.11), we obtain the following monotonic stability condition:

$$- y_\ell k_\mu V_o^2 < \frac{1 + y_\ell y_r}{2\tau} \qquad (3.5.2.3)$$

By using Routh's criterion, we also obtain the following oscillatory stability condition:

$$y_\ell k_\mu V_o^2 < \frac{1}{\tau_\mu} \frac{(1 + y_\ell y_r)(1 + \frac{2\tau}{\tau_\mu} + y_\ell y_r) + \tau^2 \Omega_\mu^2}{\tau^2 \Omega_\mu^2} \qquad (3.5.2.4)$$

We will now make a comparison between the results just obtained and the ones obtained by Schulze on a generator-driven resonator (S4). At first, conditions (3.5.2.3) and (3.5.2.4), which apply to a resonator operating in a self-excited loop, look quite similar to conditions (3.2.4) and (3.2.5), which apply to a generator-driven resonator. In both cases, we find that monotonic instability can occur only on the low-frequency side ($y_\ell < 0$, $y < 0$) and that oscillatory instability can occur only on the high-frequency side ($y_\ell > 0$, $y > 0$). We also find that there is a range of y_ℓ or y around 0 where the system will have monotonic and oscillatory stability, the resonance point ($y_\ell = 0$, $y = 0$) being unconditionally stable at all field values. Furthermore, the stability boundaries are nearly identical in magnitude.

However, there are two main differences between the two cases. Firstly, the self-excited loop results apply to a system locked in phase and amplitude (we recall that an unlocked self-excited loop did not present ponderomotive instabilities in the field range of interest), whereas the generator-driven results apply to an unlocked system, and the stability conditions will be modified when phase and

amplitude feedback are introduced.

Secondly, the nature of the y's are different. They were defined as:

$$y = \tau \left(\omega_g - \omega_{co} \right)$$

$$y_\ell = \tau \left(\omega_{\ell o} - \omega_{co} \right) = \tan \theta_\ell \qquad (3.5.2.5)$$

where ω_g, ω_{co}, $\omega_{\ell o}$ are respectively the generator frequency, the eigenfrequency of the resonator, and the frequency of the unlocked self-excited loop. Whereas y_ℓ is a totally controllable quantity (being the tangent of the phase shift introduced by the loop phase shifter), y is not a controllable quantity since ω_g, the frequency of the generator, is assumed to be fixed, and ω_c, eigenfrequency of the resonator, can vary by several bandwidths due to excitation of the mechanical modes by external vibrations. Thus, when the resonator is operated in a self-excited loop, θ_ℓ can be adjusted so that y_ℓ lies in the stable range. In the generator-driven case, y cannot be adjusted at will to prevent ponderomotive instabilities, and external feedback has to be provided to stabilize the system. This restriction can be removed by allowing the generator frequency to track the resonator eigenfrequency by the use of a voltage-controlled oscillator. However, the phase of the field is not yet stable, and feedback still has to be provided to stabilize the phase. Also, if the generator frequency is allowed to track the resonator eigenfrequency very

closely, the resonator cannot be considered anymore as being driven by a generator, but must be considered as being operated in a self-excited loop. (See Appendix A)

3.5.3 Stability with arbitrary amplitude and phase feedback

We will now proceed into the stability analysis of a locked self-excited loop in presence of electromechanical coupling, and of arbitrary phase and amplitude feedback.

The monotonic stability criterion can be found easily. Since we know that when no electromechanical coupling is present ($k_\mu V_o^2 = 0$) the system is stable for arbitrary k_a and k_ϕ, the monotonic stability condition can simply be stated as:

$$H(k_a, k_\phi, k_\mu)\Big|_{s=0} > 0 \qquad (3.5.3.1)$$

Using the expressions obtained earlier for the various transfer functions, we get:

$$- y_\ell k_\mu V_o^2 < \frac{1}{2\tau}(1 + y_\ell y_r)(1 + k_a) \qquad (3.5.3.2)$$

It is immediately apparent from the above expression that monotonic stability can be greatly improved by the introduction of amplitude feedback, and that the stability boundary can be pushed arbitarily far by increasing the amplitude feedback gain. We note that k_ϕ is not present in this expression, which means that monotonic stability

is not affected by the presence of phase feedback. However, we have to remember that some phase feedback has to be present to provide frequency locking around ω_r and that k_ϕ has to be large enough so that the use of the linearized system is valid.

Finding the oscillatory stability condition is more complicated, and because of the complex nature of $H (k_\ell, k_\phi, k_\mu)$, the use of Routh's criterion would lead to very lengthy calculations. We can, however, find an expression for the stability boundary. We recall that oscillatory instability will start to occur when a root of the characteristic equation becomes purely imaginary; that is, the stability boundary can be expressed as:

$$H(k_a, k_\phi, k_\mu)\Big|_{s=j\Omega} = 0 \qquad (3.5.3.3)$$

In other words, we have to find Ω and $k_\mu V_{ot}^2$ so that both real and imaginary parts of $H (k_a, k_\phi, k_\mu)\Big|_{s = j\Omega}$ are equal to 0. V_{ot} is the threshold field or field at which instability will start to occur, all other parameters being held constant.

After replacing the transfer functions by their expressions, and some manipulations, we obtain:

$$H(k_a,k_\phi,k_\mu) = \frac{1 + y_\ell y_r}{\tau(1 + y_\ell^2)(\tau s + 1)} \left[\frac{\tau s(1 + y_\ell^2)(\tau s + 1)}{1 + y_\ell y_r} + \frac{k_a \tau s(1 + y_\ell^2)}{1 + y_\ell y_r} \right.$$

$$+ k_\phi(\tau s + 1 + y_\ell y_r) + k_a k_\phi(1 + y_\ell y_r) + \frac{2\tau k_\phi y_\ell \Omega_\mu^2 k_\mu V_{ot}^2}{s^2 + \frac{2}{\tau_\mu} s + \Omega_\mu^2} \Bigg] \qquad (3.5.3.4)$$

Since we are interested only in the roots of H, we will drop the term in front of the brackets, and concentrate only on the expression inside.

We next replace s by $j\Omega$, and by equating to 0 the real and imaginary parts of the expression inside the brackets, we get the following relations:

$$-\tau^2\Omega^2 \frac{1 + y_\ell^2}{1 + y_\ell y_r} + k_\phi(k_a + 1)(1 + y_\ell y_r) = \frac{2k_\phi y_\ell \Omega_\mu^2 k_\mu V_{ot}^2}{(\Omega^2 - \Omega_\mu^2)^2 + \frac{4}{\tau_\mu^2}\Omega^2} (\Omega^2 - \Omega_\mu^2)$$

$$(k_a + 1) \frac{1 + y_\ell^2}{1 + y_\ell y_r} + k_\phi = \frac{2k_\phi y_\ell \Omega_\mu^2 k_\mu V_{ot}^2}{(\Omega^2 - \Omega_\mu^2)^2 + \frac{4}{\tau_\mu^2}\Omega^2} \frac{2}{\tau_\mu} \qquad (3.5.3.5)$$

By taking the ratio of these two expressions, we obtain the instability frequency:

$$\Omega^2 = \Omega_\mu^2 \left\{ 1 + \frac{2\tau}{\tau_\mu} \frac{- \dfrac{1 + y_\ell^2}{1 + y_\ell y_r} + \dfrac{k_\phi (k_a + 1)(1 + y_\ell y_r)}{\tau^2 \Omega_\mu^2}}{\dfrac{2\tau}{\tau_\mu} + (k_a + 1)\dfrac{1 + y_\ell^2}{1 + y_\ell y_r} + k_\phi} \right\} \qquad (3.5.3.6)$$

We notice that if the feedback gains become sufficiently large, the oscillation frequency can become significantly different from the mechanical frequency. In particular, for the two frequencies to be assumed as identical in the calculations without introducing any significant error, the following condition must be satisfied:

$$\frac{\tau}{\tau_\mu} \frac{1}{\tau^2 \Omega_\mu^2} \frac{k_\phi (k_a + 1)}{k_\phi + k_a + 1} << 1 \qquad (3.5.3.7)$$

By using the solution for Ω obtained above, we get the following stability boundary:

$$y_\ell k_\mu V_{ot}^2 = \frac{1}{\tau_\mu} \frac{(k_a + 1)(1 + y_\ell^2) + k_\phi (1 + y_\ell y_r)}{\tau^2 \Omega_\mu^2 \, k_\phi (1 + y_\ell y_r)}$$

$$\times \left\{ \tau^2 \Omega_\mu^2 + \left(\frac{k_\phi (k_a + 1)(1 + y_\ell y_r)^2 - \tau^2 \Omega_\mu^2 (1 + y_\ell^2)}{(k_a + 1 + \frac{2\tau}{\tau_\mu})(1 + y_\ell^2) + k_\phi (1 + y_\ell y_r)} \right)^2 \right.$$

$$+\frac{2\tau}{\tau_\mu}\left.\frac{k_\phi(k_a+1)(1+y_\ell y_r)^2-\tau^2\Omega_\mu^2(1+y_\ell^2)}{(k_a+1+\frac{2\tau}{\tau_\mu})(1+y_\ell^2)+k_\phi(1+y_\ell y_r)}\right\} \tag{3.5.3.8}$$

We will define $\frac{1}{\tau_\mu}B_{os}(k_a,k_\phi)$ as being the right-hand side of Eq. (3.5.3.8). $B_{os}(k_a,k_\phi)=y_\ell\tau_\mu k_\mu V_{ot}^2$ is a dimensionless number defining the equation of the stability boundary in the feedback parameters space as a function of the electromechanical parameters. To obtain the stability condition from the stability boundary, we go to the limit:

$$k_a = 0$$
$$k_\phi \to \infty \tag{3.5.3.9}$$

where we obtained the stability condition (3.5.2.4).

From the stability boundary (3.5.3.8), we obtain:

$$B_{os}(0,\infty) = \frac{\tau^2\Omega_\mu^2+(1+y_\ell y_r)^2+\frac{2\tau}{\tau_\mu}(1+y_\ell y_r)}{\tau^2\Omega_\mu^2} \tag{3.5.3.10}$$

Therefore, the oscillatory stability condition in presence of arbitrary phase and amplitude feedback is:

$$y_\ell k_\mu V_o^2 < \frac{1}{\tau_\mu} B_{os}(k_a,k_\phi) \qquad (3.5.3.11)$$

$B_{os}(k_a,k_\phi)$ is a complicated function of the system parameters, however, in the limits:

$$\begin{aligned} y_\ell^2 &<< 1 \\ |y_\ell y_r| &<< 1 \\ \frac{\tau}{\tau_\mu} &<< 1 \\ k_a + 1 &>> \tau\Omega_\mu \\ k_\phi &>> \tau\Omega_\mu \end{aligned} \qquad (3.5.3.12)$$

which are the normal operating conditions, it simplifies to:

$$B_{os}(k_a,k_\phi) \simeq \frac{k_\phi (k_a + 1)^2}{\tau^2 \Omega_\mu^2 (k_a + 1 + k_\phi)} \qquad (3.5.3.15)$$

Therefore, the oscillatory stability threshold can be pushed arbitrarily far by using high amplitude and phase feedback gains.

3.6 Performance of the stabilization system

In the previous section, we saw that when a resonator was operated in a self-excited loop, simple phase and amplitude feedback could provide locking to an external phase and amplitude reference while preserving the stability of the system under electromechanical

coupling. In this section, we will estimate the residual phase error $\delta\phi$ and amplitude error δv in such a system.

Since $\delta\phi$ and δv have their origin in the variations of the resonator eigenfrequency caused by external noise and vibrations which are random processes, exact expressions for the time dependence of $\delta\phi$ and δv are impossible to find. Instead, we will obtain expressions for the mean-square amplitude and phase errors $<\delta v^2>$ and $<\delta\phi^2>$ respectively defined as:

$$<\delta v^2> = \lim_{T\to\infty} \frac{1}{2T} \int_{-T}^{+T} \delta v^2(t)\, dt$$

$$<\delta\phi^2> = \lim_{T\to\infty} \frac{1}{2T} \int_{-T}^{+T} \delta\phi^2(t)\, dt \qquad (3.6.1)$$

To do this, we will use the tools and results of the theory of stationary random processes (Y2,S7). Let $x(t)$ be a stationary random process whose mean, $<x>$, will be assumed to be zero. We can define the auto-correlation function, $R_x(\tau)$, of $x(t)$ as:

$$R_x(\tau) = \lim_{T\to\infty} \frac{1}{2T} \int_{-T}^{+T} x(t)x(t+\tau)\, dt \qquad (3.6.2)$$

We can also define the spectral density, $S_x(\omega)$, of $x(t)$ as:

$$S_x(\omega) = \frac{1}{2\pi} \int_{-\infty}^{+\infty} R_x(\tau)\, e^{-j\omega\tau}\, d\tau \qquad (3.6.3)$$

The above relation indicates that $S_x(\omega)$ is the Fourier transform of $R_x(\tau)$; consequently, we also have the relation:

$$R_x(\tau) = \int_{-\infty}^{+\infty} S_x(\omega)\, e^{j\omega\tau}\, d\omega \qquad (3.6.4)$$

The mean-square value of x (t), $\langle x^2 \rangle$, can simply be expressed from the auto-correlation function and the spectral density:

$$\langle x^2 \rangle = R_x(0) = \int_{-\infty}^{+\infty} S_x(\omega)\, d\omega \qquad (3.6.5)$$

An important result of the theory of stationary random processes relates the spectral densities of the input and output of a linear system. Let x (t) be the input of a linear system of transfer function $\Phi(j\omega)$ and y (t) be its output; we then have the following relation:

$$S_y(\omega) = S_x(\omega)\, |\Phi(j\omega)|^2 \qquad (3.6.6)$$

In this particular case, we obviously have:

$$S_a(\omega) = S_\omega(\omega)\ |G_a(j\omega)|^2$$
$$S_\phi(\omega) = S_\omega(\omega)\ |G_\phi(j\omega)|^2 \qquad (3.6.7)$$

where $S_a(\omega)$, $S_\phi(\omega)$ and $S_\omega(\omega)$ are respectively the spectral density of $\delta v(t)$, $\delta\phi(t)$ and $\delta\omega_{ex}(t)$, and $G_a(j\omega)$ and $G_\phi(j\omega)$ are the transfer functions defined in equation (3.5.1.14).

We now have to find an expression for the spectral density $S_\omega(\omega)$ of the eigenfrequency deviation. The external noise will excite the mechanical modes of the resonator; since only those modes which interact with the electromagnetic field will produce frequency deviations, we will assume that a single mode is excited by the noise, and that it is the same that leads to ponderomotive instability. With this assumption, we have the following relation:

$$S_\omega(\omega) = \left| \frac{1}{\Omega_\mu^2 - \omega^2 + \frac{2}{\tau_\mu} j\omega} \right|^2 S_n(\omega) \qquad (3.6.8)$$

where $S_n(\omega)$ is the spectral density of the external noise driving the mechanical modes of the resonator. We then have the following expressions for the mean-square amplitude and phase error:

$$\langle \delta v^2 \rangle = \int_{-\infty}^{+\infty} S_n(\omega) \left| \frac{G_a(j\omega)}{\Omega_\mu^2 - \omega^2 + \frac{2}{\tau_\mu} j\omega} \right|^2 d\omega \tag{3.6.9}$$

$$\langle \delta \phi^2 \rangle = \int_{-\infty}^{+\infty} S_n(\omega) \left| \frac{G_\phi(j\omega)}{\Omega_\mu^2 - \omega^2 + \frac{2}{\tau_\mu} j\omega} \right|^2 d\omega$$

We cannot theoretically obtain an exact expression for $S_n(\omega)$, and it has to be determined experimentally. However, since the integrands are very narrowly peaked at Ω_μ and very small everywhere else, only the values of $S_n(\omega)$ around Ω_μ are of any relevance, and we will assume $S_n(\omega)$ to be constant over the whole frequency spectrum. This is equivalent to the assumption that the mechanical oscillator is driven by white noise:

$$S_n(\omega) = A^2 \tag{3.6.10}$$

We then have the following expressions for $\langle \delta v^2 \rangle$ and $\langle \delta \phi^2 \rangle$:

$$\langle \delta v^2 \rangle = A^2 \int_{-\infty}^{+\infty} \left| \frac{G_a(j\omega)}{\Omega_\mu^2 - \omega^2 + \frac{2}{\tau_\mu} j\omega} \right|^2 d\omega$$

$$\langle \delta\phi^2 \rangle = A^2 \int_{-\infty}^{+\infty} \left| \frac{G_\phi(j\omega)}{\Omega_\mu^2 - \omega^2 + \frac{2}{\tau_\mu} j\omega} \right|^2 d\omega \qquad (3.6.11)$$

For ease of calculation, and without restricting substantially the validity of the results, we will make the following simplifications in G_a and G_ϕ :

$$1 + y_\ell^2 \simeq 1$$

$$1 + y_\ell \, y_r \simeq 1 \qquad (3.6.12)$$

which means that the difference between the unlocked loop oscillation frequency (ω_ℓ) and the resonator eigenfrequency (ω_c) is much smaller than the resonator bandwidth. If necessary, the above coefficients can be reintroduced in a straightforward manner in the final results.

Using the expression found earlier for G_a (s), we obtain:

$$\frac{G_a(j\omega)}{\Omega_\mu^2 - \omega^2 + \frac{2}{\tau_\mu} j\omega} = \frac{-\sqrt{b_3}}{a_0\omega^4 + a_1\omega^3 + a_2\omega^2 + a_3\omega + a_4} \qquad (3.6.13)$$

with:

$$b_3 = k_\phi^2 \tau^2 y_\ell^2$$

$$a_0 = \tau^2$$

$$a_1 = - j\tau\left(\frac{2\tau}{\tau_\mu} + k_a + k_\phi + 1 \right)$$

$$a_2 = - \left(k_\phi(k_a + 1) + \tau^2 \Omega_\mu^2 + \frac{2\tau}{\tau_\mu}(k_a + k_\phi + 1) \right) \qquad (3.6.14)$$

$$a_3 = j\left(\frac{2}{\tau_\mu} k_\phi(k_a + 1) + \tau\Omega_\mu^2(k_a + k_\phi + 1) \right)$$

$$a_4 = k_\phi \Omega_\mu^2 \left((k_a + 1) + 2\tau y_\ell k_\mu V_o^2 \right)$$

Integrals of the form:

$$I_n = \frac{1}{2\pi j} \int_{-\infty}^{+\infty} \frac{g_n(x)}{h_n(x) h_n(-x)} \, dx$$

where:

$$g_n = b_0 x^{2n-2} + b_1 x^{2n-1} + \cdots\cdots\cdots + b_{n-1}$$

$$h_n = a_0 x^n + a_1 x^{n-1} + \cdots\cdots\cdots\cdots + a_n$$

have been tabulated (S7,J1). In our case with n=4 and $b_0=b_1=b_2=0$

we have:

$$I_4 = \frac{b_3}{2a_4} \frac{(a_0a_3 - a_1a_2)}{(a_0a_3^2 - a_1^2a_4 - a_1a_2a_3)} \qquad (3.6.15)$$

It can be noted that the stability of the system as expressed by Routh's or Hurwitz' criterion requires that the three factors containing the a's be positive (01). In particular:

$$a_4 > 0$$

is the monotonic stability condition, and

$$a_0a_3^2 - a_1^2a_4 - a_1a_2a_3 > 0$$

is the oscillatory stability condition.

Thus, we find the intuitively obvious fact that the mean-square errors are defined only within the stable range, and diverge when either stability boundary is approached.

With the above definitions for $<\delta v^2>$ and I_4 we obtain:

$$<\delta v^2> = 2\pi j A^2 I_4 \qquad (3.6.16)$$

However, expressing the mean-square amplitude error in terms of the noise is not very useful, and it would be more significant to express it in terms of the mean-square frequency deviation $<\delta\omega_{ex}^2>$. This can be obtained from:

$$\langle \delta\omega_{ex}^2 \rangle = A^2 \int_{-\infty}^{+\infty} \frac{d\omega}{\left| \Omega_\mu^2 - \omega^2 + \frac{2}{\tau_\mu} j\omega \right|^2} = 2\pi j A^2 I_2 \tag{3.6.17}$$

where:

$$I_2 = \frac{1}{2\pi j} \int_{-\infty}^{+\infty} \frac{d\omega}{\left| \Omega_\mu^2 - \omega^2 + \frac{2}{\tau_\mu} j\omega \right|^2} = - \frac{j\tau_\mu}{4\Omega_\mu^2} \tag{3.6.18}$$

Thus, we have:

$$\langle \delta v^2 \rangle = \langle \delta\omega_{ex}^2 \rangle \frac{I_4}{I_2} \tag{3.6.19}$$

Replacing the a's in (3.6.19) would lead to a very complicated formula; however, it can be greatly simplified and made easier to understand if it is expressed in terms of the stability boundaries. Earlier, we defined $B_{os}(k_a, k_\phi)$ as a dimensionless function of the feedback parameters such that the oscillatory stability condition can be expressed as:

$$y_\ell \tau_\mu k_\mu V_o^2 < B_{os}(k_a, k_\phi) \tag{3.6.20}$$

In a similar manner, we define:

$$B_{mo}(k_a) = \frac{1}{2} (1 + y_\ell y_r)(1 + k_a) \tag{3.6.21}$$

so that the monotonic stability condition can be expressed as:

$$- y_{\ell}\tau k_{\mu} V_o^2 \; < \; B_{mo}(k_a) \tag{3.6.22}$$

We then obtain the following expression for $<\delta v^2>$:

$$<\delta v^2> \; = \; <\delta\omega_{ex}^2> \frac{y_{\ell}^2}{2\Omega_{\mu}^2}$$

$$x\left[\frac{k_{\phi}(k_a+1)(k_{\phi}+k_a+1)+\frac{2\tau}{\tau_{\mu}}\left[(k_a+k_{\phi}+1)^2+\tau^2\Omega_{\mu}^2\right]+\left(\frac{2\tau}{\tau_{\mu}}\right)^2(k_a+k_{\phi}+1)}{(k_a+k_{\phi}+1+\frac{2\tau}{\tau_{\mu}})^2\;(B_{mo}+y_{\ell}\tau k_{\mu}V_o^2)(B_{os}-y_{\ell}\tau_{\mu}k_{\mu}V_o^2)}\right]$$

(3.6.23)

The dependence of the mean-square amplitude error on the loop phase shift is represented in Figure (3.14).

$<\delta\phi^2>$ can be obtained in a similar manner. The a's in I_4 are identical, but now:

$$b_2 = \tau^4$$

$$b_3 = \tau^2(k_a + 1)^2$$

$$I_4 = \frac{a_1a_4b_2 + b_3(a_0a_3 - a_1a_2)}{2a_4(a_0a_3^2 + a_1^2a_4 - a_1a_2a_3)} \tag{3.6.24}$$

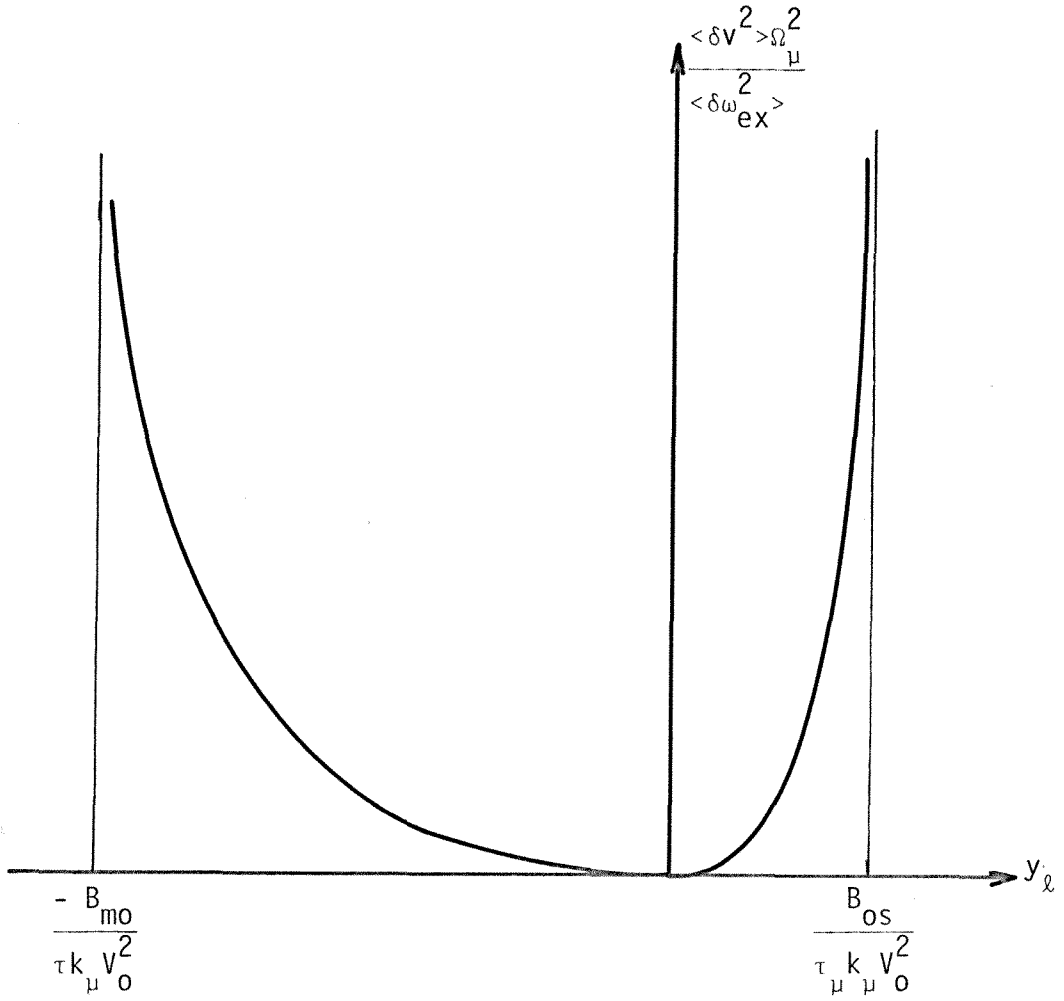

Fig.3.14. Mean-square amplitude error vs. tangent of the loop phase shift

We obtain for $\langle\delta\phi^2\rangle$:

$$\langle\delta\phi^2\rangle = \frac{\langle\delta\omega_{ex}^2\rangle}{2\Omega_\mu^2 k_\phi^2}$$

$$\times \left\{ 2\tau^2\Omega_\mu^2 k_\phi (k_a+k_\phi+1+\frac{2\tau}{\tau_\mu})(B_{mo} + y_\ell \tau k_\mu V_o^2) \right.$$

$$\left. +(k_a+1)^2\left[k_\phi(k_a+1)(k_\phi+k_a+1)+\frac{2\tau}{\tau_\mu}\left((k_a+k_\phi+1)^2+\tau^2\Omega_\mu^2\right)+\frac{4\tau^2}{\tau_\mu^2}(k_a+k_\phi+1)\right]\right\}$$

$$\times \left\{ (k_a+k_\phi+1+\frac{2\tau}{\tau_\mu})^2 (B_{mo} + y_\ell \tau k_\mu V_o^2)(B_{os} - y_\ell \tau_\mu k_\mu V_o^2) \right\}^{-1}$$

(3.6.25)

The dependence of the mean-square phase error on the loop phase shift is represented in Figure (3.15).

It should be pointed out that in the graph (3.14) of $\langle\delta v^2\rangle$ and in the graph (3.15) of $\langle\delta\phi^2\rangle$, the oscillatory stability asymptote on the right of the vertical axis has been placed much further from this axis, as compared to the left asymptote, than occurs in reality.

From these two graphs, we can draw some conclusions. First of all, we see that when the loop phase shift is adjusted so that the unlocked self-excited loop operates on resonance ($y_\ell = 0$), the mean-square amplitude error is equal to 0. This is just a consequence of the fact that on resonance, phase and amplitude feedbacks are decoupled. Also, we see that when either stability boundary is

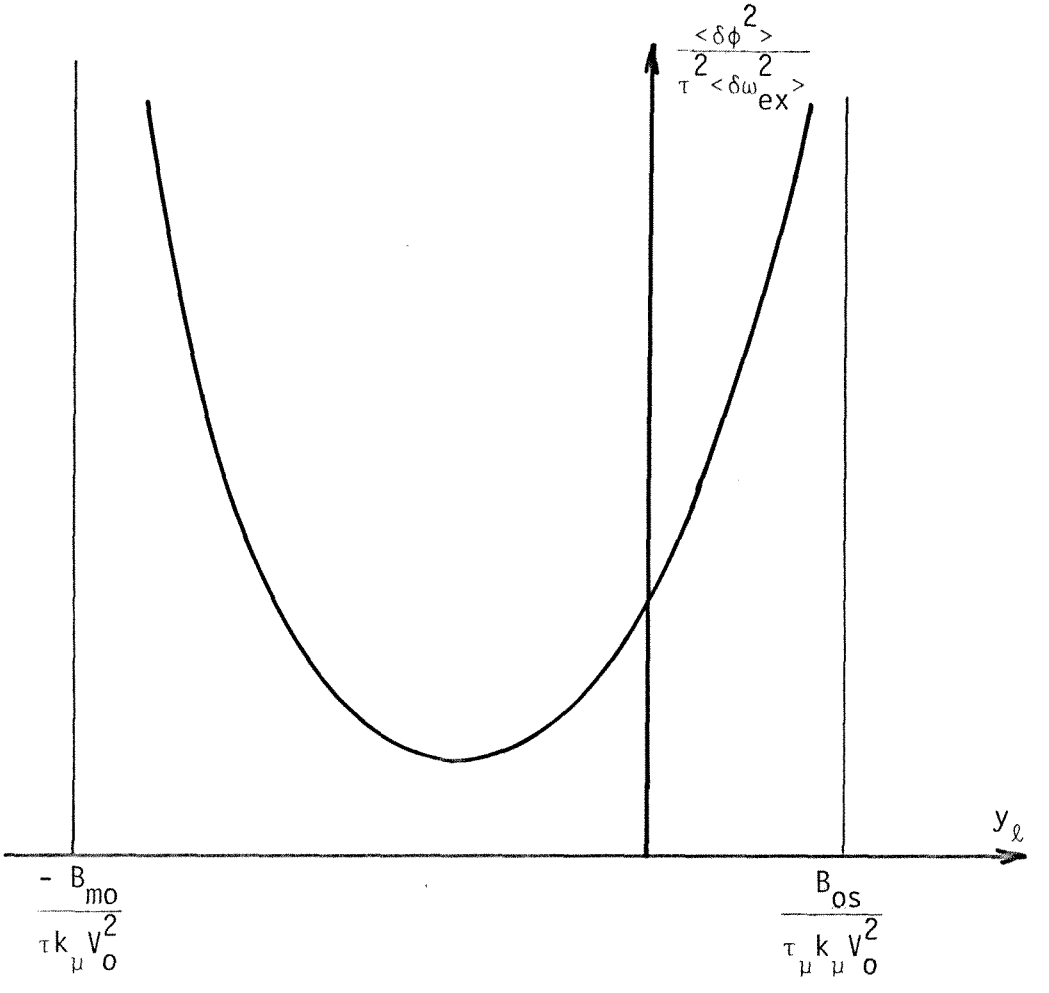

Fig. 3.15 Mean-square phase error vs. tangent of the loop phase shift

approached, the mean-square errors increase rapidly and eventually diverge. Lastly, we see that it might be preferable to operate off resonance on the low frequency side ($y_\ell < 0$). This has the consequence of decreasing the mean-square phase error while increasing the mean-square amplitude error. Thus, depending upon the application, a balance between phase and amplitude errors can be achieved. This decreasing of the phase error is due to the fact that the phase modulation creates an amplitude modulation through the transfer function G_{ta} (see Fig. 3.12), which, in turn, drives the mechanical mode to produce an additional phase modulation. When the loop operates on the low frequency side, ($y_\ell < 0$), this additional phase modulation has a sign opposite to the original phase modulation, effectively operating as an internal damping of the mechanical mode of the resonator.

In the practical limits:

$$\begin{aligned} \frac{\tau}{\tau_\mu} &<< 1 \\ k_a + 1 &>> \tau\Omega_\mu \\ k_\phi &>> \tau\Omega_\mu \end{aligned}$$

expressions (3.6.23) and (3.6.25) for $\langle\delta v^2\rangle$ and $\langle\delta\phi^2\rangle$ simplify to:

$$\langle\delta v^2\rangle = \langle\delta\omega_{ex}^2\rangle \frac{y_\ell^2}{2\Omega_\mu^2} \frac{k_\phi(k_a+1)}{(k_a+k_\phi+1)(B_{mo} + y_\ell\tau k_\mu V_o^2)(B_{os} - y_\ell\tau_\mu k_\mu V_o^2)}$$

$$\langle\delta\phi^2\rangle = \frac{\langle\delta\omega_{ex}^2\rangle}{2\Omega_\mu^2} \frac{(k_a+1)^3}{k_\phi(k_a+k_\phi+1)(B_{mo} + y_\ell\tau k_\mu V_o^2)(B_{os} - y_\ell\tau_\mu k_\mu V_o^2)} \tag{3.6.26}$$

with:

$$B_{mo} = \frac{1 + k_a}{2}$$

$$B_{os} = \frac{k_\phi(k_a + 1)^2}{\tau^2\Omega_\mu^2(k_\phi + k_a + 1)} \tag{3.6.27}$$

In particular:

$$\langle\delta\phi^2\rangle \Big|_{y_\ell=0} = \frac{\tau^2\langle\delta\omega_{ex}^2\rangle}{k_\phi^2} \tag{3.6.28}$$

We also have the following relationship between mean-square phase and amplitude error:

$$\frac{\langle\delta v^2\rangle}{\langle\delta\phi^2\rangle} = y_\ell^2 \frac{k_\phi^2}{(k_a + 1)^2} \tag{3.6.29}$$

This relationship can be easily extended to the instantaneous values of $\delta v(t)$ and $\delta\phi(t)$ since they are very strongly correlated. In effect, from Equations (3.5.1.14), we have:

$$\frac{G_a(s)}{G_\phi(s)} = \frac{y_\ell(1 + y_\ell y_r)}{1 + y_\ell^2} \quad \frac{k_\phi}{k_a + 1 + \tau s} \tag{3.6.30}$$

So, when

$$k_a + 1 \gg \tau\Omega_\mu \tag{3.6.31}$$

$\delta v(t)$ and $\delta\phi(t)$ are proportional and related by:

$$\frac{\delta v(t)}{\delta\phi(t)} = \frac{y_\ell(1 + y_\ell y_r)}{1 + y_\ell^2} \quad \frac{k_\phi}{k_a + 1} \tag{3.6.32}$$

In Chapter I we obtained an equation for the energy gain W of a particle going through a resonator which was as follows:

$$W = q \cos \phi \; E(\beta_o) \; T(\beta) \tag{3.6.33}$$

Keeping in mind that $E(\beta_o)$ is proportional to the instantaneous field V in the resonator, we obtain by differentiation the energy error caused by the phase and amplitude error:

$$\frac{\Delta W}{W} = -\tan \phi_s \; \delta\phi + \delta v \tag{3.6.34}$$

where ϕ_s is the synchronous phase.

This equation applies to a single bunch of particles going through a single resonator. If we assume that the beam entering the accelerator is purely monochromatic, the energy spread of such a beam at the output averaged over many bunches going through n identical resonators will be:

$$\left(\frac{\Delta W_t}{W_t}\right)^2 = \frac{1}{n}\left(\tan^2\phi_s\ \delta\phi^2 + \delta v^2\right) \qquad (3.6.35)$$

where $W_t = nW$ is the total energy gain. To obtain the above equation, we assumed that δv and $\delta\phi$ were independent random variables, and it clearly shows that in order to keep the beam as monochromatic as possible, both $\delta\phi$ and δv have to be minimized.

However, the previous analysis shows that with this particular feedback system, δv and $\delta\phi$ are very strongly correlated; in fact, in the limit (3.6.31), they can be considered as being proportional as indicated by equation (3.6.32). It should be emphasized that although δv and $\delta\phi$ are random variables, the proportionality is not between magnitudes or mean-square values, but between instantaneous values. So that a new expression for the energy gain error, modified by this correlation, is:

$$\frac{\Delta W}{W} = \delta\phi\left[-\tan\phi_s + \frac{y_\ell k_\phi}{k_a + 1}\ \frac{1+y_\ell y_r}{1+y_\ell^2}\right] \qquad (3.6.36)$$

which, in practical cases, simplifies to:

$$\frac{\Delta W}{W} = \delta\phi \left[- \tan \phi_s + y_\ell \frac{k_\phi}{k_a + 1} \right] \qquad (3.6.37)$$

The above equation shows that if the feedback parameters are carefully chosen (especially y_ℓ), the energy gain error can be made to vanish although phase and amplitude errors are still present. In other words, the feedback parameters can be chosen so that the effects of the residual phase and amplitude errors compensate for each other, and the beam quality is preserved. This occurs if:

$$y_\ell \frac{k_\phi}{k_a + 1} = \tan \phi_s \qquad (3.6.38)$$

Since $\phi_s = -20^o$, this would imply working on the low frequency side which, as we already mentioned, is to be preferred as the system is more stable than on the high frequency side.

More complicated feedback transfer functions can be devised in order to decrease δv and $\delta\phi$: terms proportional to $\frac{d\delta v}{dt}$ and $\frac{d\delta\phi}{dt}$ can be added together with feedback from $\delta\phi$ to δv_g and from δv to δt. However, if this decrease of δv and $\delta\phi$ is obtained at the expense of giving up the proportionality relationship, a net increase in ΔW could result.

This cancellation of the energy gain error is a direct result of the proportionality between instantaneous values of the residual phase

and amplitude errors. In practice, however, this proportionality will not be absolute at all times because of two reasons. Firstly, this proportionality, as indicated by equation (3.6.32), was obtained from a study of the linearized system, and under large frequency excursions, equation (3.6.32) might become only an approximation. Secondly, under high feedback gains, some elements in the feedback system might present a non-linear behavior. Although exact cancellation of the energy gain error will probably not happen in reality, operating the feedback system under conditions where equation (3.6.38) is satisfied, however, should result in a significant decrease of the residual energy gain error.

3.7 Conclusions

In this chapter, we derived a set of differential equations describing a resonator in a self-excited loop. Using these differential equations, it was shown that when the loop was free-running the amplitude of the field was stable, and the loop did not present ponderomotive instabilities. When the loop was locked to an external amplitude and phase reference, ponderomotive instabilities could occur; however, the loop could be made stable by adjustment of the loop phase shift and the stable range could be increased by using high feedback gains. It was also shown that the feedback parameters could be chosen in such a way as to greatly reduce the residual energy gain error while phase and amplitude errors were still present.

Chapter IV

DESCRIPTION OF A FEEDBACK SYSTEM FOR PHASE AND AMPLITUDE STABILIZATION OF SUPERCONDUCTING RESONATORS

In this chapter, we will present the design and realization of a phase and amplitude stabilization system for a superconducting resonator. This system was not simply designed to provide experimental verification of the analysis of the previous chapter, nor was it designed only to provide stabilization of a single resonator. It was conceived as a building block of the stabilization and control system of a full scale many-resonator accelerator. With this in mind, the control system had to fulfill two requirements. Firstly, it had to be flexible enough so that any control function deemed necessary could be implemented easily; secondly, there should be easy access to and easy manipulation of all the parameters of the system either manually or automatically.

In order to provide the design flexibility mentioned above, the control system was designed to operate at audio-frequency (D.C. - 200 kHz) where the signals are more easily and more economically manipulated than at the RF frequency of the resonator. The range of feasible signal manipulations is also vastly greater at audio frequency than at radio-frequency. This has the added advantage that the control system can be designed independently of the frequency of the resonator; only the RF - IF interface has to be modified. Thus, this control system can be used to stabilize resonators with eigenfrequencies ranging from less than 50 MHz to more than 5 GHz.

The access to all the parameters and the automatic operation of

the control system was obtained by having all the parameters entered digitally by a microprocessor.

Thus, this control system is composed of three levels:

- RF level: power amplifier and resonator (150 MHz)
- IF level: feedback and signal manipulation (D.C. - 200 kHz)
- Digital level: parameter setting and decision making

And of two interfaces:

- RF - IF
- IF - Digital

We will now proceed into the description of the feedback system without going into technical details.

This stabilization system is novel in several ways:

- The controlled element is not a resonator but a self-excited loop containing a resonator.

- No external voltage-controlled reactance was used; instead, stabilization was provided by negative electronic feedback.

- All the control takes place at audio-frequency.

A block diagram of the stabilization system is shown in Fig. (4.1). The three most important parts of this system are:

- The RF - IF interface

Fig. 4.1. Block diagram of the stabilization system of a single resonator.

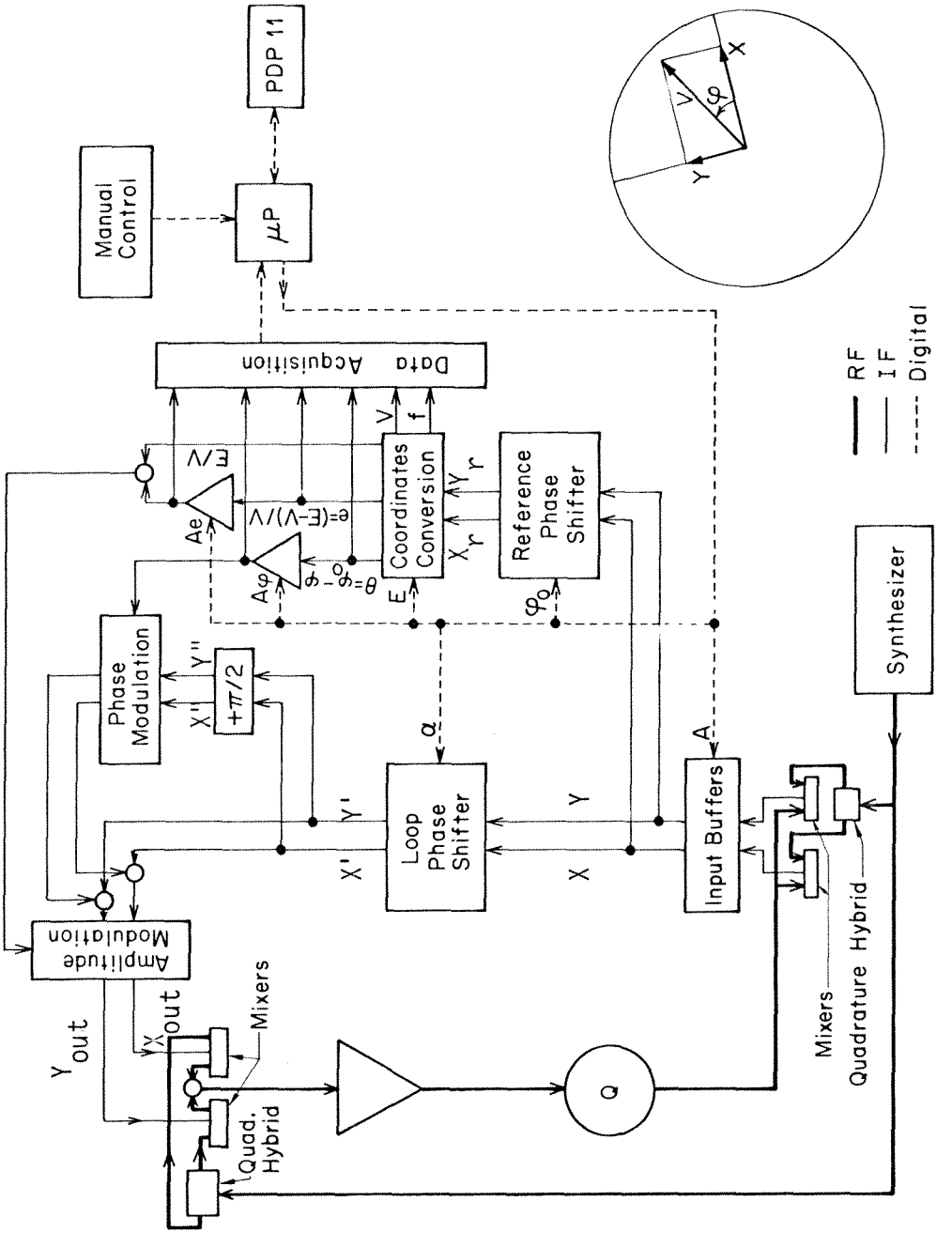
PDP 11
Manual Control
μP
Data Acquisition
V
f
E/V
Ae
e=(E-V)/V
Aφ
θ=φ-φo
Coordinates Conversion
Xr
Yr
Reference Phase Shifter
φo
E
Phase Modulation
Y''
X''
+π/2
α
A
Loop Phase Shifter
Y'
X'
Y
X
Input Buffers
Amplitude Modulation
Yout
Xout
Mixers
Quad. Hybrid
Q
Mixers
Quadrature Hybrid
Synthesizer
RF
IF
Digital
V
φ
X
Y

- The drive loop which completes the rf section of the self-excited loop,

- The control loop where phase and amplitude errors are determined, and where feedback takes place.

4.1 RF - IF Interface

As was mentioned in the introduction, both phase and amplitude of the field in the resonator have to be stabilized. This means that in the RF to IF conversion, two IF signals have to be extracted from the RF signal coming from the resonator in order to obtain all the information required. This interface is shown in Fig. (4.2).

The down-conversion can be realized by mixers operating as phase detectors. If the RF input is low enough so that the mixer operates in its linear range, the instantaneous IF output is proportional to both the RF amplitude and the cosine of the phase difference between the RF and Local Oscillator inputs. The two IF signals which are required are obtained by first splitting the local oscillator signal by a quadrature hybrid. A quadrature hybrid is a one input - two outputs device whose two outputs are 3 dB lower than the input; one being in phase with the input, and the other being shifted by -90^{o}.

Thus, one obtains two IF signals whose common frequency is the difference between the loop frequency and the reference frequency, and whose amplitudes are proportional to the amplitude of the field in the resonator. In other words, X and Y are the components of the resonator field in the rotating frame of the reference. From X and Y,

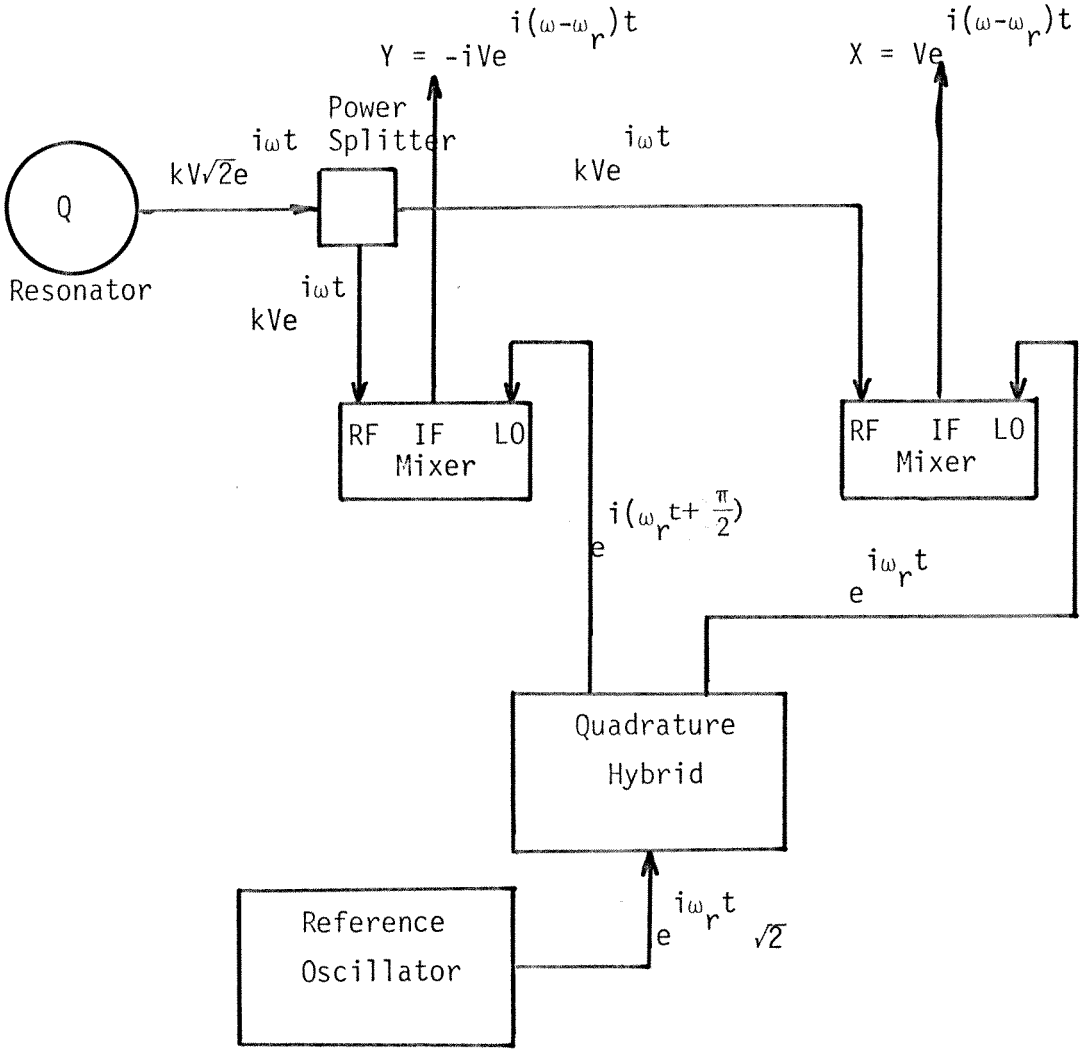

Fig. 4.2. The RF to IF interface used to convert the signal coming from the resonator into two low frequency signals. The IF to RF interface is identical with the exception that the mixers operate as current-controlled attenuators and the power splitter as a power combiner

V and ϕ can be unambiguously determined. There is of course, a proportionality constant between the resonator field amplitude and the IF signals amplitude, but this constant will be omitted from now on and V will represent simultaneously the field amplitude and the IF signal amplitude. The additive constant between the absolute phase of the resonator field and Arctan $\frac{Y}{X}$ will also be omitted, and both will be represented by ϕ.

The two IF signals X and Y are the ones which are manipulated in the control system to provide two outputs X_{out} and Y_{out} (in fact, the outputs are two currents, IX_{out} and IY_{out}, which are proportional to X_{out} and Y_{out}). The up-conversion from IF to RF is done in the same manner as the down-conversion with the exception that the mixers now operate as current-controlled attenuators, and the power splitter now operates as a power combiner.

4.2 Drive-loop

We will now describe the IF portion of the self-excited loop. X and Y are first amplified by two programmable gain amplifiers, whose common gain is set digitally, to bring the low-level mixers' output to usable levels.

The two important blocks of a self-excited loop are the phase shifter and the limiter. The unusual requirements placed upon these two is that they have to be usable down to DC. In fact, when the loop is locked, X and Y are DC signals since the local oscillator provides the RF phase reference to which the resonator has to be locked. In this particular application, since both components of a signal are available, X and Y, it is meaningful to speak about negative

frequency, and the system designed to operate between D.C. and 200 kHz had an equivalent RF bandwidth of 400 kHz.

The phase shifter had to be designed to provide a continuously variable phase shift from 0 to 2π, but independent of the input signals' amplitude and frequency. This was realized by using four multiplying digital to analog converters yielding two outputs which were linear combinations of the two inputs as shown in Fig. 4.3; the digitally-set coefficients of this linear combination being the sine and the cosine of the shifting angle.

The limiter, shown in Fig. 4.4, was realized by using an analog multiplier in each of the channels whose first input was either X' or Y' and whose second input was an analog signal proportional to $\frac{E}{V}$ provided by the coordinate conversion module which will be described in the control loop. E is the amplitude reference set digitally, and $V = \sqrt{X^2 + Y^2}$ is the field amplitude.

Thus, we obtain two signals which are the components of a signal whose phase is equal to the input phase plus a constant, and whose amplitude is independent of the input amplitude. This part of the system operates as a phase shifter and a limiter in a self-excited loop. The self-excited loop is completed by converting the outputs of the limiter from voltages to currents, and returning them to the up conversion part of the RF - IF interface.

4.3 Control loop

As has been described until now, the system operates as an unlocked self-excited loop. To be useful as an accelerating structure control system, phase and amplitude stabilization has to be provided

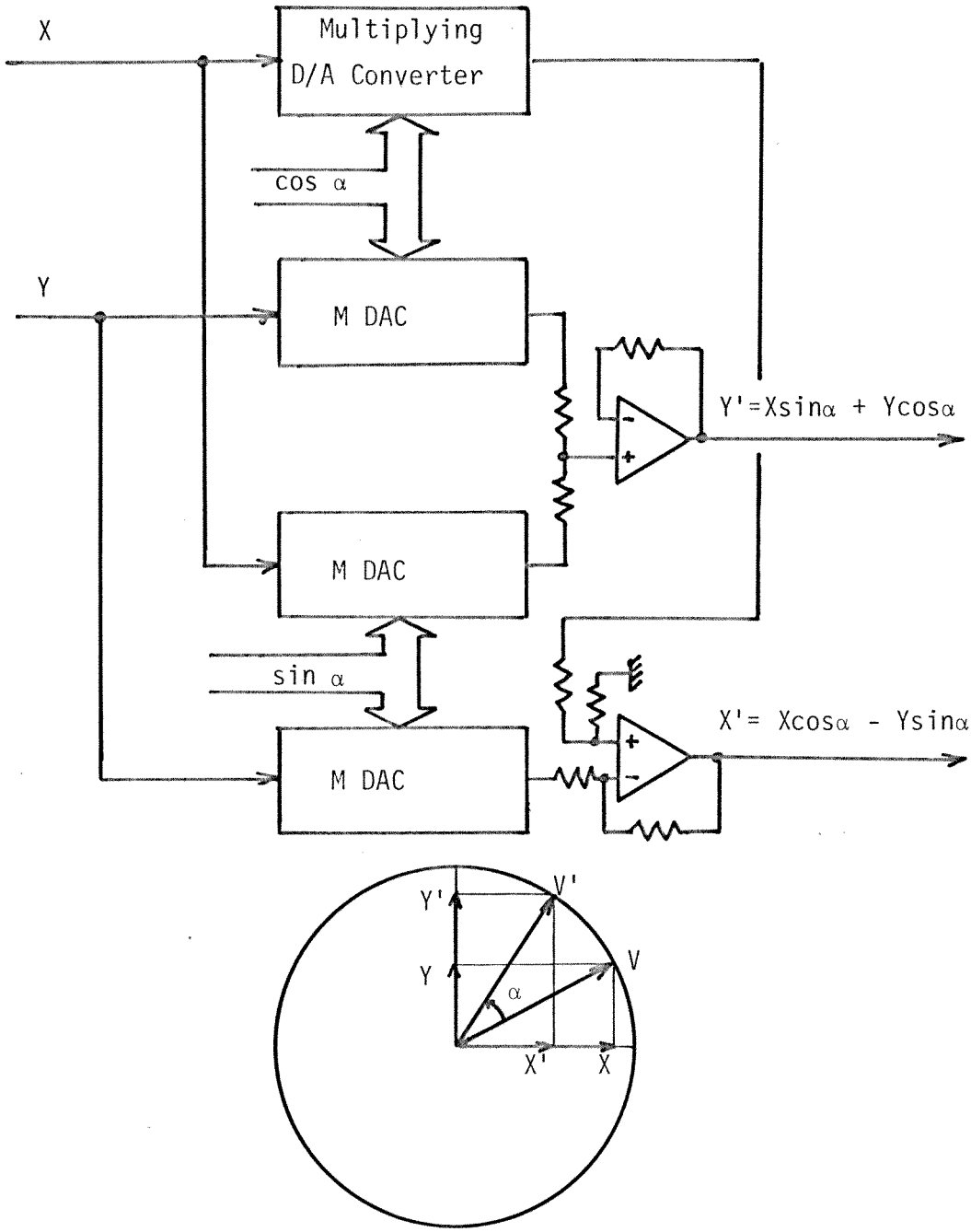

Fig. 4.3. Schematics of the digitally controlled phase shifter

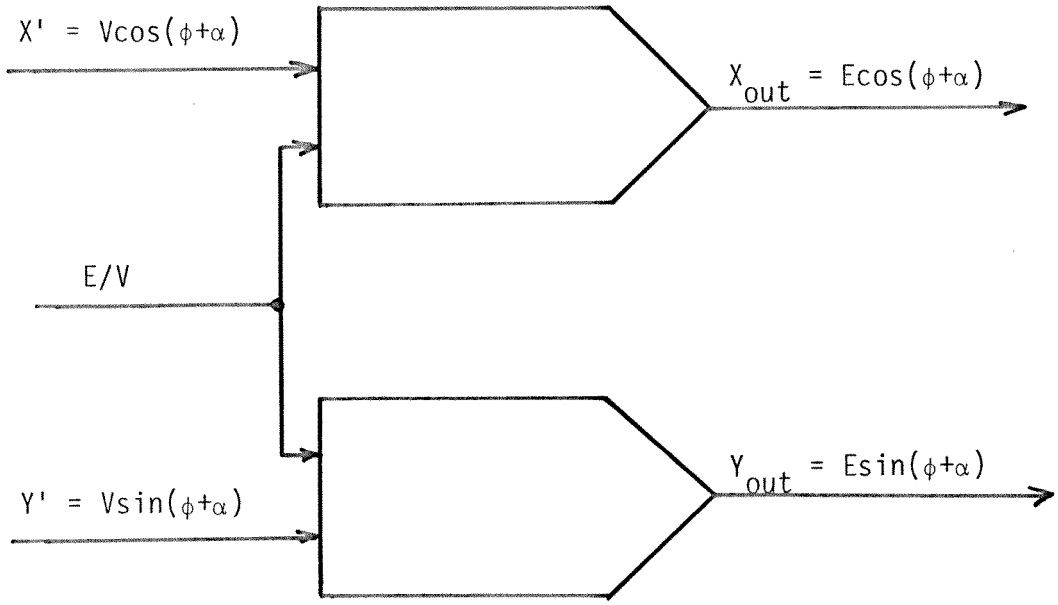

Fig. 4.4. Schematics of the limiter

which is the role of the control loop.

The heart of the control loop is the coordinate conversion module. Since the variables of interest are V and ϕ, amplitude and phase, and the variables to which we have access are $X = V \cos \phi$ and $Y = V \sin \phi$, some form of rectangular to polar coordinates conversion has to be provided.

We will mention now a second phase shifter (of angle $-\phi_0$) placed before the coordinate conversion. All the resonators have to be locked to the same phase (or frequency) reference; however, to allow for different cable length and the time of flight of the particles between the different accelerating resonators, a certain constant phase difference has to be allowed between the field in each resonator and the phase reference. This is the purpose of this second phase shifter, to account for this phase difference. The phase of the signal represented by the two outputs of the reference phase shifter is then the phase error between the phase of the field in the resonator and the phase to which it should be locked.

Obtaining V from X and Y is relatively easy by solving the implicit equation:

$$\frac{X^2 + Y^2}{V} = V$$

This can be done, as shown in Fig. 4.5, by using analog multiplier-dividers which are three inputs - one output devices (one input being differential) with the following transfer function:

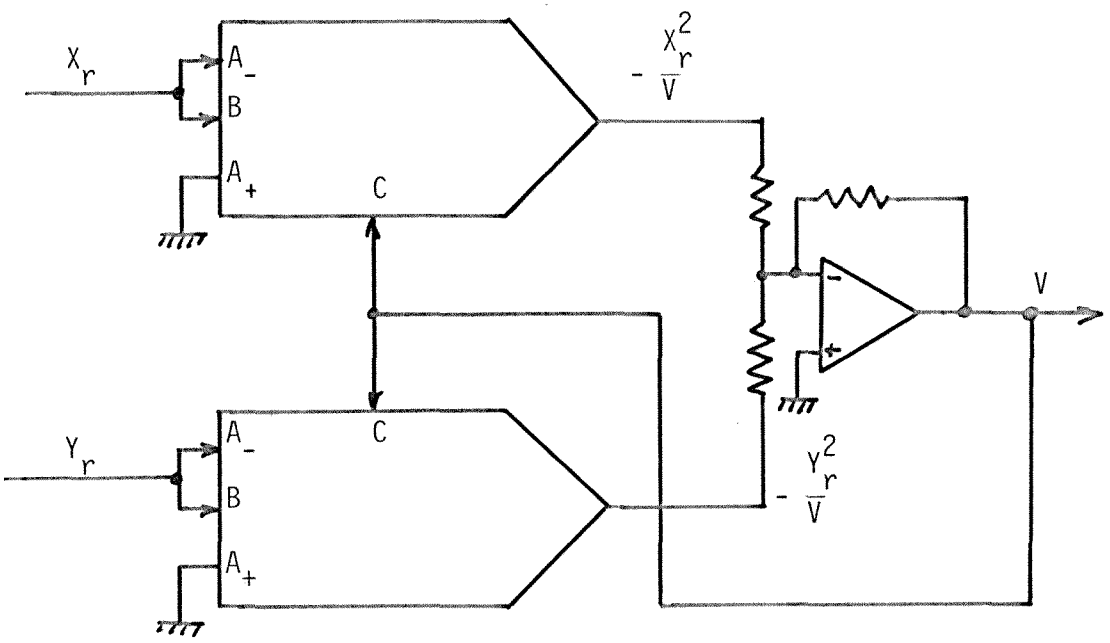

Fig. 4.5. Schematics of the determination of the amplitude of a vector from its Cartesian components

$$V_{out} = \frac{(A_+ - A_-)\, B}{C}$$

The phase conversion, which is equivalent to solving the equation:

$$\theta = \text{Arctan}\ \frac{Y}{X}$$

is more difficult to realize.

In fact, an exact solution is impossible, and some approximation will have to be found.

A suitable approximation was found to be:

$$\theta' = \frac{\sin\theta}{a + b\cos\theta} = \frac{Y}{aV + bX}$$

where a and b are free parameters which can be chosen to minimize either the relative or absolute error over any symetrical range around $\theta = 0$. $a + b = 1$ yields a relative error of the order of θ^3 around 0, and $a = 0.642$, $b = 0.358$ minimizes the relative error in the range $\left[-\frac{\pi}{2}, +\frac{\pi}{2}\right]$ to $\pm$ 0.8%. The second and third quadrants are unimportant since in the locked state $\theta \simeq 0$.

The above approximation can be implemented easily with an analog multiplier-divider. Three other useful signals are also generated in this module: E/ V where E is a digitally-set amplitude reference and is used in the limiter described above, e = (E - V)/ V which is a normalized amplitude error, and f which is the instantaneous frequency difference between the self-excited loop and the

frequency reference. f was defined and implemented as:

$$f = \frac{X\dot{Y} - \dot{X}Y}{V^2}$$

Thus, f gives us the magnitude and sign of the frequency difference, and is independent of the phase and amplitude of the input.

To provide amplitude stabilization, the normalized amplitude error e is amplified by a digitally programmable gain amplifier (of gain A_e) added to E/V to control the limiter output. This provides us with a smooth transition between unlocked and locked amplitude states. Even when no amplitude feedback is provided, the loop is still oscillating and the amplitude is stable. An even smoother transition is accomplished when the input buffers gain is adjusted so that at operating field V = E in the unlocked state.

Phase stabilization is accomplished by adding a signal in quadrature with the loop signal which is controlled by the phase error between the self-excited loop and the phase reference, as shown in Fig. 4.1. This is accomplished by using the two outputs of the loop phase shifter X' and Y', making the transformation:

$$X'' = -Y'$$
$$Y'' = X'$$

then multiplying each of them by $A_\phi\theta$ where A_ϕ is the digitally-set gain of a programmable gain amplifier and θ is the phase error, and

adding them to the inputs of the limiter-amplitude modulation module.

Thus, the output signal of the feedback system is:

$$V \left[\frac{E}{V} + A_a \left(\frac{E - V}{V} \right) \right] \left[1 + i A_\phi \theta \right]$$

or:

$$E \left[1 + A_a \left(\frac{E - V}{E} \right) \right] \left[1 + i A_\phi \theta \right]$$

which is identical in form to what was used in the analysis of the previous chapter as indicated by Equation (3.5.1.2).

In the design of this system, great care was taken to prevent the introduction of any unintentional coupling between phase and amplitude feedback which could hamper the stability of the system by exciting the mechanical mode of the resonator.

Chapter V

EXPERIMENTS

A prototype of the feedback system analyzed in Chapter III and described in Chapter IV has been designed and built to stabilize resonators for use as accelerating structures for heavy-ions. A series of experiments has been performed to test this system in conjunction with a 150 MHz lead (Pb) plated split-ring resonator at 4.2^{o} K.

Some of the stabilization experiments have already been published elsewhere (D7). In those experiments, the feedback system analyzed here has been successfully used to stabilize a 150 MHz split-ring resonator at an average accelerating field of 2 MV/m with a residual amplitude error $\delta v < \pm 0.1\%$ and phase error $\delta\phi < \pm 0.1^{o}$.

Fig. (5.1) shows an experimental determination of the probability density of the instantaneous eigenfrequency of an unlocked resonator in a laboratory environment. These results were obtained by the microprocessor performing 10,000 measurements in 40 sec of (f) the difference between the loop frequency which tracks the resonator eigenfrequency, and the reference synthesizer frequency. This typical peak to peak excursion of 100 Hz in the resonator eigenfrequency ($\sim$150 MHz) is much larger than the intrinsic bandwidth of the resonator ($\sim$20 Hz).

Fig. (5.2) shows an experimental determination of the normalized auto-correlation function, $\rho_f(\tau)$, of the frequency deviation:

$$\rho_f(\tau) = \frac{R_f(\tau)}{R_f(0)}$$

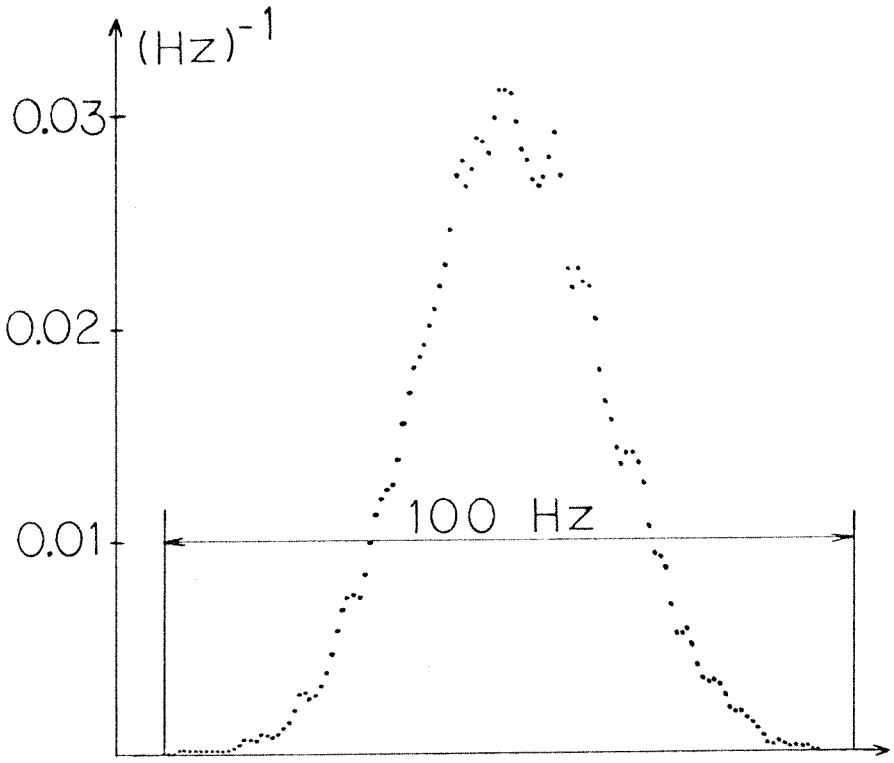

Fig. 5.1. Probability density of the resonant frequency of a 150 MHz superconducting split-ring resonator.

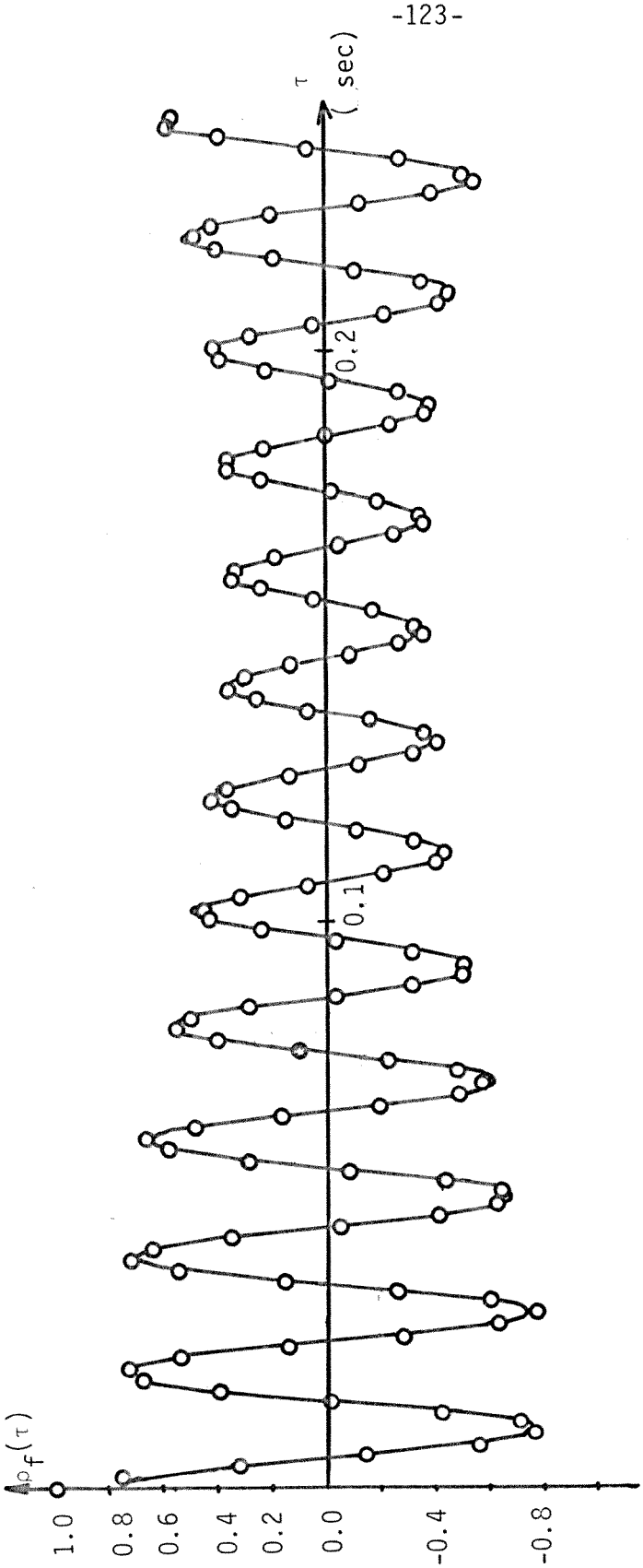

Fig. 5.2. Normalized autocorrelarion function of the resonator eigenfrequecy variation.

where

$$R_f(\tau) = \lim_{T \to +\infty} \frac{1}{2T} \int_{-T}^{+T} \delta f(t)\ \delta f(t+\tau)\ dt$$

$$\delta f = f - \langle f \rangle$$

These results were also obtained by the microprocessor making measurements of (f) every 2 msec.

The auto-correlation function shows that two mechanical modes are excited by vibrations and interact with the electromagnetic field. These two modes were identified at room temperature by stroboscopic means. One is a torsional and bending mode of the loop where the drift tubes move in opposite direction along the beam line and has a frequency $\Omega_1 \simeq 47$ Hz. The other is a bending mode of the loop where the drift tubes move in a plane perpendicular to the beam line and has a frequency $\Omega_2 \simeq 50$ Hz.

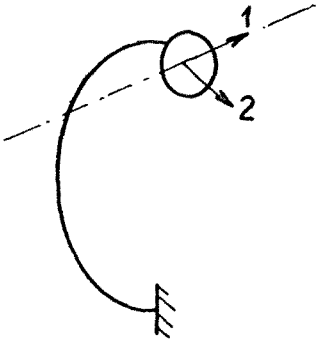

In Fig. (5.2), the solid line represents a least-square fit to the experimental points by a function of the form:

$$\rho\ (\tau) = A_1 \cos \Omega_1 \tau + A_2 \cos \Omega_2 \tau$$

with $A_1 = 0.55$ $\Omega_1/2\pi = 50$ Hz

$A_2 = 0.21$ $\Omega_2/2\pi = 46.8$ Hz

Such a trial function assumes that the eigenfrequency deviation is due to two independent mechanical oscillators excited by white noise with Q's much larger than 1. It can be noted that $A_1 + A_2 < 1$. This is to take into account a superimposed high frequency noise introduced by the electronics which had the effect of decreasing the value of the normalized auto-correlation function for all values of $\tau \neq 0$.

The contribution of mode 2 to the total frequency shift can, in principle, be determined from the electromagnetic field distribution inside the resonator. The contribution of mode 1, however, is more difficult to estimate; since it is very sensitive to the position of the drift tubes along the beam line.

It can be seen from Fig. (5.3) that the electric force excited by one end plate on its facing drift tube nearly cancels the force exerted by the other drift tube. However, a small displacement of any drift tube along the beam line will result in a net electric force and an increased contribution of the mechanical mode 1 to the eigenfrequency variation by an amount which is difficult to predict, and varies from resonator to resonator.

For example, the total radiation pressure frequency shift at an average accelerating field of 2 MV/m was reduced from 4 KHz to 400 Hz

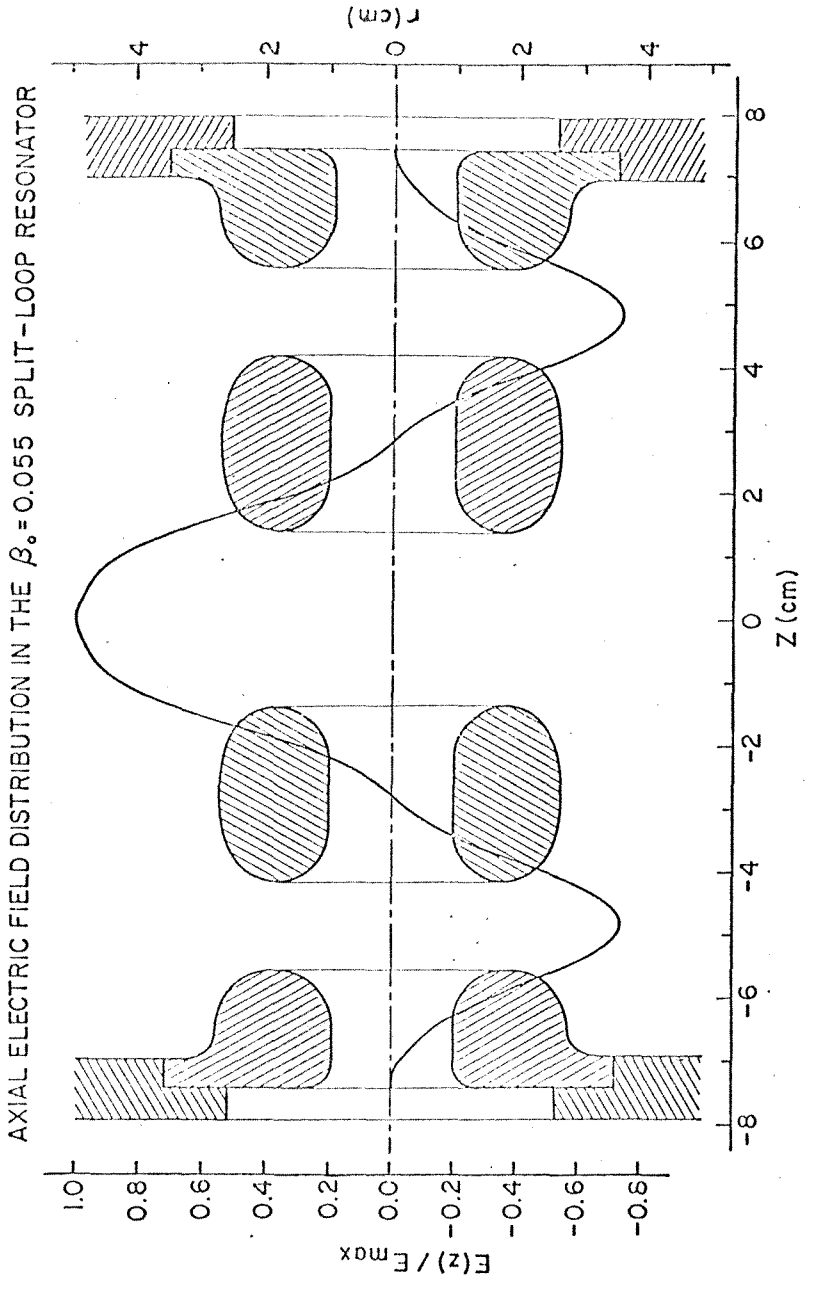

Fig. 5.3. Axial electric field profile of a split-ring resonator.

by adjusting the position of the drift tubes along the beam line. It can be seen from Fig. (5.2), where the fundamental frequency is 50 Hz, that the main contribution to the frequency shift comes from the mechanical mode 2.

We found in Chapter III that when the amplitude feedback gain is sufficiently high ($k_a + 1 >> \tau\Omega_\mu$), there exists a simple relationship between residual phase and amplitude error as expressed by equation (3.6.32).

This relationship was tested with the feedback system described in Chapter IV and a 150 MHz resonator locked to an external reference. The results are shown in Fig. (5.4) where $\frac{k_a+1}{k_\phi}\frac{\delta v}{\delta\phi}$ (in %/deg) is plotted as a function of θ_ℓ, the loop phase shift. The solid line is $\frac{\pi}{1.8}\sin\theta_\ell\cos\theta_\ell$ which is what is expected from the relation with $y_r = 0$. The only adjustable parameter is a constant offset in θ_ℓ since the absolute loop phase shift is impossible to measure. Fig. (5.4) shows an excellent agreement between analysis and experiments.

In another series of experiments, the oscillatory stability boundary was measured and compared with theory.

In the first experiment, the field amplitude V_0 and the phase feedback gain k_ϕ were held constant, and the loop phase shift θ_ℓ, at which ponderomotive oscillatory instability started to occur, was measured as a function of the amplitude feedback gain k_a. The results are presented in Fig. (5.5) where the solid line is what is expected from theory. This was obtained from:

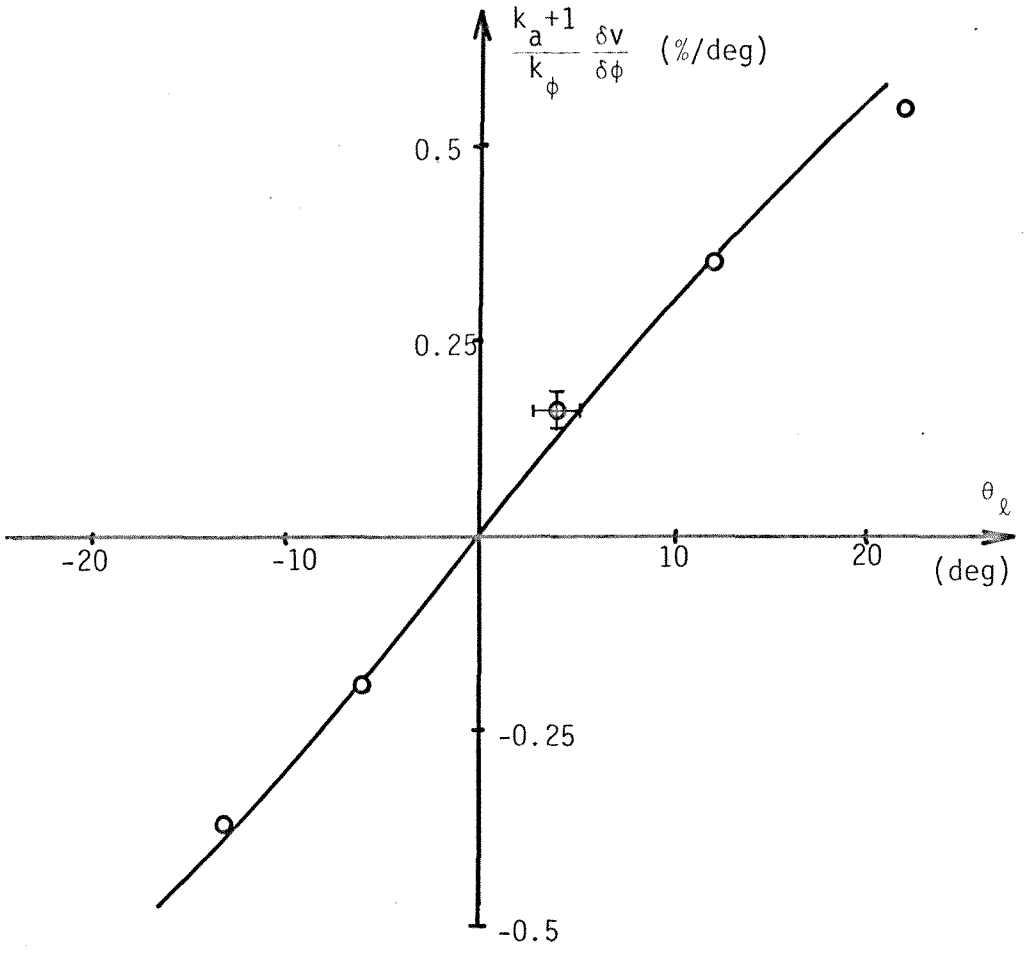

Fig. 5.4. Normalized ratio of residual amplitude and phase error vs. loop phase shift.

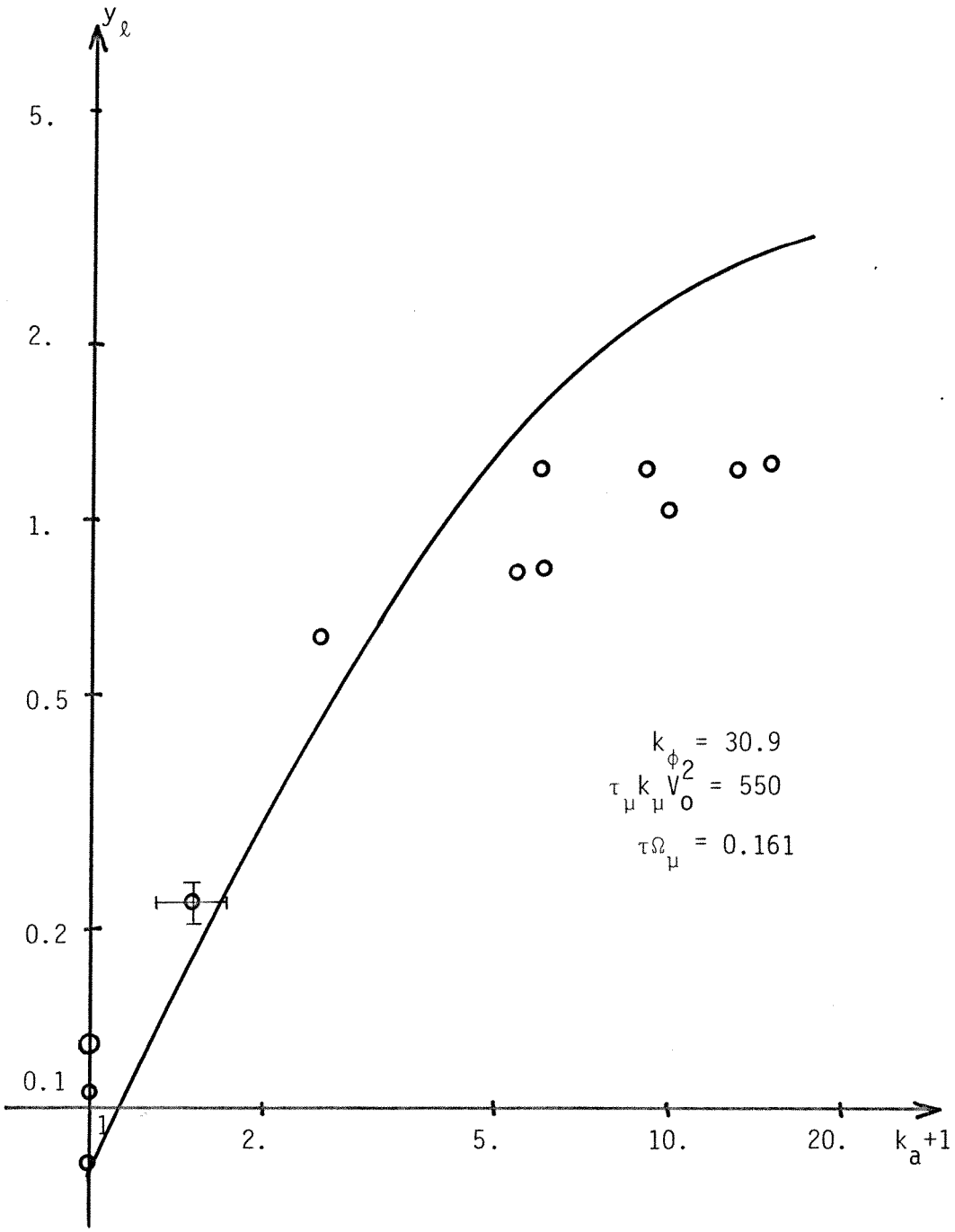

Fig. 5.5. Oscillatory stability boundary vs. amplitude feedback gain.

$$y_\ell = \frac{B_{os}\ (\ k_a,\ k_\phi\ )}{\tau_\mu\ k_\mu\ V_o^2}$$

by solving for y_ℓ as a function of k_a. This solution had to be found by successive approximations since y_ℓ is also present in B_{os}. In the expression for B_{os}, we made the approximation: $y_r = 0$, and besides an offset in θ_ℓ which was determined from Fig. (5.4), all the parameters were either measured or calculated.

The agreement between theory and experiment is excellent, especially at low values of y_ℓ and k_a. At higher values of y_ℓ, however, there seems to be some discrepancies. These discrepancies have their origin not in some inexactitude of the analysis, but in the breakdown of the feedback system. As we mentioned in Chapter II, the coupling of the resonator is adjusted so that the maximum frequency excursion is half the bandwidth of the resonator; this means that y_r varies in the range $\left|-1,\ +1\right|$.

However, for the loop and the feedback system to be operating, condition (3.5.1.6) must be satisfied, and we see that when y_ℓ gets of the order of 1, the feedback system can become unstable independently of ponderomotive effects.

The same experiment was made where y_ℓ was measured as a function of k_ϕ for fixed k_a and is shown in Fig. (5.6). Here again, the agreement between theory and experiment is excellent.

In conclusion, the experiments successfully demonstrated the principle of phase and amplitude stabilization of resonators operated

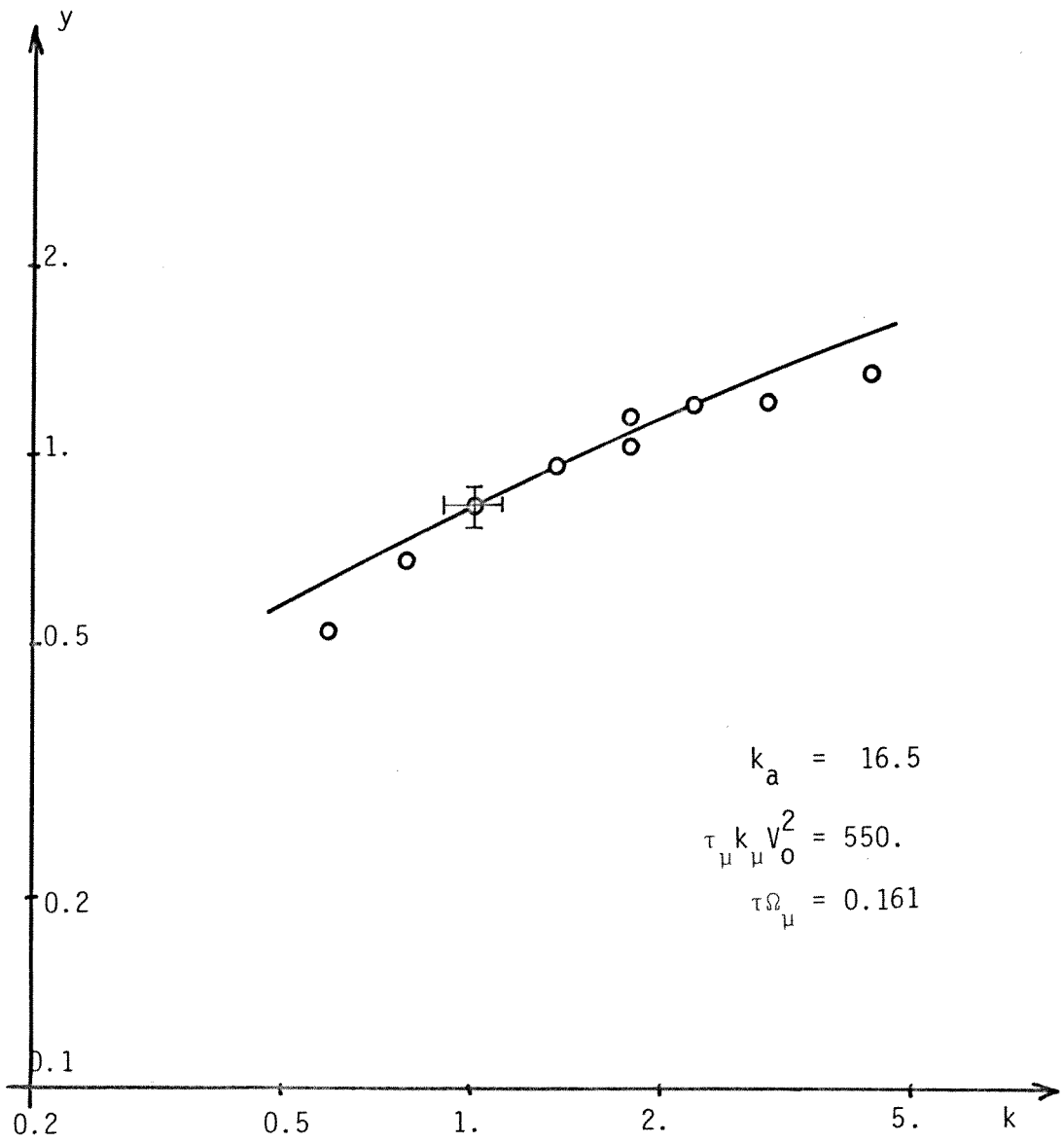

Fig. 5.6. Oscillatory stability boundary vs. phase feedback gain.

in self-excited loops by electronic feedback. They also confirmed the results of the analysis pertaining to the relative values of the residual phase and amplitude errors, and of the oscillatory stability of the electromechanical system.

Appendix A

RESONATOR DRIVEN BY A VOLTAGE-CONTROLLED OSCILLATOR

Throughout this thesis, we have studied a resonator operated in a self-excited loop, and in some instances, we have made references to another case where the resonator is driven by a fixed frequency generator. A third case, however, can occur in practice where the resonator is driven by a voltage-controlled oscillator (V.C.O.), that is, a generator whose frequency is not fixed, but is controlled by an external variable, in this case, the phase shift across the resonator as shown in figure (A.1).

Since the generator frequency is not fixed, the resonator input is best represented in terms of a real amplitude and an absolute RF phase:

$$v_g = V_g e^{i\alpha} \tag{A.1}$$

The resonator output can be represented in several ways whose convenience varies depending upon the application. The most common is to assign to the output the same RF phase as the input, and then include any phase shift between input and output into a complex amplitude:

$$v = \tilde{V} e^{i\alpha} \tag{A.2}$$

Another way is to describe the fields in terms of a real amplitude and an absolute RF phase:

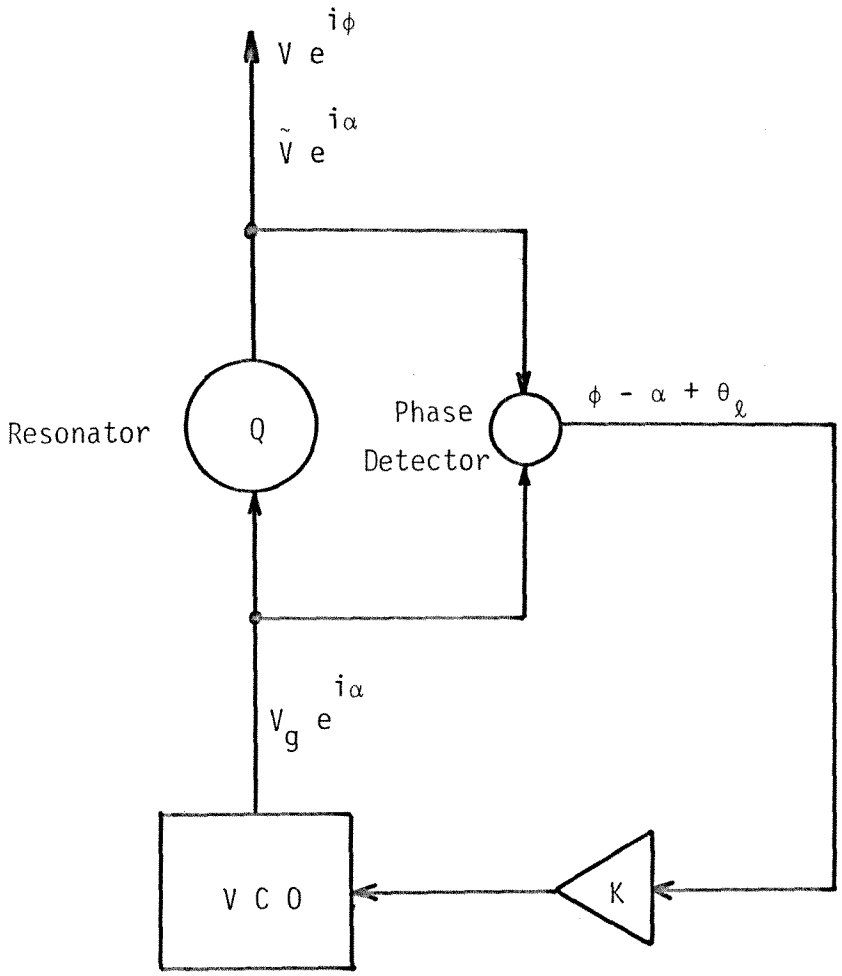

Fig. A.1. Block diagram of a resonator driven by a voltage-controlled oscillator

$$v = V e^{i\phi} \tag{A.3}$$

The phase difference between input and output is sensed by a phase detector, and after addition of an arbitrary phase offset θ_ℓ, this signal is amplified by an amplifier of gain K to control the V.C.O. frequency which is now:

$$\frac{d\alpha}{dt} = \omega_{go}\left[1 + K(\phi - \alpha + \theta_\ell)\right] \tag{A.4}$$

where ω_{go} is the frequency of the V.C.O. when no phase locking is provided.

We also define θ_c as being the phase shift across the resonator.

$$\theta_c = \phi - \alpha = \left(\frac{1}{\omega_{go}}\frac{d\alpha}{dt} - 1\right)\frac{1}{K} - \theta_\ell \tag{A.5}$$

As usual, the resonator is represented in terms of a single electromagnetic mode:

$$\ddot{v} + \frac{2}{\tau}\dot{v} + \omega_c^2 v = \frac{2}{\tau}\dot{v}_g \tag{A.6}$$

By replacing v and v_g in (A.6) by their expressions (A.1) and (A.2), one gets the following differential equation:

$$\ddot{\tilde{V}} + \dot{\tilde{V}}(2i\dot{\alpha} + \frac{2}{\tau}) + \tilde{V}(i\ddot{\alpha} + \frac{2}{\tau}i\dot{\alpha} + \omega_c^2 - \dot{\alpha}^2) = \frac{2}{\tau}(\dot{V}_g + i\dot{\alpha}V_g) \tag{A.7}$$

If (A.3) instead is used for v, we get:

$$\ddot{V} + \dot{V}(2i\dot{\phi} + \frac{2}{\tau}) + V(i\ddot{\phi} + \frac{2}{\tau}i\dot{\phi} + \omega_c^2 - \dot{\phi}^2) = \frac{2}{\tau}(\dot{V}_g + i\dot{\alpha}V_g) \quad (A.8)$$

By using (A.4) and (A.5), (A.7) and (A.8) transform respectively to:

$$\ddot{\tilde{V}} + \dot{\tilde{V}}\left[2i\omega_{go}(1 + K(\theta_c + \theta_\ell)) + \frac{2}{\tau}\right]$$

$$+ \tilde{V}\left[iK\omega_{go}\dot{\theta}_c + \frac{2}{\tau}i\omega_{go}(1 + K(\theta_c + \theta_\ell)) + \omega_c^2 - \omega_{go}^2(1 + K(\theta_c + \theta_\ell))^2\right]$$

$$= \frac{2}{\tau}\left[\dot{V}_g + i\omega_{go}(1 + K(\theta_c + \theta_\ell))V_g\right] \quad (A.9)$$

and to:

$$\ddot{V} + \dot{V}(2i\dot{\phi} + \frac{2}{\tau}) + V(i\ddot{\phi} + \frac{2}{\tau}i\dot{\phi} + \omega_c^2 - \dot{\phi}^2)$$

$$= \frac{2}{\tau}\, e^{i\left[\theta_\ell - \frac{1}{K}(\frac{1}{\omega_{go}}\frac{d\alpha}{dt} - 1)\right]}\left(\dot{V}_g + i(\dot{\phi} - \frac{\ddot{\alpha}}{K\omega_{go}})V_g\right) \quad (A.10)$$

It should remembered that although (A.9) and (A.10) look very different, they describe the same time evolution of the fields in the resonator. The differences have their origin in the two different representations used for the fields.

One important limit case which is obvious to understand is when the phase-locking system does not operate. In this instance, it is expected that the above differential equation reduces to the one

describing a resonator driven by a fixed frequency generator. In effect, if we set K=0 in (A.9), we get:

$$\ddot{\tilde{V}} + \dot{\tilde{V}}(2i\omega_{go} + \frac{2}{\tau}) + \tilde{V}(\frac{2}{\tau}i\omega_{go} + \omega_c^2 - \omega_{go}^2) = \frac{2}{\tau}(\dot{V}_g + i\omega_{go}V_g) \tag{A.11}$$

which describes a resonator driven by a generator of frequency ω_{go}.

Another important limit case is when phase-locking is perfect, so that the generator frequency is determined only by the phase shift across the resonator. If we set K=∞ in (A.10), we get:

$$\ddot{V} + \dot{V}(2i\dot{\phi} + \frac{2}{\tau}) + V(i\ddot{\phi} + \frac{2}{\tau}i\dot{\phi} + \omega_c^2 - \dot{\phi}^2) = \frac{2}{\tau}e^{i\theta_\ell}(\dot{V}_g + i\dot{\phi}V_g) \tag{A.12}$$

which is just the differential equation describing a resonator operated in a self-excited loop whose loop phase shift is θ_ℓ and whose limiter output is V_g.

Thus, the two cases where the resonator is driven by a fixed frequency generator, or is operated in a self-excited loop, can be considered as limits of a third, more general, case where the resonator is driven by a voltage-controlled oscillator.

REFERENCES

B1 J. Bardeen, L.N. Cooper, J.R. Schrieffer, Phys. Rev. 108, 1175-1204 (1957)

B2 I. Ben-Zvi, J.G. Castle, P.H. Ceperley, IEEE trans. NS-19, 226-230 (1972)

B3 L. Bollinger, IEEE Trans. NS-24, No 3, 1076-1080 (1977)

B4 F.E. Borgnis, C.H. Papas, Handbuch der Physik, edited by S. Flugge (Springer, Berlin, 1958), Vol. 16, p. 411

D1 G.J. Dick, K.W. Shepard, Appl. Phys. Lett., Vol. 24, No 1, 40-42 (1974)

D2 G.J. Dick, K.W. Shepard, 1972 Applied Superconductivity Conference, IEEE Publ. No 72ch0682-5-TABSC, 649-652

D3 O.D. Despe, K.W. Johnson, T.K. Khoe, IEEE trans. NS-20, No 3, 71-75 (1973)

D4 G.J. Dick, IEEE Trans. MAG-11, No 2, 441-442 (1975)

D5 J.J. D'Azzo, C.H. Houpis, Linear control system analysis and design: conventional and modern, Mc Graw-Hill (1975)

D6 G.J. Dick, J.R. Delayen, H.C. Yen, IEEE Trans. NS-24, No 3, 1130-1132 (1977)

D7 J.R. Delayen, G.J. Dick, J.E. Mercereau, IEEE trans NS-24, No 3, 1759-1761 (1977)

F1 W.M. Fairbank, J.M. Pierce, P.B. Wilson, Proc. 8th Low Temp. Phys. Conf., 324-325 (1962)

H1 B.H. Hillenbrand, H. Martens, H. Pfister, K. Schnitze, G. Ziegler IEEE Trans. MAG-11, No 2, 420-422 (1975)

H2 G. Hochschild, D. Schulze, F. Spielbock, IEEE Trans. NS-20, No 3, 116-118 (1973)

J1 H.M. James, N.B. Nichols, R.S. Phillips, Theory of servomechanisms, MIT Radiation Laboratory Series, No 25, Mc Graw-Hill (1947)

K1 M.M. Karliner, V.E. Shapiro, I.A. Shekhtman, Soviet Physics, Technical Physics, Vol 11, No 11, 1501,1507 (1967)

K2 M. Kuntze, Proceedings of the 1976 proton linear accelerator conference, Chalk River, AECL-5677, 86-94, (1976)

N1 V.L. Newhouse, Applied Superconductivity, Vol 1 & 2, Academic Press, New York (1975)

O1 R.C. Oldenbourg, H. Sartorius, The dynamics of automatic controls A.S.M.E. (1948)

P1 P.Z. Peebles Jr., IEEE Trans NS-20, No 3, 113-115 (1973)

S1 H.A. Schwettmann, J.M. Pierce, P.B. Wilson, W.M. Fairbank, Advan. Cryogen. Eng. 10, sect. M-U, p. 88 (1965)

S2 A.J. Sierk, C.J. Hamer, T.A. Tombrello, Particle Accelerators, Vol. 2, 149-167, (1971)

S3 K.W. Shepard, J.E. Mercereau, G.J. Dick, IEEE Trans. NS-22, No 3, 1179-1182 (1975)

S4 D. Schulze, KFK Report 1493, Kernforschungszentrum, Karlsruhe (1971), ANL Translation 944 (1972)

S5 K.W. Shepard, C.H. Scheibelhut, R. Benaroya, L.M. Bollinger, IEEE Trans. NS-24, No 3, 1147-1149 (1977)

S6 V.E. Shapiro, Soviet Physics, JETP 28, 301,304 (1969)

S7 V.V. Solodovnikov, Introduction to the statistical dynamics of automatic control systems, Dover (1960)

T1 J.P. Turneaure, Ph.D. Thesis, Stanford University (1967)

Y1 H.C. Yen, Ph.D. Thesis, California Institute of Technology (1977)

Y2 A.M. Yaglom, An introduction to the theory of stationary random functions, Dover (1973)